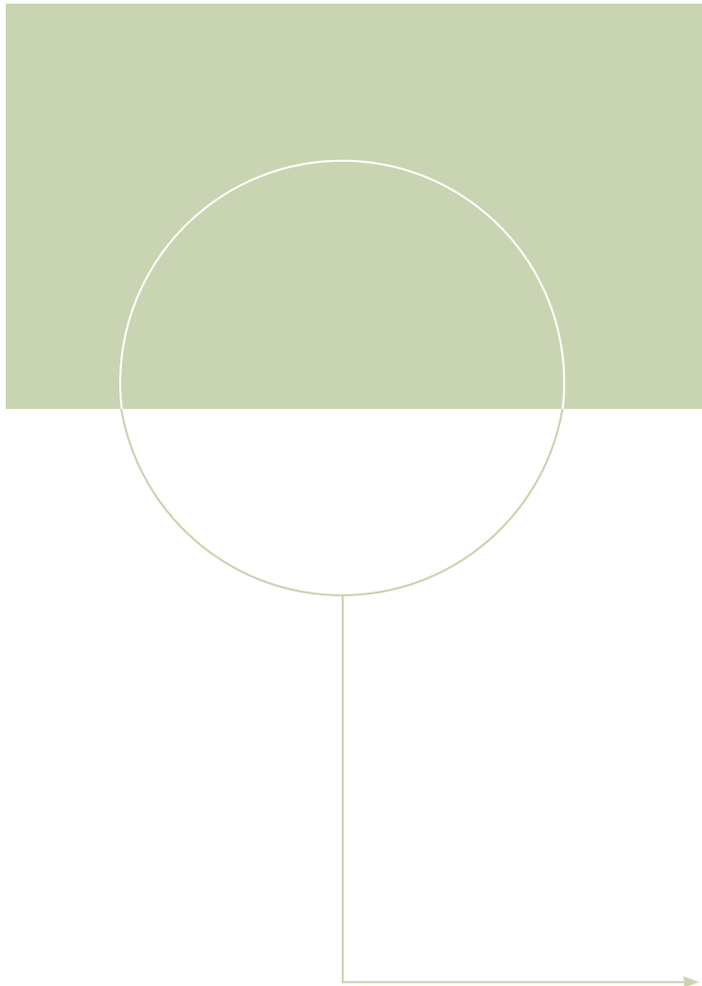

Master's thesis

2022

Benjamin Colin Sørli Josefsen

NTNU
Norwegian University of
Science and Technology
Faculty of Natural Sciences
Department of Materials Science and Engineering

Benjamin Colin Sørli Josefsen

Electrochemical Detection of Silver Ions in Nickel Chloride Based Process Solutions

June 2022

NTNU
Norwegian University of
Science and Technology

NTNU
Norwegian University of
Science and Technology

NTNU

Norwegian University of
Science and Technology

Electrochemical Detection of Silver Ions in Nickel Chloride Based Process Solutions

Benjamin Colin Sørli Josefsen

Chemical Engineering and Biotechnology
Submission date: June 2022
Supervisor: Frode Seland
Co-supervisor: Øyvind Mikkelsen
Elke Thisted
Torkild Eivindson

Norwegian University of Science and Technology
Department of Materials Science and Engineering

Preface

I want to thank my supervisor Professor Frode Seland for his superb guidance throughout this master thesis. Your infinite knowledge and good ideas have been essential throughout the period.

A big thank you is also addressed to Glencore Nikkelverk AS for letting me execute this thesis. I would also like to thank my co-supervisors at Glencore Nikkelverk AS, Torkild Eivindson, and Elke Thisted. Thanks for providing me with process solutions for use in measurements, as well as giving me valuable insight into the industrial aspect. In addition, I would like to thank my co-supervisor, Professor Øyvind Mikkelsen, for valuable input about electrochemical online detection.

Siri Marie Skaftun deserves a massive thank. I am incredibly grateful for everything you have helped me with over the past year, as laboratory training, finding sources of error, and giving feedback on my thesis. Your help has really been invaluable.

I would also like to thank Anita Storsve, Elin Albertsen, and Marthe Folstad for providing laboratory equipment and chemicals. Finally, I would like to thank my friends for many entertaining and funny lunch breaks this semester. The hours on the sofa in the break area have been a bright spot on heavy days.

Abstract

Silver ions are present as impurities in the electrolyte used for nickel electrowinning. A method for monitoring the silver concentration in process solutions is needed to ensure that silver ions have been removed to a sufficient degree before electrowinning. Electrochemical measurements can be used for online monitoring, and the silver ion concentration may be recorded several times each hour. The aim of this thesis was to develop an electrochemical method for detecting silver ions in actual nickel process solutions with a high chloride content.

In anodic stripping voltammetry, a fast scan rate gives a large current peak when stripping off a metal. However, if several metal ions have deposited on the electrode surface, their current peaks might overlap. Overlapping current peaks may lead to detection problems. Measures, chemically or electrochemically, can often be taken to distinguish the peaks. A possibility is to use a slow scan rate when stripping off the metals and consequently get separated small current peaks. On the other side, this will give an increased lower detection limit for the metal ion of interest. An alternative might be to divide the stripping into several sweeps, where the unwanted metal is stripped off by a slow scan rate and the metal of interest is stripped off with a fast scan rate.

In this work, anodic stripping voltammetry methods, such as linear sweep and differential pulse voltammetry, were tested for qualitative detection of silver ions in nickel chloride based process solutions. The morphology and composition of the electrodeposited material were studied by using scanning electron microscope and energy dispersive spectroscopy. Anodic stripping voltammetry methods were further tested with the stripping divided into several sweeps(divided stripping) to isolate the current signals. The possibility of using a nickel wire as a pseudo-reference electrode was also investigated.

Both linear sweep and differential pulse voltammetry was found to be possible methods for silver ion detection in nickel chloride based process solutions. Before the voltammetry measurement, silver was electrodeposited at a constant potential. However, both silver and bismuth were depositing on glassy carbon in most of the potential range for silver deposition. To avoid interference of the current peaks from the two metals, a divided stripping was used, where bismuth was stripped off by a slow scan rate before silver was stripped off by a fast scan rate. The reproducibility and sensitivity were better for linear

sweep voltammetry than differential pulse voltammetry when using divided stripping to isolate the silver signal.

An electrochemical method was developed for qualitative detection of silver ions in a 1/10 dilution of the process solution. Using a rotating glassy carbon disk as working electrode, silver was detected by deposition at $-0.3\,\mathrm{V}$ vs Ag/AgCl for 500 s and then using linear sweep voltammetry with two sweeps and a rotation speed of 1600 rpm. In the first sweep from -0.3 to 0.0 V vs Ag/AgCl, a scan rate of $5\,\mathrm{mV\,s^{-1}}$ was used. In the second sweep, between 0.0 and 0.4 V vs Ag/AgCl, a scan rate of $100\,\mathrm{mV\,s^{-1}}$ was used. Finally, the electrode was left in the solution at open circuit for 500 s to clean the working electrode surface.

Calibration curves were made by repeating the method described above for a number of different silver concentrations. The calibration curves were based both on charge and peak height of the silver peak. The charge gave a slightly better estimate of the silver ion concentration than the peak height, with coefficients of determination of 0.998 and 0.992, respectively. The lowest tested silver concentration corresponds to $0.5\,\mathrm{mg\,L^{-1}}$ Ag^+ in the undiluted process solution.

A nickel wire worked as a pseudo-reference electrode in nickel process solution and seems to be a relatively good replacement for a Ag/AgCl reference electrode. The stability was relatively good over longer time periods, but fluctuations in the potential on a short-time basis were observed. The stability and reproducibility of silver quantification were a little worse when using a nickel pseudo-reference electrode instead of an Ag/AgCl reference electrode, but still acceptable.

Sammendrag

Sølvioner er tilstede som urenheter i elektrolytten som brukes til elektrolyse av nikkel. En metode for å overvåke sølvkonsentrasjonen i prosessløsning er nødvendig for å sikre at sølvioner er fjernet i tilstrekkelig grad før elektrolysen. Elektrokjemiske målinger kan brukes til online overvåking, og sølvionkonsentrasjonen kan registreres flere ganger hver time. Målet med denne oppgaven var å utvikle en elektrokjemisk metode for å detektere sølvioner i faktiske nikkelprosessløsninger med høyt kloridinnhold.

I anodisk stripping-voltammetri gir en rask sveiphastighet en stor strømtopp når man stripper av et metall. Imidlertid, hvis flere metallioner har avsatt seg på elektrodeoverflaten, kan strømtoppene deres overlappe. Overlappende strømtopper kan føre til deteksjonsproblemer. Kjemiske eller elektrokjemiske tiltak kan bli gjort for å skille toppene. En mulighet er å bruke en langsom sveiphastighet ved stripping av metallene og følgelig få separerte små strømtopper. På den andre siden vil dette senke sensitiviteten for deteksjon av metallionet av interesse. Et alternativ kan være å dele strippingen i flere sveip, hvor det uønskede metallet fjernes med en langsom sveiphastighet og metallet av interesse fjernes med en høy sveiphastighet.

I dette arbeidet ble anodiske stripping-voltammetrimetoder, som lineært sveip og differensiell pulsvoltammetri, testet for kvalitativ deteksjon av sølvioner i nikkelkloridbaserte prosessløsninger. Morfologien og sammensetningen til det elektroavsatte materialet ble studert ved å bruke skanning elektronmikroskop og energidispersiv spektroskopi. Anodiske stripping-voltammetrimetoder ble ytterligere testet med strippingen delt inn i flere sveip (delt stripping) for å isolere strømsignalene. Muligheten for å bruke en nikkeltråd som pseudoreferanseelektrode ble også undersøkt.

Både lineær sveipvoltammetri og differensiell pulsvoltammetri ble funnet å være mulige metoder for sølviondeteksjon i nikkelkloridbaserte prosessløsninger. Før voltammetrimålingen ble sølv avsatt electrokjemisk med konstant potensial. Imidlertid ble både sølv og vismut avsatt på glasskarbon i det meste av det potensielle området for sølvavsetning. For å unngå interferens mellom strømtoppene fra de to metallene, ble det brukt en delt stripping, hvor vismut ble strippet av med en langsom sveiphastighet før sølv ble strippet av med en høy sveiphastighet. Reproduserbarheten og følsomheten var bedre for lineær sveipvoltammetri enn differensialpulsvoltammetri ved bruk av delt stripping for å isolere

sølvsignalet.

Det ble utviklet en elektrokjemisk metode for kvalitativ påvisning av sølvioner i en 1/10 fortynning av prosessløsningen. Ved å bruke en roterende glasskarbondisk som arbeidselektrode ble sølv detektert ved avsetning ved $-0.3\,\mathrm{V}$ vs Ag/AgCl i 500 s og deretter ved bruk av lineær sveipvoltammetri med to sveip og en rotasjonshastighet på 1600 rpm. I det første sveipet, fra -0,3 til $0.0\,\mathrm{V}$ vs Ag/AgCl, var en sveiphastighet på $5\,\mathrm{mV\,s^{-1}}$ brukt. I det andre sveipet, mellom 0,0 og $0.4\,\mathrm{V}$ vs Ag/AgCl, var en sveiphastighet på $100\,\mathrm{mV\,s^{-1}}$ brukt. Til slutt ble elektroden stående i løsningen ved åpen krets i 500 s for å rengjøre arbeidselektrodeoverflaten.

Kalibreringskurver ble laget ved å gjenta metoden beskrevet ovenfor for en rekke forskjellige sølvkonsentrasjoner. Kalibreringskurvene var basert både på ladning og topphøyde på sølvtoppen. Ladningen ga et litt bedre estimat på sølvionekonsentrasjonen enn topphøyden, med bestemmelseskoeffisienter på henholdsvis 0,998 og 0,992. Den laveste testede sølvkonsentrasjonen tilsvarer $0.5\,\mathrm{mg\,L^{-1}}$ $\mathrm{Ag^+}$ i den ufortynnede prosessløsningen.

En nikkeltråd fungerte som en pseudoreferanseelektrode i en nikkelprosesselektrolytt, og ser ut til å være en relativt god erstatning for en Ag/AgCl-referanseelektrode. Stabiliteten var relativt god over en lengre tidsperiode, men det ble observert svingninger i potensialet på kort sikt. Stabiliteten og reproduserbarheten til prosedyren for sølvkvantifisering var litt dårligere ved bruk av en nikkel-pseudoreferanseelektrode i stedet for en Ag/AgCl-referanseelektrode, men fortsatt akseptabel.

Contents

1 Introduction

1.1 Background and motivation

In hydrometallurgy, metal ions are first extracted from ores by leaching, then purified, and finally refined by electrowinning. Metal ores typically have a relatively low concentration of primary metal. Therefore, the process of purifying and increasing the primary metal concentration is critical to get a pure metal.[1] Some trace metals, such as noble metals, are also valuable pay metals and may be advantageous to capture and sell.

Trace metal concentrations are monitored continuously to ensure pure process solutions before electrowinning. By monitoring the content of the process solution, measures can be taken to remove impurities that are present in too large concentrations. Because of the low concentrations of the impurities, manually collected samples are highly sensitive to contamination. Despite this, manual sample collection and preparation are widely used in the industry. Examples of instruments with good sensitivity and the possibility to detect a wide range of different elements are inductive coupled plasma-mass spectrometry (ICP-MS), atomic absorption spectrometer (AAS), inductively coupled plasma atomic emission spectroscopy (ICP-OES), and pH meter with an ion-selective membrane.[2][3][4][5][6][7][8] Colorimetry is also a widely used measuring method that uses the color of the solution to estimate the content of a complex in a solution.[9] To minimize the risk of contamination of the sample and human sources of error, automatizing sample preparation and measuring by implementing an online monitoring system is widespread. Fully automated online monitoring systems exist and are constructed to do sampling, sample preparation, and measuring the solution content. Voltammetry is an example of a measuring technique used for online monitoring of trace metals. This can give regular updates on the solution content all day without a workforce, with little risk of sample contamination and little need for maintenance.[10] Most of the previously mentioned instruments are difficult to automate and affordably.[11] Calibration of the instruments is needed regularly, and the instruments are large and expensive.[12] The pH meter with the ion-selective membrane is an exception but is very limited to which elements it can detect.[7][8]

Voltammetry is an electrochemical technique where the current is measured as a function of the applied potential. The current signal can be used to estimate the concentration

of one or more predefined electroactive species based on calibration.[13] Voltammetry is widely used for automatic online detection of trace metals, for example, nickel and cobalt, in wastewater from the industry.[10][14] Systems for voltammetric measurements can be cheap, small, and easy to set up compared to ICP-MS and AAS. Since the technique is based on the reduction potential of metal ions in the given solution, problems can occur if several metals have a reduction potential in the same region. This can make it difficult to distinguish the signals and find a concentration. The complexation of metal ions changes the detection potential. This can make it difficult to predict where the metal can be detected if the process solution content varies over time.[15]

Nickel electrowinning is an example of a hydrometallurgical process. Nickel ores typically contain about 1% nickel and a lot of impurities and different trace metals. Concentrating and smelting of the ore material are generally performed before the material enters the refining process. The intermediate product formed after the smelting of sulfide ores of nickel is called matte. Glencore Nikkelverk AS (Nikkelverket) in Kristiansand produces about 90000 tons of nickel annually by nickel electrowinning. They receive mattes with a material typically containing 50-75% nickel. In addition, the material contains some raw materials for co-products, such as copper, cobalt, precious metals, and many different trace metals. Silver is a precious metal produced at Nikkelverket. It is desirable to collect silver ions to avoid impurities in the finished nickel metal and because it is a valuable pay metal. By removing silver ions from the solution, it can be sold for the high silver prices instead of the lower nickel prices.[16][17] In addition, the nickel metal will not have to be downgraded as a result of high silver content. If the silver ion content of the process solution can be continuously monitored, measures can be taken to minimize the consequences of an increased silver ion concentration.

Currently, the silver ion content in the process solution is analyzed by AAS at Nikkelverket. This is a lengthy process, with several steps with possible sources of error. Sampling should be done in an upstream process flow to get a representative sample. The instrument needs to be calibrated, the sample needs to be diluted and analyzed without contamination, and the result must be reported. This process demands workforce in addition to being uncertain considering the sources of error. Electrochemical online monitoring of the silver ion content will likely need little maintenance, give more accurate and frequent data, be cheaper, and require less workforce than continuing with AAS.

Electrochemical detection of silver ions in chloride electrolytes has already been shown for a synthetic nickel chloride solution.[18] Silver ion concentrations corresponding to $10\,\mathrm{mg\,L^{-1}}$ in an undiluted process solution have been detected electrochemically in a synthetic nickel process solution containing nickel, chloride, sulfate, iron, manganese, bismuth, and silver. The solution used for the measurements corresponds to a 1/10 dilution of the process solution content seen in Table 1.1. The silver signal was recorded by first depositing silver on a glassy carbon or a platinum rotating disk electrode and then stripping it off. This was done by chronoamperometry and linear sweep voltammetry. Signals from bismuth deposition can interfere with the silver signal for some deposition potentials, especially at platinum electrodes. Since silver has a slightly higher deposition potential than bismuth in the diluted synthetic process solution, the effect of bismuth can be removed by increasing the deposition potential. The best way of detecting silver was found to be by using a glassy carbon working electrode with a deposition potential of -0.1 V vs. Ag/AgCl, a deposition time of 100 s, a scan rate of $50\,\mathrm{mV\,s^{-1}}$, and a rotation speed of 1600 rpm. Due to the potential change resulting from silver chloride complex formation, a 1/10 dilution of the synthetic process solution gave the best conditions for silver detection.[18][19]

Table 1.1: Concentration of selected elements in a typical process solution.

Element	Concentration	Unit
Ni^{2+}	250	$\mathrm{g\,L^{-1}}$
Cl^{-}	300	$\mathrm{g\,L^{-1}}$
$SO_4{}^{2-}$	50	$\mathrm{g\,L^{-1}}$
Fe^{2+}	12	$\mathrm{g\,L^{-1}}$
Mn^{2+}	10	$\mathrm{mg\,L^{-1}}$
Bi^{2+}	5	$\mathrm{mg\,L^{-1}}$
Ag^{+}	< 1	$\mathrm{mg\,L^{-1}}$

A stable reference electrode (RE) is crucial for reliable results in electrochemical measurements. Silver/silver chloride RE is widely used due to its known potential and stability despite changes in the electrolyte composition. However, in strong electrolytes, the solution in the RE chamber will be contaminated over time, causing potential drift. Silver/silver chloride REs can be challenging to maintain and are relatively expensive to buy. An alternative to ordinary REs is pseudo-reference electrodes (pseudo-RE), a metal wire in equilibrium with ions in the solution. A nickel wire might be a possible pseudo-RE

in a nickel process solution. It will corrode over time, but the wire is cheap and easy to replace when the degree of corrosion is too large. It might be a suitable replacement for an ordinary RE if it gives a stable potential over time.[20]

1.2 Aim and scope of the work

The aim of the master thesis work is to develop an electrochemical method to detect silver ions in a nickel chloride process solution. Different electrochemical methods for detection of silver and isolation of its current signal will be tested and compared. This is to be able to make a reproducible method for silver detection that can be used to make a calibration. The possibility of using a nickel pseudo-RE will also be explored.

Firstly, the silver signal in real process solutions will be mapped. After that, different electrochemical methods and stripping programs will be tested to find a reproducible silver detection method. The stability of a nickel wire as a pseudo-reference electrode will also be studied. In addition, a calibration curve for silver detection will be made.

2 Theory

2.1 Mass transport in electrolytes

Mass transport in a solution can occur due to three different mechanisms. The modes of transport are due to a gradient of concentration, pressure, or electrical potential in the solution and are respectively named diffusion, convection, and migration. The way an experiment is designed determines which mechanism or mechanisms are dominant.[15][21]

2.1.1 Diffusion

The transport of ions, atoms, and molecules in a solution due to a chemical potential gradient, such as concentration differences, is called diffusion. A concentration gradient will arise near electrode surfaces where reactions take place.[15][21]

The diffusive flux, J_i^{dif}, is proportional to the concentration gradient, $\frac{dc_i}{dx}$, and follows Fick's first law:

$$J_i^{dif} = -D_i(\frac{dc_i}{dx}) \tag{2.1}$$

where J_i^{dif} is the amount of the species i transported through an area per second due to diffusion and D_i is the diffusion coefficient for species i. The position, x, is zero at the electrode surface and the negative sign indicates movement from high to low concentration.[21][22]

2.1.2 Convection

Convection is a driving force for mass transport in solutions caused by a pressure gradient. This gradient can be either forced or natural. Forced convection happens due to an external force on the solution, such as pumps, stirring, or heating of the solution Natural convection is caused by natural density changes in the solution and can happen due to temperature gradients.

The convective flux, J_i^{conv}, is proportional to the velocity, υ, and follows:

$$J_i^{conv} = \upsilon_x c_i \tag{2.2}$$

where J_i^{conv} is the amount of the species i transported through an area per second due to

convection and c_i is the concentration of species i.

In many cases, it may be preferable to control the convection. By stirring the solution, the convection mass transport contribution can be dominant over mass transport from diffusion. [15][21]

2.1.3 Migration

Charged species, such as ions, can move due to an electrical gradient in the solution. This is called migration and is the primary way that charge is moved in a solution between electrodes. The migration flux, J_i^{mig} is expressed as:

$$J_i^{mig} = -u_i \cdot c_i(\frac{d\Phi}{dl}) \tag{2.3}$$

where u_i is the mobility of species i, c_i is the concentration of species i, and $\frac{d\Phi}{dl}$ is the potential gradient. For low concentrations of the charged species compared to the amount of the non electroactive part of the electrolyte, the supporting electrolyte, the contribution from migration can be neglected compared to the diffusion of the charged species.[15][21]

2.1.4 Total mass transport flux

The contribution from diffusion, convection, and migration gives the following equation for the total mass transport flux:

$$J_i = J_i^{dif} + J_i^{conv} + J_i^{mig} = -D_i(\frac{dc_i}{dx}) + v_x c_i - u_i \cdot c_i(\frac{d\Phi}{dl}) \tag{2.4}$$

Since convection is an effective force of mass transport, it is often used in electrochemical experiments. One of the most common ways to do this is by stirring the solution using a rotating disk electrodes. This is because its effect on mass transport is well defined. The voltammetric consequence of this stirring can consequently be predicted quantitatively.[21]

2.1.5 Rotating disk electrode

A rotating disk electrode (RDE) is a type of working electrode (WE) used to perform steady-state studies by rotating the circular disc with a chosen velocity, ω. The RDE stirs the solution, working as a pump, continuously supplying the electrode surface with

new reactant. The rotation causes a well defined flow field for the electrolyte. [15][22] RDE is commonly used to control convection.[21] Introducing convection to a system can increase the current signal by 3-100 times, giving higher sensibility.[23]

In experiments using RDE, the limiting current density, i_{lim}, is dependent on the velocity as seen from the Levich equation:

$$i_{\text{lim}} = 0.62nF\nu^{-1/6}D^{2/3}c_b\omega^{1/2} = B \cdot \omega^{1/2} \tag{2.5}$$

where D is the diffusion coefficient, and c_b is the bulk concentration (the concentration of the bulk, far from the electrode). i_{lim} is proportional to the square root of the rotation rate.[21][24]

2.2 Electrodeposition

Electrodeposition is the electrochemical reduction of a metal ion on the WE surface. This may be done by applying a predefined potential and reducing the metal. A generalized reaction for metal deposition of a metal M^{z+} is as follows:

$$M^{z+} + ze^- \rightleftharpoons M \tag{2.6}$$

For an electrochemical reaction to occur, the electrode potential must exceed a thermodynamic potential called the reversible electrode potential, E. The Nernst equation uses the standard potential, E°, to calculate E:

$$E = E^\circ - \frac{RT}{nF} \cdot \ln Q \tag{2.7}$$

where R is the gas constant, T is the temperature, n is the number of electrons being transferred in the reaction, F is the Faraday constant, and Q is the reaction quotient.[21][25] In reality, an additional overpotential is needed for the reaction to occur. The overpotential is the magnitude of deviation of the electrode potential, compared to the equilibrium value. The difference between the actual deposition potential and the reversible electrode potential at equilibrium can be seen as the overpotential.[22][26][27] The effect of overpotential can, for example, be observed for stripping of deposited bismuth. The bismuth stripping peak moves to a more positive potential when silver ions are added to the solu-

tion. This indicates that silver increases the stability of deposited bismuth, hence causing a higher overpotential for bismuth stripping. [28].

An increased deposition time will give an increased amount of the trace metal deposited on the electrode, in accordance with Faraday's law:

$$m_i = \frac{M_i I t}{nF} \tag{2.8}$$

where m_i is the mass of species i electrodeposited, M_i is the molar mass of species i, I is the current, and t is the deposition time.[21][29][30]

Electrochemical codeposition of metals is the deposition of two or more metals simultaneously on the electrode surface. When trying to detect a metal electrochemically, the current signals from the different metals may interfere. This makes quantifying the content of a single metal difficult. Electrochemical codeposition, i.e. simultaneous electrodeoposition of multiple metallic phases, can occur if the electrode potential is sufficiently low for different metal ions to be reduced to their respective metal. The deposition potential of a metal ion can, in some cases, be altered by complexation to avoid codeposition and separate the current signals.[26][31]

2.2.1 Nucleation and growth

In the initial process for electrodeposition of a metal, nuclei form at the surface. The rate of nucleation is strongly dependent on the overpotential and the mass transport. There are several models for nucleation and growth in diffusion limited cases, for example, the one from Scharifker and Hills [32]. This model gives two limiting cases for the formation rate: instantaneous and progressive nucleation. In instantaneous nucleation, nuclei immediately form at all available sites, while the number of nuclei increases with time in progressive nucleation, as shown in Figure 2.1. The nucleation in cases with forced convection has been less studied. However, in an article from Hyde, Klymenko, and Compton [33], a very complex equation for nucleation in systems with forced convection is derived.

Metals have different overpotentials for electrodeposition on different surfaces, depending on material and structure. Two metals may deposit differently on the same electrode surface. The potential gap between the deposition of two metals may also vary with the electrode material, electrolyte composition and temperature. If a metal has a lower

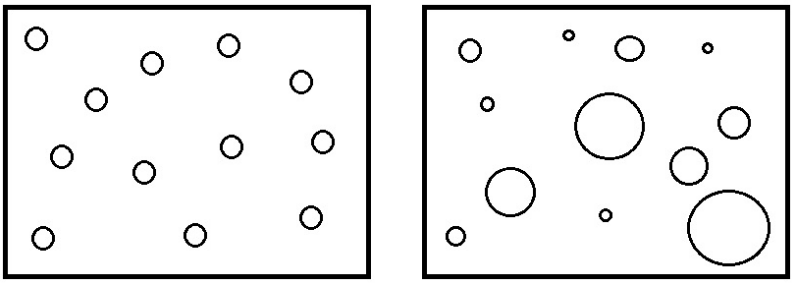

Figure 2.1: Illustration of instantaneous nucleation (left) and progressive nucleation (right), reproduced from Skaftun [34].

Figure 2.2: Illustration of nucleation growing into a thin film on the surface, reproduced from Popov [35].

overpotential for deposition on itself than the electrode surface material, larger nuclei with a 3D structure will form on the surface. On the other hand, if the overpotential is lower for deposition on the surface, the metal will deposit as a uniform film. The formation of a film can be seen in Figure 2.2.[26][27][31]

2.2.2 Activity in strong electrolytes

In weak electrolytes, the activity of water can be approximated to be unity. However, for strong electrolytes, the water activity can differ from unity. The activity of water in nickel chloride solutions has been estimated by Åkre [36] for concentrations up to 4 mol $NiCl_2$/kg H_2O. In a 1/10 dilution of the process solution, the molality of nickel chloride will be in the region of 0.4-0.45mol/kgH_2O. This gives a water activity of about 0.97-0.98 according to Åkre [36], making unity a good approximation. In the process solution, other ions and complexes exist, and the effect of these in collaboration on the water activity is complex and difficult to estimate theoretically. However, their concentrations are significantly lower than of nickel chloride, making the concentration of nickel chloride a good estimation for finding the water activity.

Generally, the activity of a species i can be found from the following equation:

$$a_i = \gamma_i \cdot m_i \tag{2.9}$$

where m_i and γ_i are the molality concentration and the activity coefficient of species i, respectively. The mean activity coefficient is the ratio between the activity and the actual concentration and can be found experimentally or estimated by equations.[36][21]

The mean ionic activity coefficient in a weak electrolyte can be estimated by Debye–Hückel equation:

$$\log \gamma_{\pm} = -\frac{A|z_+ z_-|\sqrt{I}}{1 + B\dot{a}\sqrt{I}} \tag{2.10}$$

where $\gamma_{\pm}$ is the mean ionic activity coefficient, A and B are constants, z_+ and z_- are the charge number of cations and anions, respectively, I is ionic strength, and $\dot{a}$ is an ion-size related parameter. In strong electrolytes with a high concentration of ions, the Debye–Hückel equation deviates a lot from experimental values. Stokes and Robinsons equation is an alternative equation for estimation of the mean ionic activity coefficient:

$$\log \gamma_{\pm} = -\frac{A|z_+ z_-|\sqrt{I}}{1 + B\dot{a}\sqrt{I}} - \frac{h}{v}\log a_w - \log\left[1 + 0.018(v-h)m\right] \tag{2.11}$$

where h is the hydration number, a_w is the water activity, and v is the stoichiometric coefficient.[36][37][38]

The mean ionic activity coefficient can further be used to estimate the single-ion activity coefficients. For a metal chloride salt with the formula MCl_2, the single-ion activity coefficient of M^{2+} and Cl^- can be found from the mean activity coefficient of MCl_2:

$$\log \gamma_{M^{2+}} = 2\log \gamma_{\pm} + 0.00782hm\Phi + \log\left[1 + 0.018(3-h)m\right] \tag{2.12}$$

$$2\log \gamma_{M^{2+}} = \log \gamma_{\pm} - 0.00782hm\Phi - \log\left[1 + 0.018(3-h)m\right] \tag{2.13}$$

where Φ is the osmotic coefficient that characterizes the deviation of the solvent from ideal behavior. This is a better way of estimating the activity of species, which can be used, for example, in the calculation of the reversible electrode potential.[36] [37]

2.3 Complexation

In solutions containing several different atoms and ions, complexation is commonly observed. Complexation is the formation of a complex, which is a large molecule or ion made from several other ions and molecules. The complex is made up of a central metal ion, surrounded by ligands, which are ions or molecules connected to the central ion. [39][40] A generalized equation for the formation of a complex, $[ML_x]^{z+xp}$, by a metal, M, and a ligand, L, is written as:

$$M^{z+} + xL^{p} \rightleftharpoons [ML_x]^{z+xp} \tag{2.14}$$

A high ligand concentration favors the formation of the complex, making it more challenging to reduce the metal ion. This is because the metal ion is surrounded by a stabilizing shroud of ligands, making access more difficult. When reducing a central metal ion from a complex, Equation 2.14 must proceed from right to left to produce the metal ion from the complex. After that, the metal ion can be reduced according to Equation 2.6. The metal ion concentration will be low when the ligand concentration is high, causing a much lower reduction potential than for solutions without complexation.[15][26] A high local metal ion concentration will arise close to the electrode surface when oxidizing the metal. A complexing agent present in the solution can cause an increased concentration gradient at the electrode due to the rapid formation of the complex. This increases the stripping rate, giving higher peak currents and more narrow peaks in stripping voltammograms.[41][42]

2.3.1 Silver chloride complexes

In aqueous solutions chloride and silver ions form silver chloride, which has low solubility in water: [43]

$$Ag^{+}(aq) + Cl^{-}(aq) \rightleftharpoons AgCl(s) \tag{2.15}$$

If the chloride concentration of a solution is large compared to the silver ion concentration, several different silver chloride complex ions will form. These complex ions are soluble in water and are formed according to the following chemical equations:

$$AgCl(s) + Cl^{-}(aq) \rightleftharpoons [AgCl_2]^{-}(aq) \tag{2.16}$$

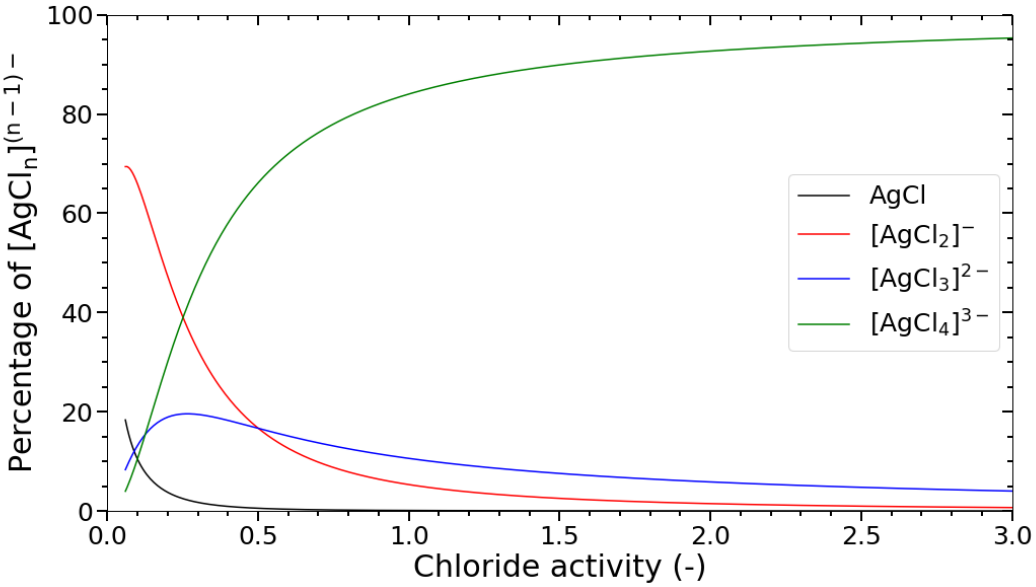

Figure 2.3: The percentage of silver chloride and silver chloride complexes as a function of chloride activity for a solution containing 10^{-3} mol L^{-1} silver ions. Modified from Lampre et al. 2000.[44]

$$[AgCl_2]^-(aq) + Cl^-(aq) \rightleftharpoons [AgCl_3]^{2-}(aq) \tag{2.17}$$

$$[AgCl_3]^{2-}(aq) + Cl^-(aq) \rightleftharpoons [AgCl_4]^{3-}(aq) \tag{2.18}$$

where silver dichloride, silver trichloride, and silver tetrachloride are formed, respectively.[44] Figure 2.3 shows how the percentage of each complex changes as a function of the chloride activity.

2.3.2 Standard electrode potential of complexes

In strong electrolytes and aqueous process solutions, the thermodynamics properties often vary significantly from ideal behavior. These solutions typically contain a lot of different ions in large concentrations, giving a high ionic strength. Because of the high ion concentrations, the complex system of equilibria and the formation of complex ions, constants, and parameters are often not tabulated directly in handbooks. However, many constants can be derived from tabulated values.

E° of an electrode reaction is the potential in a cell where a species A is reduced, hydrogen gas is oxidized, and all activities are one.[45] Many electrode reactions are tabulated versus the hydrogen electrode at standard conditions in, for example, SI Chemical Data and CRC

Handbook of Chemistry and Physics.[43][46] These tables use the hydrogen electrode at standard conditions as the reference. The hydrogen reduction reaction consequently has a defined standard potential of 0 V and is referred to as the standard hydrogen electrode (SHE).[21][47][48] The SHE reaction is:

$$2\mathrm{H}^+(aq) + 2\mathrm{e}^- \rightleftharpoons \mathrm{H}_2(g) \tag{2.19}$$

The reduction of silver ions is described by the following reaction:

$$\mathrm{Ag}^+ + e^- \longrightarrow \mathrm{Ag} \tag{2.20}$$

and has a E° of 0.80 V vs. SHE. However, this reduction potential will change if the solution content is changed from standard conditions. An example is the formation of silver complexes. In a chloride solution, silver chloride complexes can be formed, leading to a change in the standard electrode potential. Tables do not contain standard electrode potentials for silver chloride complexes, but they can, however, be calculated. Silver dichloride, $[\mathrm{AgCl_2}]^-$, is one complex that can be formed in chloride solutions. Reduction of $[\mathrm{AgCl_2}]^-$ can be expressed by the following equation:

$$[\mathrm{AgCl_2}]^- + e^- \longrightarrow \mathrm{Ag} + 2\mathrm{Cl}^- \tag{2.21}$$

The relationship between the standard cell potential and the standard Gibbs free energy of formation is expressed as follows:

$$E^\circ = \frac{-\Delta G^\circ}{nF} \tag{2.22}$$

The standard Gibbs free energy of formation can further be expressed by the equilibrium constant:

$$\Delta G^\circ = -RT \ln K \tag{2.23}$$

The equilibrium constant can be calculated using formation constants and solubility products. For Equation 2.21, the equilibrium constant can be calculated by the cumulative

formation constant for the following equation

$$\mathrm{AgCl}(s) + \mathrm{Cl}^- \longrightarrow [\mathrm{AgCl_2}]^- \tag{2.24}$$

which is tabulated in SI Chemical Data [43] as $\log \beta = -4.50$ and the solubility product constant for the following equation:

$$\mathrm{AgCl}(s) \longrightarrow \mathrm{Ag}^+ + \mathrm{Cl}^- \tag{2.25}$$

which is $K_{sp} = 1.8 \cdot 10^{-10}$.[43] By subtracting Equation 2.25 from Equation 2.24, the formation reaction for silver dichloride from silver ions can be expressed as:

$$\mathrm{Ag}^+ + 2\mathrm{Cl}^- \longrightarrow [\mathrm{AgCl_2}]^- \tag{2.26}$$

The equilibrium constant for the reaction in Equation 2.26 can then be calculated as:

$$K = \beta \cdot \frac{1}{K_{sp}} = 10^{-4.5} \cdot \frac{1}{1.8 \cdot 10^{-10}} = 1.76 \cdot 10^5 \tag{2.27}$$

Further, the equilibrium constant can be used to calculate the standard Gibbs free energy of formation for Equation 2.26:

$$\begin{aligned} \Delta G^\circ = -RT \ln K = -8.314\,\mathrm{J\,K^{-1}\,mol} \cdot 298\,\mathrm{K} \cdot \ln 1.76 \cdot 10^5 \cdot \frac{1\,\mathrm{kJ}}{1000\,\mathrm{J}} \\ = -29.922\,\mathrm{kJ\,mol^{-1}} \approx -30\,\mathrm{kJ\,mol^{-1}} \end{aligned} \tag{2.28}$$

The standard Gibbs free energy of formation for reduction of silver ions (Equation 2.20) can be calculated as follows:

$$\Delta G_1{}^\circ = \Delta G_{\mathrm{Ag}}{}^\circ - \Delta G_{\mathrm{Ag^+}}{}^\circ = 0\,\mathrm{kJ\,mol^{-1}} - 77\,\mathrm{kJ\,mol^{-1}} = -77\,\mathrm{kJ\,mol^{-1}} \tag{2.29}$$

By subtracting the standard Gibbs free energy of formation for Equation 2.26 from the standard Gibbs free energy of formation for Equation 2.20, the standard Gibbs free energy

of formation for Equation 2.21 is found:

$$\Delta G_3{}^\circ = \Delta G_1{}^\circ - \Delta G_2{}^\circ = -77\,\mathrm{kJ\,mol^{-1}} - (-30\,\mathrm{kJ\,mol^{-1}}) = -47\,\mathrm{kJ\,mol^{-1}} \tag{2.30}$$

By using this value, the standard electrode potential for Equation 2.21 can be calculated from Equation 2.22 as:

$$E^\circ = \frac{-(\Delta G_3{}^\circ)}{nF} = \frac{(47\,000\,\mathrm{J\,mol^{-1}})}{1 \cdot 96\,485\,\mathrm{C\,mol^{-1}}} = 0.49\,\mathrm{V\ vs.\ SHE} \tag{2.31}$$

Values for the cumulative formation constant from Seward [49], as seen in Table 2.1, give the same calculated values for the standard cell potential.

The reduction of silver trichloride, $[AgCl_3]^{2-}$, can be expressed as:

$$[AgCl_3]^{2-} + e^- \longrightarrow Ag + 3Cl^- \tag{2.32}$$

and the reduction of silver tetrachloride, $[AgCl_4]^{3-}$, can be expressed as:

$$[AgCl_4]^{3-} + e^- \longrightarrow Ag + 4Cl^- \tag{2.33}$$

The values for the standard cell potential can be seen in the same Table 2.1 for silver dichloride, silver trichloride, and silver tetrachloride.

When silver is reduced from silver ions as in Equation 2.20, the standard cell potential is 0.80 V vs. SHE. This is significantly higher than the standard cell potential when silver is reduced from silver dichloride complexes, as in Equation 2.21.

Table 2.1: Table containing cumulative formation constants from Seward [49] for the formation of silver dichloride, silver trichloride, and silver tetrachloride from silver ions. The values for ΔG° and E° have been calculated from the formation constants at 25°C by cumulative formation constants for 18°C.

Complex	$\log \beta_n$	ΔG° [kJ mol^{-1}]	E° [V]
$[AgCl_2]^-$	5.31	-30.3	0.487
$[AgCl_3]^{2-}$	5.44	-31.0	0.477
$[AgCl_4]^{3-}$	4.19	-23.9	0.549

2.3.3 Chloride concentration effect on the reversible electrode potential of silver

The chloride concentration has a great influence on the reversible electrode potential, E, of silver because of the formation of silver chloride complexes. A simplified reduction reaction for the silver tetrachloride complex can be written as:

$$[AgCl_4]^{3-} + e^- \longrightarrow Ag + 4Cl^- \tag{2.34}$$

In reality, the complex is encircled by water molecules:

$$[AgCl_4 \cdot (H_2O)_x]^{3-} + e^- \longrightarrow Ag + 4Cl^- + xH_2O \tag{2.35}$$

where x is the unknown amount of water in the complex.

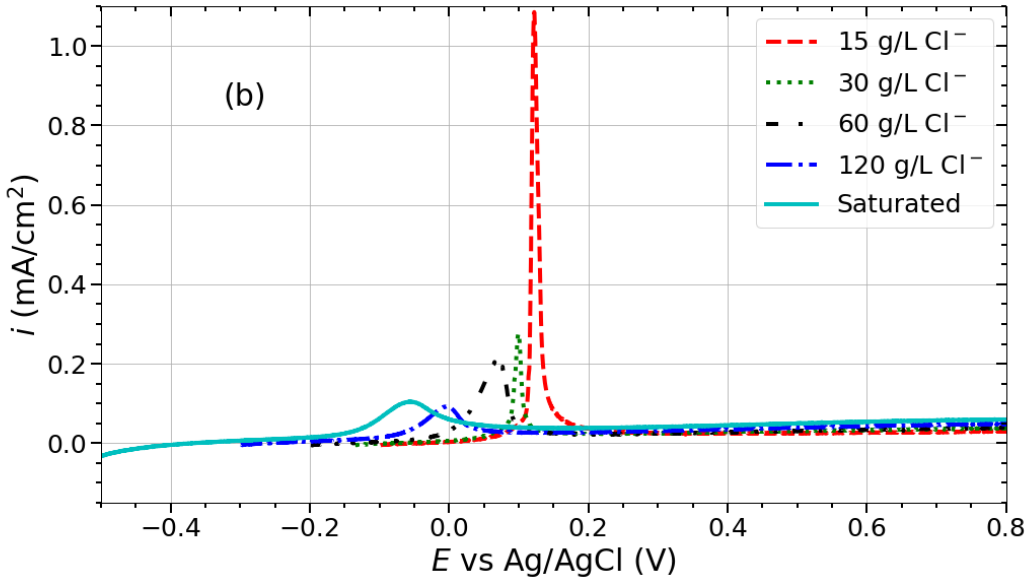

Figure 2.4: Effect of the chloride concentration on the silver peak in stripping voltammetry. The experimental parameters used are as follows: glassy carbon working electrode, 100 mV s^{-1} scan rate, 100 s deposition time, rotation rate of 1600 rpm, and deposition potential between -0.1 and −0.5 V vs. Ag/AgCl. [18]

Figure 2.4 shows how the silver potential shifts towards a lower potential for an increased chloride concentration. This can be seen from the Nernst equation for the reaction in

Equation 2.35:

$$E = E^\circ - \frac{RT}{nF} \cdot \ln \frac{a_{\mathrm{Ag}} \cdot a_{\mathrm{Cl^-}}^4}{a_{[\mathrm{AgCl_4}]^{3-}} \cdot a_{\mathrm{H_2O}}^x} \tag{2.36}$$

where a_{Ag}, $a_{\mathrm{Cl^-}}$, $a_{[\mathrm{AgCl_4}]^{3-}}$, and $a_{\mathrm{H_2O}}$ are the activities of Ag, $\mathrm{Cl^-}$, $[\mathrm{AgCl_4}]^{3-}$ and $\mathrm{H_2O}$, respectively.[21][22][50][25] When the chloride concentration is increased, the activity of chloride will increase, giving a lower reversible electrode potential.

In a solution containing $30\,\mathrm{g\,L^{-1}}$ $\mathrm{Cl^-}$ and $0.1\,\mathrm{mg\,L^{-1}}$ $\mathrm{Ag^+}$, corresponding to $0.85\,\mathrm{mol\,L^{-1}}$ and $9.3 \cdot 10^{-5}\mathrm{mol\,L^{-1}}$ respectively, it is reasonable to estimate that all of the silver ions exist as silver tetrachloride (Figure 2.3). For simplicity, the activities of ions are estimated to be equal to their concentrations and activity of water and silver is set to unity. This is a good simplification in some cases. By using the calculated value for the standard electrode potential from Table 2.1, the reversible electrode potential can be estimated by Equation 2.36:

$$E = E^\circ - \frac{RT}{F} \cdot \ln \frac{a_{\mathrm{Ag}} \cdot a_{\mathrm{Cl}}^4}{a_{[\mathrm{AgCl_4}]^{3-}} \cdot a_{\mathrm{H_2O}}^x} = 0.549\,\mathrm{V} - 0.0256\,\mathrm{V} \cdot \ln \frac{0.85^4}{0.000093}$$
$$= 0.33\,\mathrm{V vs\ SHE} \tag{2.37}$$

This gives a potential of 0.11 V vs. Ag/AgCl.

2.4 Anodic stripping voltammetry (ASV)

Voltammetry is an electrochemical measurement where the current is measured at the WE as a function of the applied potential.[48] A voltammetric measurement gives a graph, called a voltammogram, where the current is plotted versus the applied potential.[51] A potentiostat is often used to control the potential and measure the current produced in experiments. Under the right circumstances, oxidation and reduction reactions occurring on the WE surface can be seen as current peaks in the voltammogram. The concentration of the oxidating or reducing species needs to be large enough, and the WE needs to be of a material where the reaction can occur. The area of the peak is proportional to the concentration of the species. This is used when setting up a voltammetric measurement to measure the amount of a trace metal. By comparing the area of the peak to a calibration, the concentration can be found.[13]

Anodic stripping voltammetry (ASV) is a voltammetric measurement in two steps, often used to measure the content of a trace metal in a solution.[13] In the first step, a trace metal is electrodeposited on the WE surface by applying a predefined potential where the metal is reduced. Electrodepositing is used to concentrate the amount of a trace metal on the electrode. This is done to get a large enough amount of the metal to get a quantifiable current response. The trace metal concentration can then be estimated based on the current signal. The potential applied needs to be low enough for the reduction of the trace metal to happen without reducing other metals that can interfere with the oxidation current. The deposition time is proportional to the amount of trace metal deposited and needs to be chosen depending on the concentration range of the trace metal in the solution.

In the second step, the trace metal is stripped off by increasing the potential in the anodic direction in a certain way and measuring the current. There are several types of ASV, mainly distinguished by the stripping program. Linear sweep voltammetry, differential pulse voltammetry, and square wave voltammetry are the most common and are widely used in industry. [29][30]

2.4.1 Anodic linear sweep voltammetry

Anodic linear sweep voltammetry (ALSV) is a type of ASV where the potential is scanned linearly in the anodic direction, as shown in Figure 2.5. This is the simplest type of ASV and has a lower sensitivity for trace metal detection than others. One of the advantages of ALSV is the possibility to make stops in the scan or scan with different scan rates in different parts of the potential range. This is useful if several metals deposit simultaneously and are oxidized at nearby potentials. By dividing the stripping into several scans, it can become easier to distinguish the current signals from each other. Contaminating metals will then not disturb the current signal used to determine the concentration of the metal of interest.

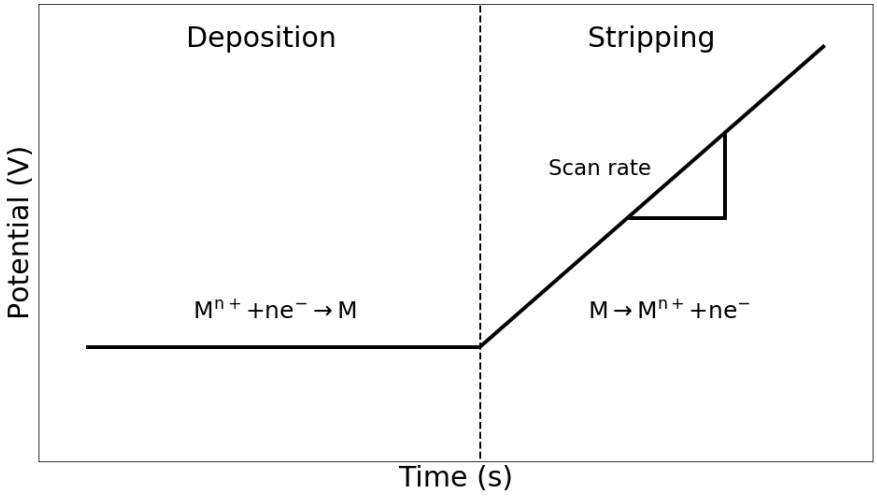

Figure 2.5: Development of electrode potential with time during anodic linear sweep voltammetry. Reprinted from Josefsen [18].

2.4.2 Differential pulse voltammetry

Differential pulse voltammetry (DPV) is a more advanced technique where the background current is taken into account. This method can compensate for background current by applying a potential pulse at regular intervals in the linear sweep voltammetry, as shown in Figure 2.6.

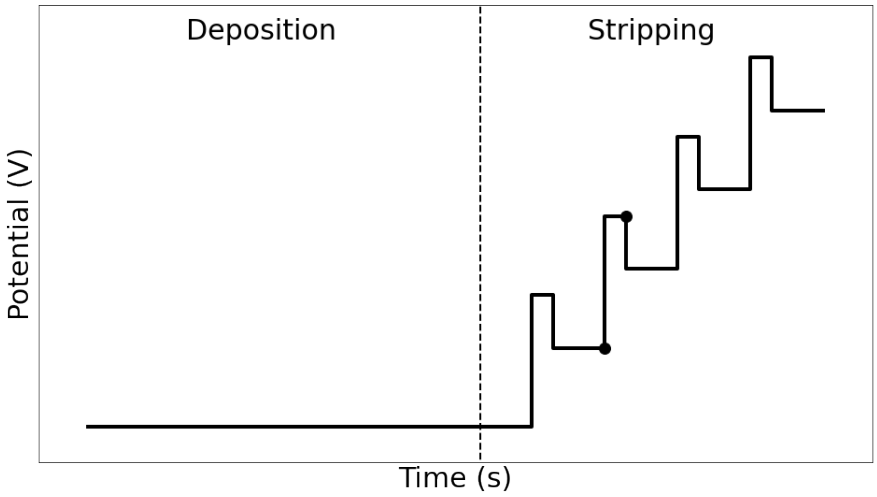

Figure 2.6: The potential versus time figure, showing how potential is applied to the working electrode in differential pulse voltammetry. The two points is where the current is sampled.[29]

The current is sampled before the pulse is applied and at the end of the pulse, seen as the two points in the figure. The difference in current between the two points is plotted against the potential, where the charging currents are reduced compared to linear sweep voltammetry. This gives DPV a better sensitivity compared to ALSV.[29][52]

2.4.3 Square wave voltammetry

Square wave voltammetry (SWV) is one of the most used voltammetric methods, mostly because of its high sensitivity to surface reactions at the electrode. An example potential program is shown in Figure 2.7.

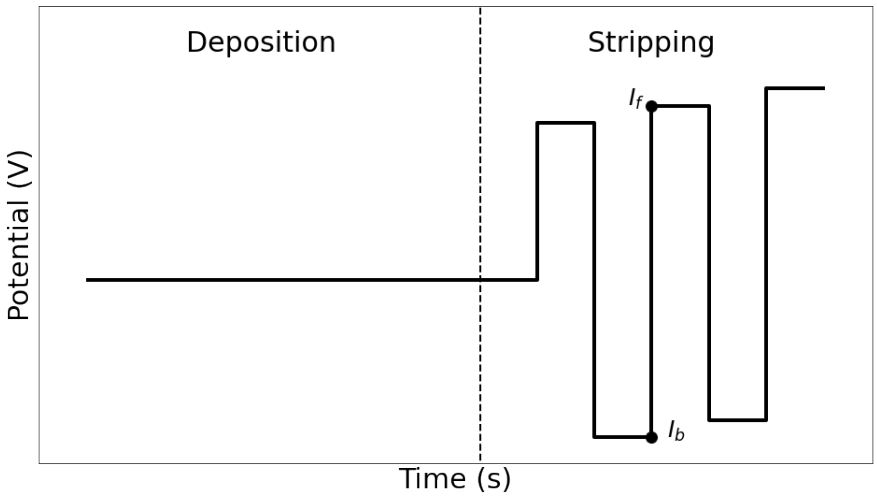

Figure 2.7: Potential program for square wave voltammetry. I_f and I_b are the points where the forward and backward currents are sampled, respectively.[53]

The current is measured at both the minimum and maximum of a pulse. At the minimum, the backward or reverse current is measured, I_b, and at the maximum, the forward current is measured, I_f.[53] This can give valuable information about the reversibility of the reaction and about the electrode structure. The difference between the currents from two consecutive pulses is used as the current response and plotted against the potential. SWV can be used for stripping measurements or directly without a deposition step.[29][52][53]

2.4.4 Calibration

To quantify the content of a detected metal ion, the relationship between the measured current signal and the concentration needs to be found. This might be done by making a calibration curve where known amounts of the metal ion are added and compared to the current signal. By doing this for two or more concentrations, a calibration curve might be made. This gives a relationship between the height of the current peak or the charge and the concentration.[10][54] The measuring points in the calibration curve often show linearity but can also be curved or a mix.[55] The concentration of a solution with an unknown metal ion concentration can then be estimated by comparing the current signal with the calibration curve.

For linear calibration curves, the equation for the line can be found by, for example, least squares regression. The coefficient of determination, R2, tells how good the line fit is. R2 is given as a number between 0 and 1, where a high value indicates a good fit. A value of 0.94 means that 94% of the variation in y can be explained by the variation in x. [55]

2.5 Open circuit potential

Open circuit potential (OCP) is the potential at an open circuit where no external potential is applied. In other words it is the potential between the WE and the surrounding electrolyte versus a reference electrode. This potential is dependent on both the WE material and the electrolyte and will consequently change if materials are deposited on the electrode surface. In a system with a corroding material, OCP is the same as the corrosion potential. The corrosion potential can be used to figure out if corrosion of the WE surface can happen or not.[21][56]

2.5.1 Corrosion rate

The corrosion rate tells how fast a material is corroding in a solution. It can be determined experimentally and is of great use when estimating how often a unit needs to be replaced in a solution. The corrosion rate of a metal in a specific electrolyte can be found by making an Evans diagram for the oxidation and the reduction reaction. An Evans diagram is a diagram of the potential versus the logaritm of the absolute value of the current. Experimentally, this is done by scanning in the anodic direction from a potential

below open circuit potential (OCP) or in the cathodic direction from a potential above OCP. A polarization curve is plotted as the logarithm of the current density versus the potential. The asymptotes to the polarization curve are called the Tafel lines and are the overpotential curves for the reduction and oxidation reactions. The two Tafel lines may be drawn in the voltammogram to find the intersection. The intersection gives the corrosion current density, i_{corr}, and can be used to calculate the corrosion rate by rewriting Faraday's law(Equation 2.8):

$$\frac{\Delta s}{\Delta t} = \frac{M_i i_{corr}}{nF\rho} \tag{2.38}$$

where $\frac{\Delta s}{\Delta t}$ is the corrosion rate in mm/year and ρ is the density of the metal.[50][57]

2.6 Reference electrode

In voltammetric measurements, a reference electrode (RE) is often used to control the potential of the WE continuously. To avoid any overpotential contribution from the RE, the electrode can not be passing a significant current. There are two types of RE: real RE and pseudo-RE. A real RE has a known potential in a separate and well-defined electrolyte and is connected to the system by a diaphragm or a salt bridge. The potential in a real RE is controlled by a reduction and oxidation thermodynamic equilibrium on a metal, giving it a thermodynamically calculable potential. A pseudo-RE is dependent on the electrolyte composition and is often just a metal wire.

There are several different RE, and in some cases, it is preferable to show the potential versus another RE than the one used. This can be done by adding the potential difference between the two RE.[58] Typical real RE used in modern electrochemistry are silver/silver chloride electrode (Ag/AgCl), reversible hydrogen electrode (RHE), and saturated calomel electrode (SCE).[20][22][29]

2.6.1 Pseudo reference electrode

A pseudo-reference electrode (pseudo-RE), also named quasi-reversible electrode, is a metal wire immersed directly into the electrolyte. The metal is not in thermodynamic equilibrium with its oxidized form, which can be soluble or insoluble.[24][59] The pseudo-RE is dependent on the electrolyte and does not have a thermodynamically calculable potential. Therefore, it is necessary to calibrate the pseudo-RE in the specific solution by

using a RE with a known potential. In most cases, the pseudo-RE will not contaminate the electrolyte in a way that affects the measurements. A real RE might contaminate the electrolyte, for example, by leaching chloride.[51] Common pseudo-RE are platinum, gold, silver, copper, and silver/silver chloride wires.[20][29]

2.6.2 Reference electrode stability

A RE with both a good short-term and long-term stability is desired in electrochemical online monitoring. To achieve this, there are many variables to consider. Measurements rely on the RE for precision and accuracy. Therefor, it needs to be chosen with care. A drift of potential less than 10 mV per day is often acceptable.[20] A good RE should have little memory effect from previous experiments and a long operation lifetime in the electrolyte. To avoid disturbances in the measurements, ions from corrosion or leaching of the RE should not contaminate the solution in a way that causes disturbances in the current signal. [60][61]

A temperature coefficient describes how sensitive a RE is to temperature changes. This coefficient says how much the potential changes with temperature and can be determined experimentally by measurements on different temperatures. To ensure minimal potential drift, a RE with a small temperature coefficient in the operating temperature range should be chosen.[60][61]

Real RE are dependent on a stable electrolyte composition in the RE compartment. Over time, even when using a diaphragm or salt bridge, the separate electrolyte will be contaminated, causing a drift of the potential. This causes a need for maintenance that can be comprehensive or expensive.[60][61]

In many cases, a pseudo-RE is very stable over time, even when corroding. It needs little maintenance and can easily be replaced by a new wire if necessary. In some cases, a cheap material as nickel or silver, can be used as PRE, causing very low operating cost. The drawback of PREs is that they do not have a known potential, causing the need for regular calibration.[60][61]

2.7 Scanning electron microscope and energy dispersive spectroscopy

In a scanning electron microscope (SEM), the area to be investigated is irradiated with a thin focused electron beam, which gives rise to several different signals that can be detected, as seen in Figure 2.8. Secondary electrons (SE) are made due to inelastic interactions between the sample and the electron beam and originate from the surface or near the surface, as seen in Figure 2.9. To study the surface morphology of the sample, SE is therefore often used. The resolution depends on the atomic number and the acceleration voltage, where a high atomic number and low acceleration voltage gives the best resolution.[62][63][64]

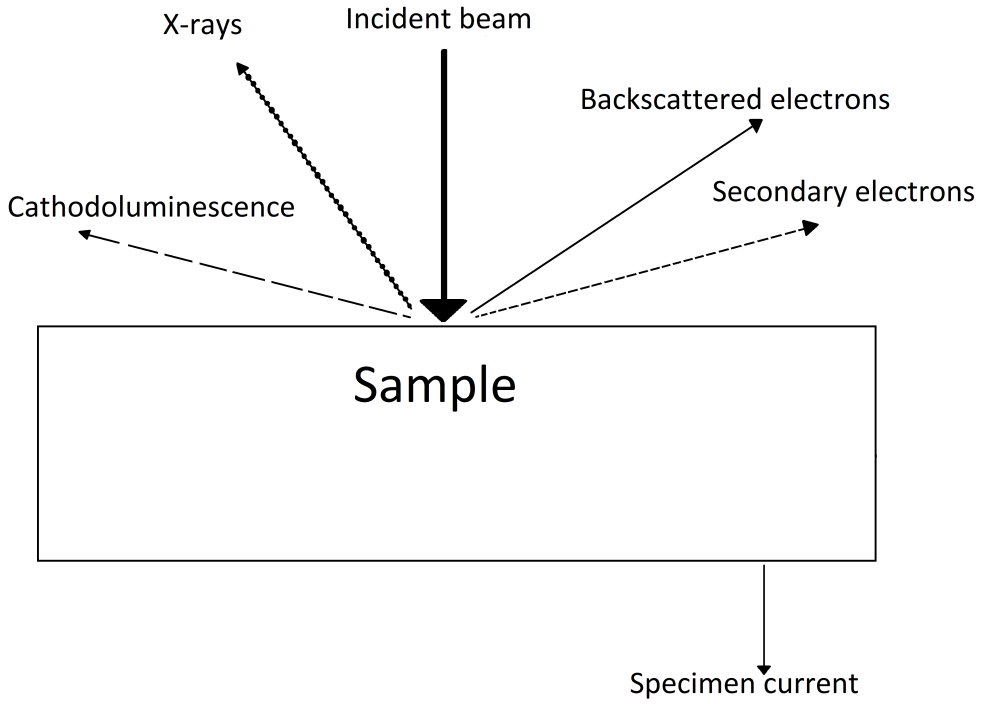

Figure 2.8: Some of the signals that can be used for detection in SEM. Based on illustrations from Beanland [62], Hjelen [63] and Alobad [65].

In energy dispersive spectroscopy (EDS), X-ray signals are analyzed to estimate the chemical composition. As seen in Figure 2.9, the penetration depth of X-rays is quite large compared to that of secondary electrons. Consequently, when studying a thin electrodeposited layer on an electrode material, a relatively large part of the signal will come from the electrode material (substrate). The detection limit and accuracy in EDS is about

1%.[62][63][64]

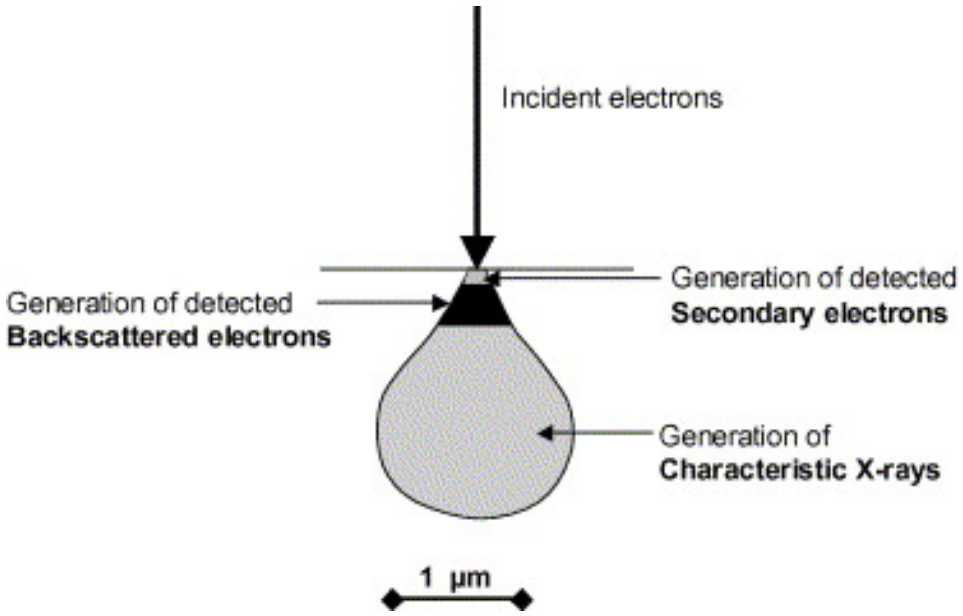

Figure 2.9: The interaction volume where some of the signals may be detected in SEM. The penetration depth for X-ray is deep, while secondary electrons are detected close to the surface. Reprinted from Scrivener [64].

2.7.1 Electrodeposited silver studied with SEM

By using SEM, it has been shown that the morphology of electrodeposited silver on a glassy carbon electrode is largely dependent on the deposition parameters.[66] The particle size of silver increases with an increased deposition potential until a specific upper limit. However, the amount of particles increases with a decreasing deposition potential. The amount of particles is also dependent on the deposition time and increases with an increased deposition time. The size of the particles is, on the other hand, not as influenced by deposition time.

3 Experimental

3.1 Chemicals and apparatus

To conduct the electrochemical measurements, a typical three-electrode electrochemical setup was used, as shown in Figure 3.1. A 150 mL glass cell of conventional design, a rotator, a rotation speed controller, and a potentiostat were used in the setup, in addition to the electrodes. Glassy carbon (GC) with a geometrical surface area of 0.196 cm^2 was used as working electrode (WE). The reference electrode (RE) was either a silver/silver chloride electrode (Ag/AgCl) or a nickel pseudo-RE. Both reference electrodes were mainly used directly in the solution. The Ag/AgCl reference was stated to have a potential of 0.199 V vs. SHE. Graphite was used as the counter electrode (CE). All experiments were performed at room temperature (23 ± 1 °C). All experiments were conducted in a fume hood because of the risk of chlorine gas evolution. To control the potential between the WE and RE and measure the current during the measurements, an Autolab PGSTAT30 potentiostat was used. The data from the electrochemical measurements were managed and analyzed by the potentiostat software Nova.

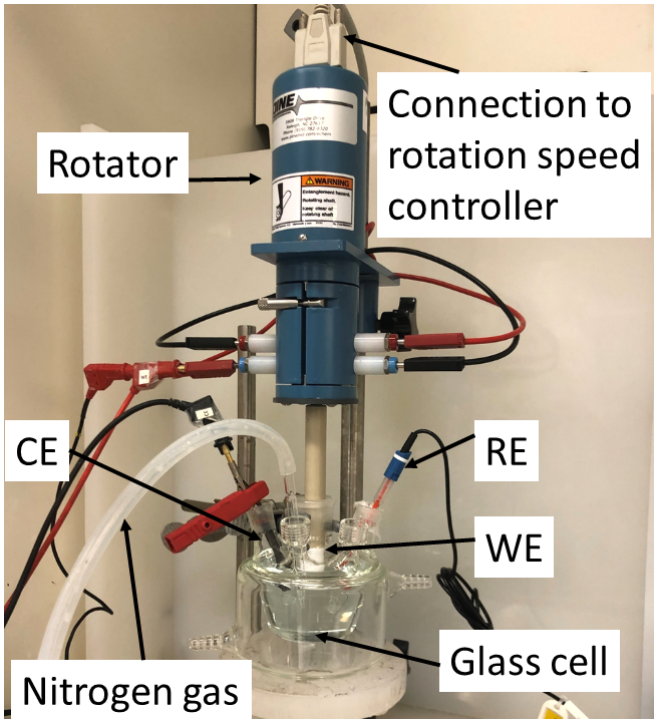

Figure 3.1: Electrochemical setup for measurements with rotating disc electrode.[67]

The surface of the WE with deposits was studied with SEM and EDS (LVSEM, Hitachi S-3400N). When preparing samples for SEM and EDS, the WE was coupled with a titanium

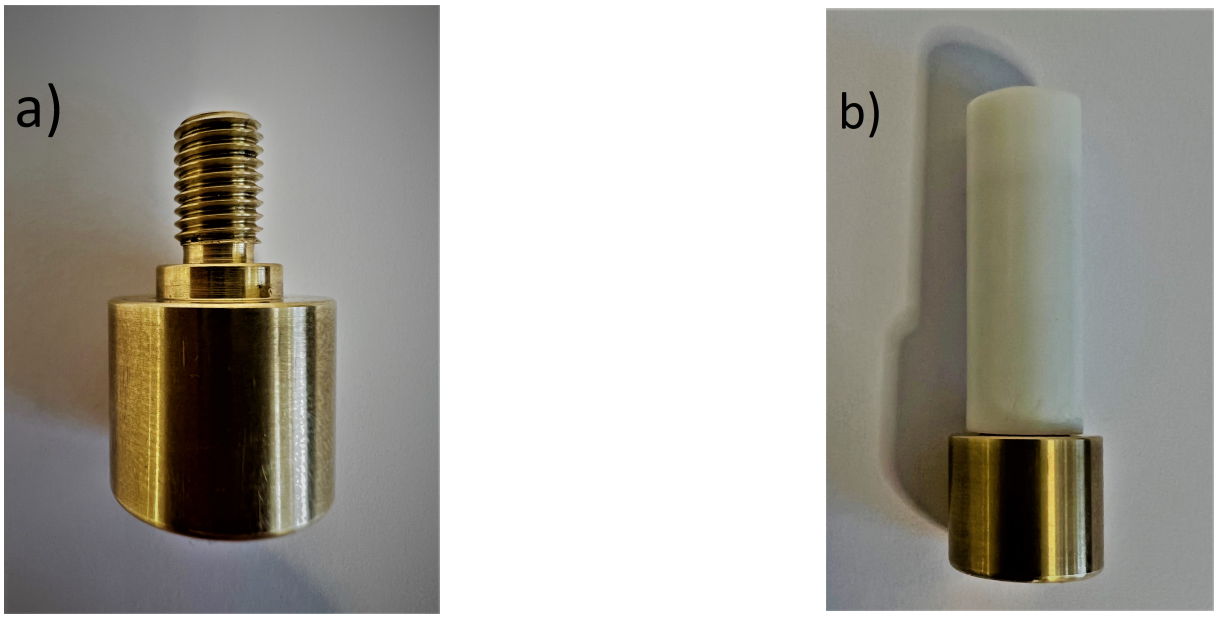

Figure 3.2: Pictures of the electrode holder for use in SEM. The holder can be seen with and without the electrode connected on the left (a) and right image (b), respectively.

wire in a heat shrink tube. The titanium wire stayed in the electrolyte while the WE was removed so that the electrode potential was controlled. Titanium was chosen since it has a very low electrochemical response in the tested electrolytes and potentials. A holder in brass (Figures 3.2 a and b) for rotating disk electrodes was made by the mechanical workshop at NTNU so that the rotating disc electrode could be loaded directly into the SEM. An overview of all equipment used can be found in Table 3.1.

Table 3.1: List of instruments and software used.

Equipment	Manufacturer	Name
Potentiostat/Galvanostat	Metrohm	Autolab PGSTAT30
Rotator	Pine Research	MSR Rotator
Rotation rate control unit	Pine Research	AFMSRCE
Advanced Electrochemical Software	Metrohm	Nova
Pipette	VWR	89079-974 100-1000µL
GC RDE Tip 5.0 mm	Pine Research	AFE3T050GC
Ag/AgCl RE	Radiometer Analytical	REF201 Red Rod RE
Alumina suspension 0.3 µm	Allied high tech	90-187510
Polishing cloth	Buehler	MicroCloth, PSA, 2.875 in
Heat shrink tube	-	-
Electrode holder for SEM	Mechanical workshop NTNU	-
SEM	Hitachi	S-3400N

A list of all used chemicals can be found in Table 3.2. The chemicals, and their amounts, for preparing diluted synthetic process solution is shown in Table 3.3. The chemicals was dissolved by deionized water to make the synthetic solution. The content of the diluted synthetic process solution is shown in Table 3.4. The content of some of the most important elements in the used process solution diluted 1/10 with $0.1\,\mathrm{mol\,L^{-1}}$ sulphuric acid is shown in Table 3.5. The content of the undiluted process solution are shown in Appendix A.

Table 3.2: List of chemicals used.

Chemical name	Formula	Purity	Manufacturer
Sulfuric acid	H_2SO_4	98%	EMD Millipore
Silver nitrate	$AgNO_3$	$\geq$ 99.8%	Sigma-Aldrich
Sodium sulfate	$Na_2\,SO_4$	ACS, ISO	Merck
Nickel(II) chloride hexahydrate	$NiCl_2 \cdot 6H_2O$	$\geq$ 98%	Sigma-Aldrich
Iron(II) sulfate heptahydrate	$FeSO_4 \cdot 7H_2O$	$\geq$ 99.0%	Sigma-Aldrich
Bismuth(III) chloride	$BiCl_3$	$\geq$ 99.0%	Sigma-Aldrich
Manganese(II) sulfate monohydrate	$MnSO_4 \cdot H_2O$	ACS	Merck
Ammonia solution	NH_3	25%	Merck
Deionized water	H_2O	$15.0\,\mathrm{m\Omega\,cm}$	Millipore

Table 3.3: Quantity of chemicals used to prepare synthetic process solution. All values are the weight of the chemical needed to make a 1-liter solution. The chemical formulas are written without the crystal water, but the crystal water has been considered in the weights. The exact chemical formulas can be seen in Table 3.2.

H_2SO_4 $\mathrm{g\,L^{-1}}$	$NiCl_2$ $\mathrm{g\,L^{-1}}$	$FeSO_4$ $\mathrm{g\,L^{-1}}$	$MnSO_4$ $\mathrm{mg^{-1}\,L}$	$BiCl_3$ $\mathrm{mg\,L^{-1}}$
10.2	101	5.97	30.8	11.6

Table 3.4: Content of the 1/10 diluted synthetic process solution without silver ions.

Element	Unit	Concentration
Ni^{2+}	$\mathrm{g\,L^{-1}}$	25
Cl^-	$\mathrm{g\,L^{-1}}$	30
$SO_4{}^{2-}$	$\mathrm{g\,L^{-1}}$	50
Fe^{2+}	$\mathrm{g\,L^{-1}}$	1.2
Bi^{2+}	$\mathrm{mg\,L^{-1}}$	5

A silver nitrate solution was prepared by mixing 118 mg silver nitrate and 500 mL deionized water. 1 mL of this solution gives $1\,\mathrm{mg\,L^{-1}}$ silver ions in 150 mL electrolyte, corre-

Table 3.5: Content of selected elements in the process solution diluted 1/10 with $0.1\,\mathrm{mol\,L^{-1}}$ sulphuric acid.

Element	Unit	Concentration
Ni^{2+}	$\mathrm{g\,L^{-1}}$	24
Cl^{-}	$\mathrm{g\,L^{-1}}$	28
$SO_4{}^{2-}$	$\mathrm{g\,L^{-1}}$	13
Fe^{2+}	$\mathrm{g\,L^{-1}}$	0.9
Bi^{2+}	$\mathrm{mg\,L^{-1}}$	1.0
Ag^{+}	$\mathrm{mg\,L^{-1}}$	0.0

sponding to $10\,\mathrm{mg\,L^{-1}}$ in the concentrated solution. The calculations is shown in Appendix A.

3.2 Procedure

3.2.1 Start-up procedure for electrochemical measurements

Before a new experiment, all equipment in contact with the electrolyte was washed thoroughly with deionized water. In addition, the glass cell was washed with the electrolyte used in the experiment.

When adding a new electrolyte, the solution was purged with nitrogen gas (unless otherwise specified) to remove the oxygen dissolved in the solution. The purging was conducted by lowering a glass pipe connected to nitrogen gas into the solution. After purging the solution with nitrogen for 10 minutes, the bubbling rate was lowered to about one bubble per second, and the pipe was placed just above the solution.

A start-up cyclic voltammetry (CV) was conducted before starting measurements to ensure a clean WE surface giving reproducible results. This was achieved by running a CV measurement between -0.3 and 0.4 V at $100\,\mathrm{mV\,s^{-1}}$ until the voltammogram was stable. The first time a new electrode was used, it was cycled for at least 100 cycles. After that, it was cycled for at least 10 cycles every time the electrolyte was changed.

3.2.2 Examination of electrode surface

To study the deposited materials on the electrode surface, SEM and EDS was used. SEM was used to look at how the materials deposited on the surface, and EDS was used to detect what elements was present on the surface. Chronoamperometry (CA) was

executed for 1000 s at -0.1, -0.2, and -0.3 V vs. Ag/AgCl with a rotation speed of 1600 rpm. This was done in diluted process solutions both with and without 1 mL of the silver nitrate solution. The silver ion content corresponds to a concentration of 10 mg L^{-1} Ag^{+} in the undiluted process solution. When about 30 s of the CA remained, the rotating disc electrode was raised from the electrolyte and washed with deionized water without touching the electrode. An auxiliary Ti-wire remained in the electrolyte to maintain potential control, as described in section 3.1. The rotation was kept turned on afterward to dry the electrode. When the electrode was dry, the surface was studied with SEM and EDS.

3.2.3 Open circuit potential measurements after chronoamperometry

Open circuit potential (OCP) measurements after CA at -0.2 V vs. Ag/AgCl were executed for different deposition times. CA with deposition times of 100, 1000, and 10 000 s was performed, followed by OCP measurements for 60, 200, and 1000 seconds, respectively. This was done in a diluted process solution, added 1 mL of the silver nitrate solution.

3.2.4 Silver detection in synthetic process solution vs. real process solution by anodic linear sweep voltammetry

To compare silver detection in a synthetic process solution to a real process solution, anodic linear sweep voltammetry (ALSV) was used. The synthetic solution contained chloride, nickel, iron, manganese, and bismuth ions corresponding to 10% of the content in the real process solution according to Table 3.5. The diluted real process solution used contained untraceable amounts of silver ions. Therefore, 1 mL of the silver nitrate solution was added to both solutions. ALSV was executed with parameters given in Table 3.6, both with and without silver ions in the solution for both electrolytes.

3.2.5 Differential pulse measurements

Differential pulse voltammetry (DPV) measurements were performed by altering different parameters, seen in Table 3.7. This was executed in diluted process solutions with 1 mL of the silver nitrate solution.

Table 3.6: List of settings used for ALSV in synthetic and real process solutions.

Parameter	Values
Deposition potential	-0.30, -0.20, -0.10 V vs. Ag/AgCl
Deposition time	100 s
Scan rate	50 mV s^{-1}
Rotation speed	1600 rpm

Table 3.7: List of settings used for DPV measurements in process solutions. The values for the parameters that were kept constant while one and one parameter was changed are highlighted.

Parameter	Values
Deposition potential	**-0.30** , -0.20, -0.10 V vs. Ag/AgCl
Deposition time	**100**, 250 s
Modulation amplitude	0.01, 0.02, **0.05**, 0.1 V
Modulation time	0.005,**0.01**, 0.05, 0.1 V
End potential	0.4 V vs. Ag/AgCl
Rotation speed	1600 rpm

3.2.6 Divided stripping by ALSV

Stripping in two sweeps was tested to try to distinguish the signal from silver and bismuth from each other. This was done by CA for deposition, followed by a slow scan (ALSV) until an intermediate potential of 0.0 V vs. Ag/AgCl, where a faster scan was started, as seen in Figure 3.3. The parameters used are shown in Table 3.8. These measurement were executed in diluted process solutions with 1 mL of the silver nitrate solution.

The reproducibility of ALSV with divided stripping was tested by using the same parameters (Table 3.8) and repeating the measurement 13 consecutive times.

To check the effect of potential drift, divided ALSV was also tested for displacement of the potential. Both the deposition potential and the intermediate potential were changed by 0.2 and 0.5 V in both positive and negative directions compared to Table 3.8.

3.2.7 Divided stripping by differential pulse voltammetry

Divided stripping in three sweeps was tested to distinguish the silver and bismuth peaks from each other. This was done by CA for deposition, followed by three sweeps with different modulation times and amplitudes, as seen in Figure 3.4. The parameters used

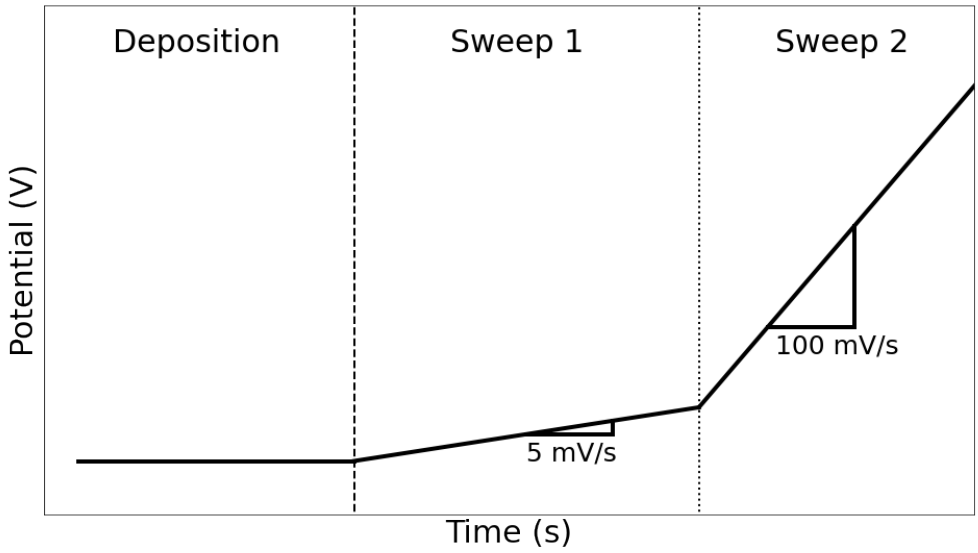

Figure 3.3: Model of how the divided stripping is constructed for ALSV. After deposition, a slow scan ($5\,\mathrm{mV\,s^{-1}}$) is used until a potential of 0.0 V vs. Ag/AgCl. The scan rate is then changed to a fast scan rate ($100\,\mathrm{mV\,s^{-1}}$).

Table 3.8: List of settings used for divided stripping by ALSV in a diluted process solutions.

Parameter	Values
Deposition potential	−0.3 V vs. Ag/AgCl
Deposition time	500 s
Scan rate 1	$5\,\mathrm{mV\,s^{-1}}$
Intermediate potential	0.0 V vs. Ag/AgCl
Scan rate 2	$100\,\mathrm{mV\,s^{-1}}$
End potential	0.4 V vs. Ag/AgCl
Time at OCP before new deposition	500 s
Rotation speed	1600 rpm

are shown in Table 3.9. These measurement was executed in diluted process solutions with 1 mL of the silver nitrate solution.

The reproducibility of DPV with three-part stripping was tested by using the same parameters (Table 3.9) and repeating the measurement 13 consecutive times.

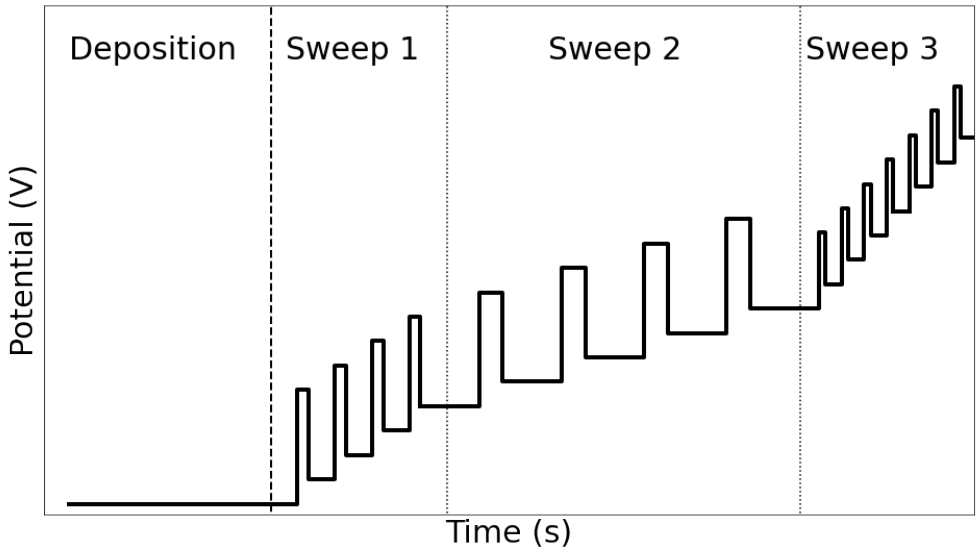

Figure 3.4: Model of how the divided stripping is constructed for DPV. The stripping is built up by three different stripping sweeps, as seen in Table 3.9.

Table 3.9: List of settings used for divided stripping by DPV in a diluted process solution.

Parameter	Values
Deposition potential	−0.3 V vs. Ag/AgCl
Deposition time	500 s
Modulation amplitude 1	0.15 V
Modulation time 1	0.05 s
Intermediate potential 1	−0.15 V vs. Ag/AgCl
Modulation amplitude 2	0.15 V
Modulation time 2	0.5 s
Intermediate potential 2	−0.12 V vs. Ag/AgCl
Modulation amplitude 3	0.10 V
Modulation time 3	0.01 s
End potential	0.4 V vs. Ag/AgCl
Time at OCP before new deposition	500 s
Rotation speed	1600 rpm

3.2.8 Calibration curve for silver detection by divided stripping

Calibration curves were made by divided stripping with ALSV for different silver ion concentrations. A diluted process solution was used, added 0, 0.05, 0.1, 0.2, 0.5 and 1 mL of the silver nitrate solution. An ALSV measurement with divided stripping was executed with the parameters seen in Table 3.8. The peak height and charge were used to make the calibration curve. A trend line was made for the measuring points that showed linearity.

3.2.9 Nickel reference electrode

An OCP measurement between the pseudo-RE and a common RE was executed to check the possibility of using a pseudo reference electrode. A Ag/AgCl reference electrode submerged into a saturated KCl was connected by a salt bridge to a diluted process solution with a nickel wire as a pseudo-RE. The salt bridge was prepared with KCl and Agar-gel. Before use, the salt bridge was washed first in deionized water three times and then three times with diluted process solution. The salt bridge was then placed into the process solution, and some solution was sucked into the pipe to make a connection between the two solutions. An OCP measurement was performed for 21 days to check the stability over time.

The corrosion rate of Ni-wire was measured by starting at $-0.55\,\mathrm{V}$ vs. a nickel pseudo-RE and scanning once in the anodic direction and once in the cathodic direction using the settings in Table 3.10. Nickel wires were used as WE, RE, and CE and placed in the same beaker. The solution was not bubbled with nitrogen gas. This is because it was supposed to simulate corrosion in a real diluted process solution.

Table 3.10: List of settings used to make an Evens diagram to find the corrosion rate.

Parameter	Values
Scan rate	$0.5\,\mathrm{mV\,s^{-1}}$
Lower potential	$-0.55\,\mathrm{V}$ vs. Ni pseudo-RE
Upper potential	$0.3\,\mathrm{V}$ vs. Ni pseudo-RE
Rotation speed	1600 rpm

ALSV was performed by the settings seen in Table 3.11. This was executed in diluted process solutions with 1 mL of the silver nitrate solution.

Table 3.11: List of settings used for ALSV in diluted process solutions with a nickel pseudo-RE.

Parameter	Values
Deposition potential	$-0.218\,\mathrm{V}$ vs. Ni pseudo-RE
Deposition time	$100\,\mathrm{s}$
Scan rate	$100\,\mathrm{mV\,s^{-1}}$
Rotation speed	1600 rpm

Stripping in two sweeps was tested for a nickel pseudo-RE. This was executed as for the Ag/AgCl RE, but by the settings shown in Table 3.12. The potential values are the only

settings that were changed from the measurements by a Ag/AgCl. These measurement was executed in diluted process solutions with 1 mL of the silver nitrate solution.

The reproducibility of ALSV with a nickel pseudo-RE with two part stripping was tested by using the parameters in Table 3.12 and repeating the measurement 13 consecutive times.

Table 3.12: List of settings used for divided stripping by ALSV in a diluted process solutions by a nickel pseudo-RE.

Parameter	Values
Deposition potential	$-0.218\,\mathrm{V}$ vs. Ni pseudo-RE
Deposition time	500 s
Scan rate 1	$5\,\mathrm{mV\,s^{-1}}$
Intermediate potential	0.082 V vs. Ni pseudo-RE
Scan rate 2	$100\,\mathrm{mV\,s^{-1}}$
End potential	0.482 V vs. Ni pseudo-RE
Time at OCP before new deposition	500 s
Rotation speed	1600 rpm

4 Results

The results from the study of the electrodeposition at different potentials and solutions are shown first in the results. Here, images from scanning electron microscope (SEM) and a table of chemical content from energy dispersive spectroscopy (EDS) of the electrodeposited material are presented. Further, voltammograms from different types of anodic stripping voltammetry are presented. In addition, voltammograms for methods for separation of current peaks are presented, as well as calibration curves and measurements for a nickel pseudo reference.

4.1 Stability, morphology, and composition of electrodeposited material

4.1.1 Electrodeposition by chronoamperometry

A plot of the current as a function of time can be seen in Figure 4.1 for deposition at different potentials in a diluted process solution, both with and without silver ions added.

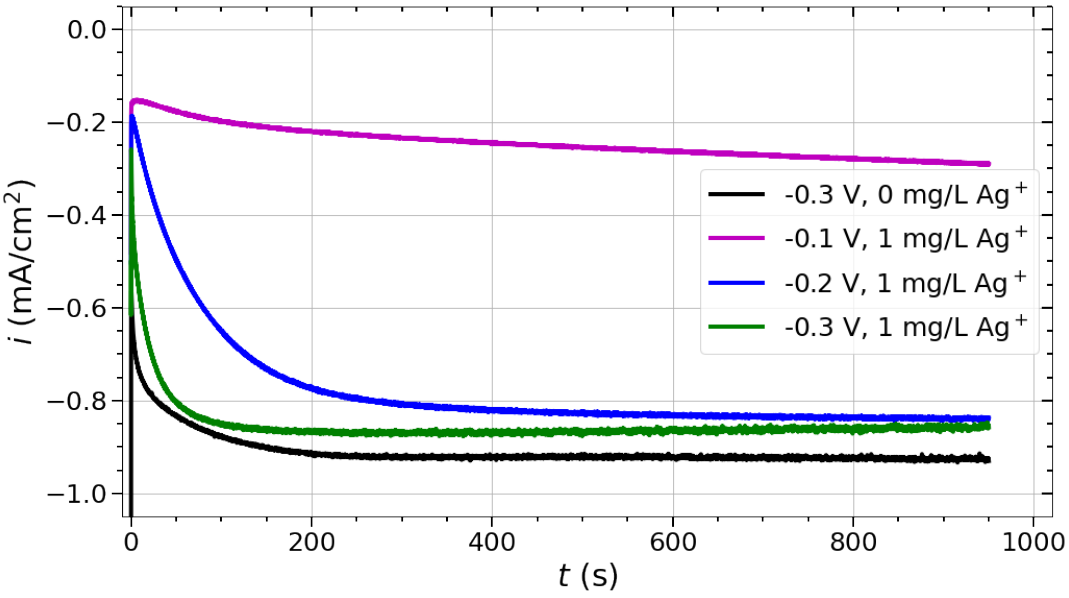

Figure 4.1: Plot of the current as a function of time during chronoamperometry at -0.1, -0.2, and −0.3 V vs. Ag/AgCl for solutions containing silver ions and −0.3 V vs. Ag/AgCl for solutions without silver ions (1 mg L^{-1}). The graphs were obtained by 1000 s deposition and rotation rate of 1600 rpm. The graphs stops at 950 s because this was when the electrode was removed from the solution.

For lower deposition potentials, the current reaches a more negative value. The current signal from chronoamperometry (CA) in the solution without silver ions shows curve with a slightly lower current and a different shape than for the solution containing silver ions.

Fitting the current signals from electrodeposition to plots with instantaneous and progressive nucleation was tested but is not shown.

4.1.2 SEM and EDS of the electrode surface

The surface of a clean glassy carbon (GC) electrode is dark, smooth, and has no deposited material (Figure 4.2 a). The EDS measurement confirms that there is no material of importance present on the surface (Table 4.1).

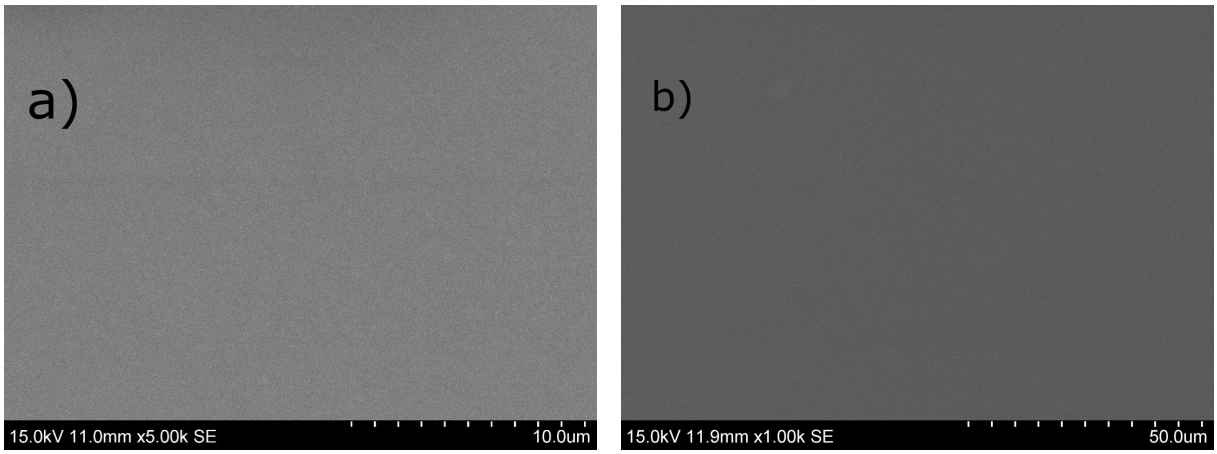

Figure 4.2: SEM image of a clean GC electrode (a) and the same electrode after electrodepositing at −0.3 V vs. Ag/AgCl for 1000 s in a diluted process solution without silver ions (b).

In experiments where the electrode was left for a short while in the solution at OCP before removal, the surface was either without any deposit or had some residual silver and chloride present, as shown in Appendix D. The potential, therefore, has to be controlled when the electrode is removed from the surface after deposition. A SEM image of the surface of a GC electrode after 1000 s deposition at −0.3 V vs. Ag/AgCl in a diluted process solution is shown in Figure 4.2 b. The surface looks like a clean electrode seen in Figure 4.2 a. There is no visible nucleation on the surface. However, the EDS measurement shows bismuth present at the surface (Table 4.1). Images from deposition at −0.1 and −0.2 V vs. Ag/AgCl in a diluted process solution are shown in Appendix D.

Table 4.1: EDS analysis of the GC electrode after electrodeposition with different combinations of deposition conditions. Carbon was excluded in EDS to get larger quantities of the more interesting elements. The remaining percentages are due to silicon which is not relevant for the results, or other elements with such a low percentage that they are not confirmed. The complete list of the content is seen in the EDS spectra in Appendix D. The row marked with $*$ is a clean GC electrode before deposition.

Deposition conditions		**Concentration**		
Ag^+ concentration $[mg\,L^{-1}]$	Deposition potential [V vs. Ag/AgCl]	O At %	Ag At %	Bi At %
0^*	-	100	0	0
0	-0.1	100	0	0
0	-0.2	93	0	7.3
0	-0.3	86	0	12
1	-0.1	91	6.3	0
1	-0.2	89	7.9	1.4
1	-0.3	83	12	2.1
1	-0.2 & 0.0	87	10	0

Figures 4.3 a-d shows SEM pictures of the GC surface after deposition for 1000 s at different deposition potentials in a diluted process solution with added silver ions corresponding to $1\,mg\,L^{-1}$ in the diluted solution ($10\,mg\,L^{-1}$ in the undiluted solution).

The GC surface after deposition at $-0.1\,V$ vs. Ag/AgCl shows some nucleation randomly distributed with different nuclei sizes (Figure 4.3 a). The nuclei look relatively spherical and homogeneous. The EDS measurement shows that silver has been deposited at the electrode surface (Table 4.1).

Figure 4.3 b shows the GC surface after deposition at $-0.2\,V$ vs. Ag/AgCl. The surface has more nuclei than after deposition for $-0.1\,V$ vs. Ag/AgCl. The nuclei size appears to be smaller than for deposition at $-0.1\,V$ vs. Ag/AgCl. The shape of the nuclei looks irregular because they are built up of several smaller nuclei. The EDS shows that both silver and bismuth are present at the electrode surface.

Figure 4.3 d shows the GC surface after deposition at $-0.2\,V$ vs. Ag/AgCl and subsequently bismuth stripping for 1000 s at $0.0\,V$ vs. Ag/AgCl. The surface looks like Figure 4.3 b, with small nuclei in collections. The difference in contrast between Figures 4.3 b and d is the main reason for the visual apparent difference between them. The EDS measurement shows that bismuth has been removed, but silver still is deposited at the electrode surface.

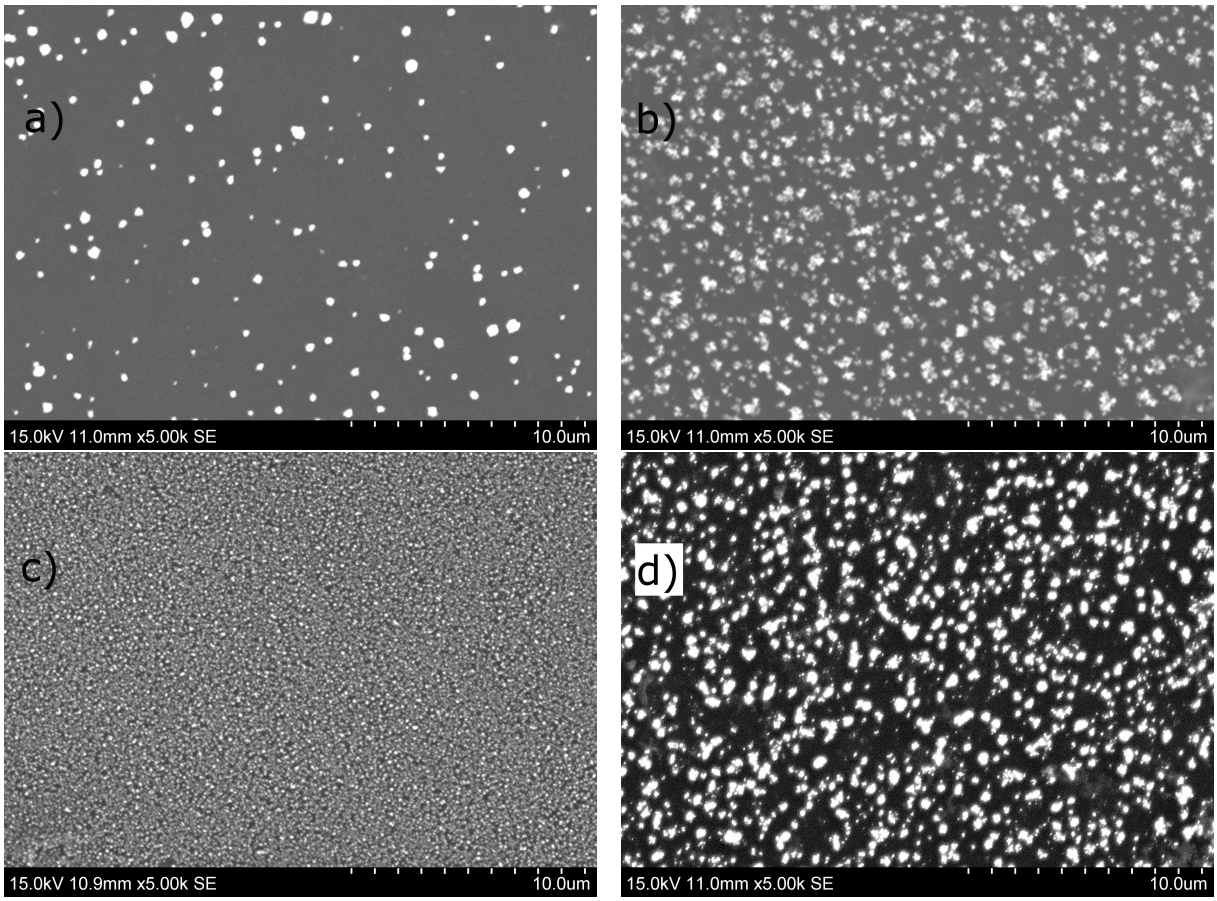

Figure 4.3: SEM image of a GC electrode after electrodepositing for 1000 s at a) −0.1 V vs. Ag/AgCl, b) −0.2 V vs. Ag/AgCl, and c)−0.3 V vs. Ag/AgCl in a diluted process solution with silver ions. Figure d) shows the SEM image of the electrode in b) after 1000 s bismuth stripping at 0.0 V vs. Ag/AgCl.

Figure 4.3 c shows the GC surface after deposition at −0.3 V vs. Ag/AgCl. The surface has tiny nuclei very close to each other. Due to the small nucleus size, it is not easy to see details in the nucleation. EDS shows that both silver and bismuth are present at the electrode surface. A trend of decreasing nucleus size for decreasing deposition potential is visible in Figures 4.3 a, b, and d.

4.1.3 Open circuit potential after electrodeposition

Open circuit potential (OCP) measurements after deposition at −0.2 V vs. Ag/AgCl for 100, 1000, and 10 000 s are shown in Figures 4.4 a-c, respectively. All three figures show two intermediate potential plateaus before reaching a stable OCP value of about 0.4 V vs. Ag/AgCl. The first potential plateau is between -0.02 and −0.06 V vs. Ag/AgCl, and the second potential plateau is at about 0.05-0.07 V vs. Ag/AgCl. The length of each

plateau increases with increasing deposition potential. The second plateau seems to be approximately three times as long as the first plateau.

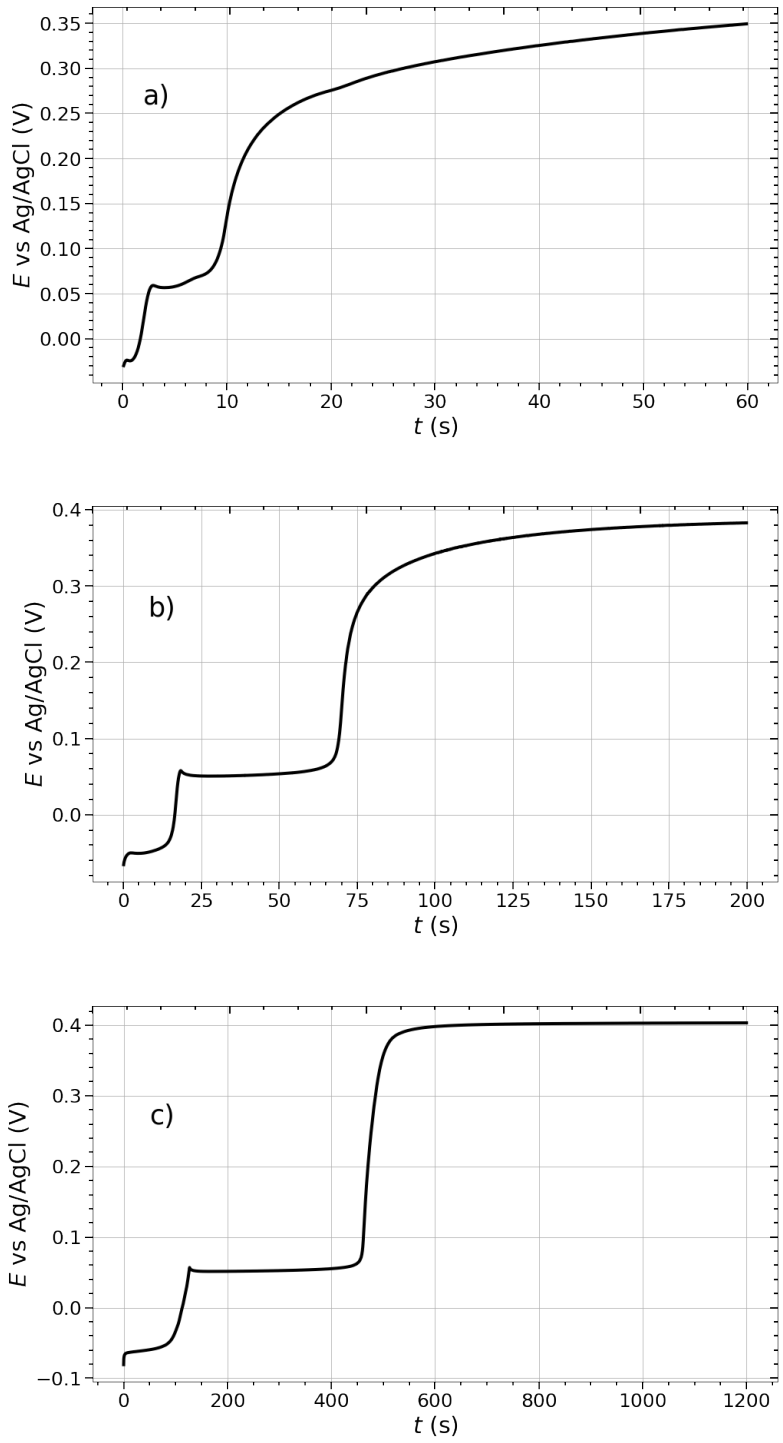

Figure 4.4: Plot of the potential as a function of time for an OCP measurement after deposition at −0.3 V vs. Ag/AgCl for a) 100 s, b) 1000 s, and c) 10 000 s. Rotation rate of 1600 rpm. The electrolyte used was a 1/10 diluted process solution, added silver ions ($1\,\mathrm{mg\,L^{-1}}$).

4.2 Anodic stripping voltammetry

4.2.1 Anodic linear sweep voltammetry in synthetic and process solution

Anodic linear sweep voltammetry (ALSV) of the 1/10 diluted process solution with and without silver ions is shown in Figure 4.5 for a deposition potential of −0.3 V vs. Ag/AgCl. The voltammogram obtained in process solution without added silver ions shows one clear peak at about −0.06 V vs. Ag/AgCl When silver ions are added to the process solution, two peaks can be observed, one at about 0.0 V vs. Ag/AgCl and one at about 0.08 V vs. Ag/AgCl. The two peaks do not overlap but have a relatively small potential gap between each other (about 0.03 V). Adding ammonium buffer to a diluted synthetic process solution was tested and can be seen in Appendix C.

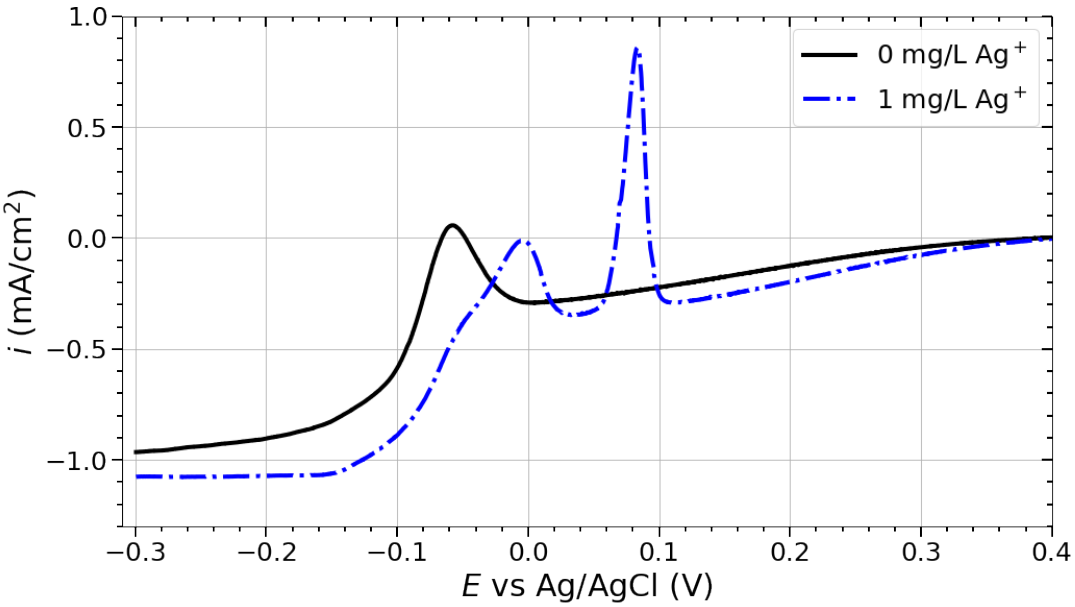

Figure 4.5: Voltammograms of a 1/10 diluted process solution with and without 1 mg L^{-1} added Ag^+-ions (corresponding to 10 mg L^{-1} in the undiluted solution). The voltammograms were obtained at 50 mV s^{-1} after 100 s deposition at −0.3 V vs. Ag/AgCl. Rotation rate 1600 rpm.

A comparison of ALSV in a diluted synthetic process solution and a diluted real process solution is shown in Figures 4.6 a and b for deposition potential of −0.1 V vs. Ag/AgCl and −0.2 V vs. Ag/AgCl, respectively. Voltammograms both with and without added silver ions are shown for both solutions.

From Figure 4.6 a, a current peak at 0.09 V vs. Ag/AgCl is observed in the voltammogram

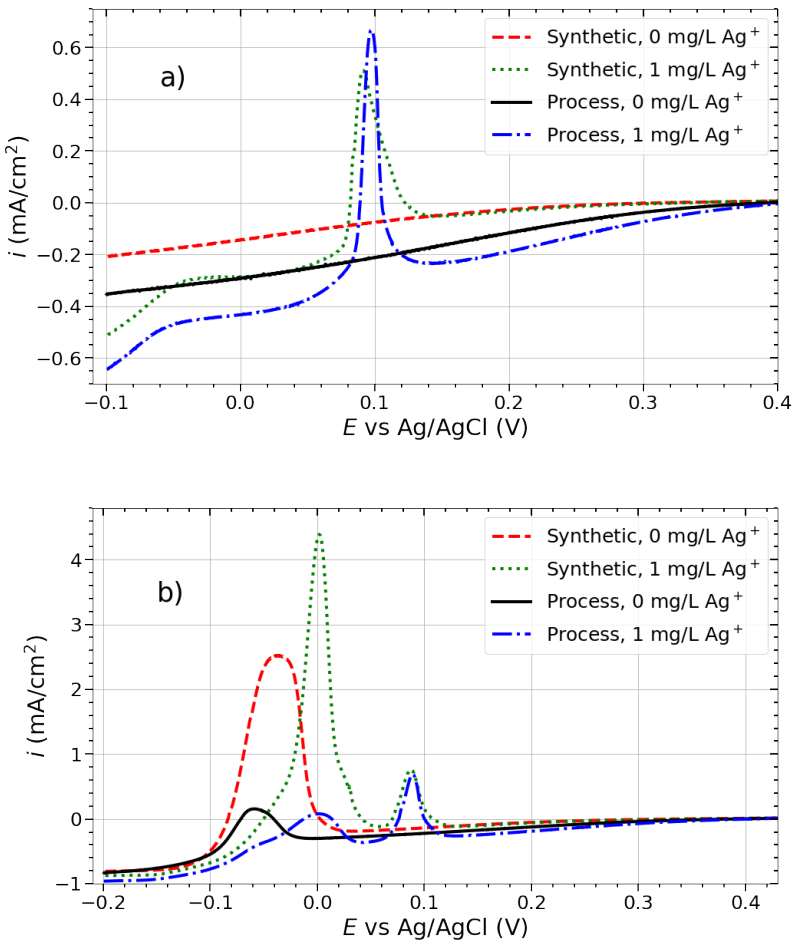

Figure 4.6: Voltammograms of ALSV in both synthetic and diluted process solution with ($1\,\mathrm{mg\,L^{-1}}$) and without Ag^+, deposited for 100 s at a) $-0.1\,\mathrm{V}$ vs. Ag/AgCl and b) $-0.2\,\mathrm{V}$ vs. Ag/AgCl. The voltammograms were obtained at $50\,\mathrm{mV\,s^{-1}}$ with a rotation rate of 1600 rpm.

for the synthetic solution with added silver ions. The voltammogram for the process solution with added silver ions shows a peak at 0.1 V vs. Ag/AgCl. Both solutions without silver ions give voltammograms without distinct features.

Both voltammograms in Figure 4.6 b containing silver ions show peaks at 0.0 V vs. Ag/AgCl and 0.09 V vs. Ag/AgCl. The first peak is much larger for the synthetic solution than for the process solution. On the other hand, the second peak has about the same size, shape, and height for both solutions. The second peak corresponds well with the peak seen in Figure 4.6 a. The solutions without silver ions show one peak at -0.06 and $-0.04\,\mathrm{V}$ vs. Ag/AgCl for the process and synthetic solution, respectively. The peak for the synthetic solution is considerably larger than for the process solution.

4.2.2 Differential pulse voltammetry in process solution

Figures 4.7 a-d show how the stripping peaks change when varying the experimental parameters in differential pulse voltammetry (DPV). The figures show voltammograms from diluted process solution with added silver ions, with varying deposition potential, deposition time, modulation amplitude, and modulation time.

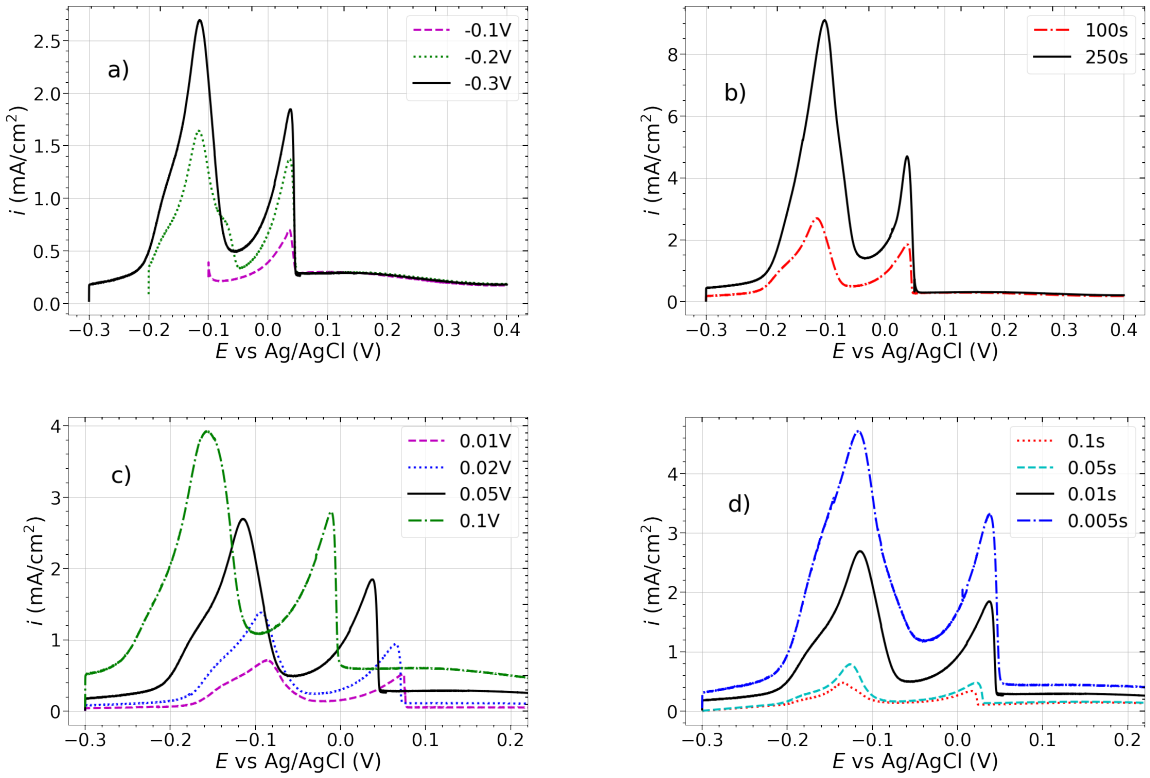

Figure 4.7: Voltammograms showing the effect of changing: a) deposition potential, b) deposition time, c) modulation amplitude, and d) modulation time in DPV on a GC electrode in a diluted process solution with added silver ions ($1\,\mathrm{mg\,L^{-1}}$). The set parameters were modulation amplitude of 0.05 V and modulation time of 0.01 s after 100 s deposition at −0.3 V vs. Ag/AgCl. Rotation rate 1600 rpm.

The effect of changing the deposition potential can be observed in Figure 4.7 a. A peak is observed at 0.04 V vs. Ag/AgCl for all three voltammograms. For deposition potential of −0.3 and −0.2 V vs. Ag/AgCl, an additional peak is observed at −0.11 V vs. Ag/AgCl. Both the peak height and width increase with a decreasing deposition potential, while the positions of the peaks are not affected by the deposition potential.

Figure 4.7 b shows the effect of deposition time on the voltammograms obtained from DPV of a diluted process solution. Two peaks can be observed with the same potential

positions as seen in Figure 4.7 a. The size of the peaks increases with an increasing deposition time, while the position of the peaks is unaffected.

The effect of the modulation amplitude on the voltammograms can be observed in Figure 4.7 c. The two peaks, corresponding to the ones observed in the previous figures, increase in size with an increased modulation amplitude. In addition, the peaks shift in the negative direction with an increasing modulation amplitude. The shift seems to correspond well with the increase in modulation amplitude. An increase from 0.05 to 0.1 V in modulation amplitude will move the peaks 0.05 V in negative direction.

Figure 4.7 d shows the effect of the modulation time on the voltammograms. The two peaks observed in all four voltammograms seem to correspond well with the peaks observed in the previous figures. The peak size is increased with a decreasing modulation time. The separation of the peaks is consequently decreasing with a decreasing modulation time.

A comparison between ALSV and DPV is shown in Figure 4.8. The plot of DPV has a clear baseline at 0.2-0.3 mA cm^{-2}. ALSV does not have a clear baseline but starts

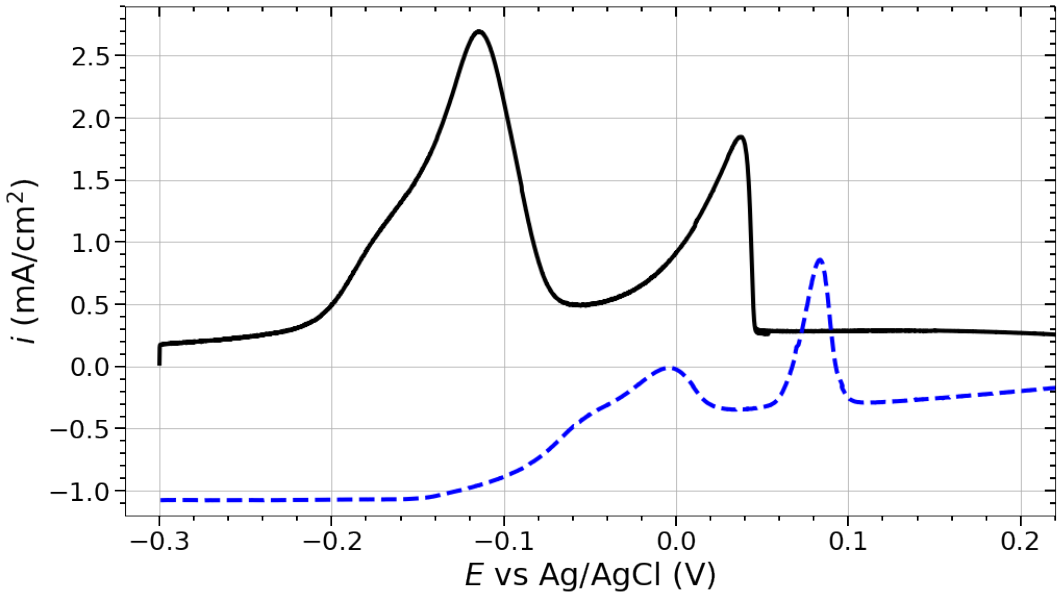

Figure 4.8: Voltammogram from DPV (black, solid curve) and ALSV (blue, dashed curve) after 100 s deposition at −0.3 V vs. Ag/AgCl in a diluted process solution with added silver ions (1 mg L^{-1})). Modulation amplitude of 0.05 V and modulation time of 0.01 s were used for the DPV. The ALSV voltammogram was obtained at 100 mV s^{-1}. Rotation rate of 1600 rpm.

at $-1.1\,\mathrm{mA\,cm^{-2}}$ and ends at $-0.2\,\mathrm{mA\,cm^{-2}}$. The two peaks seen in the voltammogram for DPV are larger than the peaks seen in the voltammogram for ALSV.

4.3 Divided stripping and reproducibility

4.3.1 Linear divided stripping for silver/silver chloride reference electrode

The voltammogram from anodic stripping with two individual sweeps after 500 s deposition is shown in Figure 4.9. The procedure takes about 1180 s and can measure the content about three times each hour. From the first stripping sweep, a very small peak is observed at about $-0.03\,\mathrm{V}$. The second stripping sweep has a notably larger peak at $0.11\,\mathrm{V}$. The two peaks seem to fit with the peaks observed in Figure 4.5. There is good separation of the two peaks with this method.

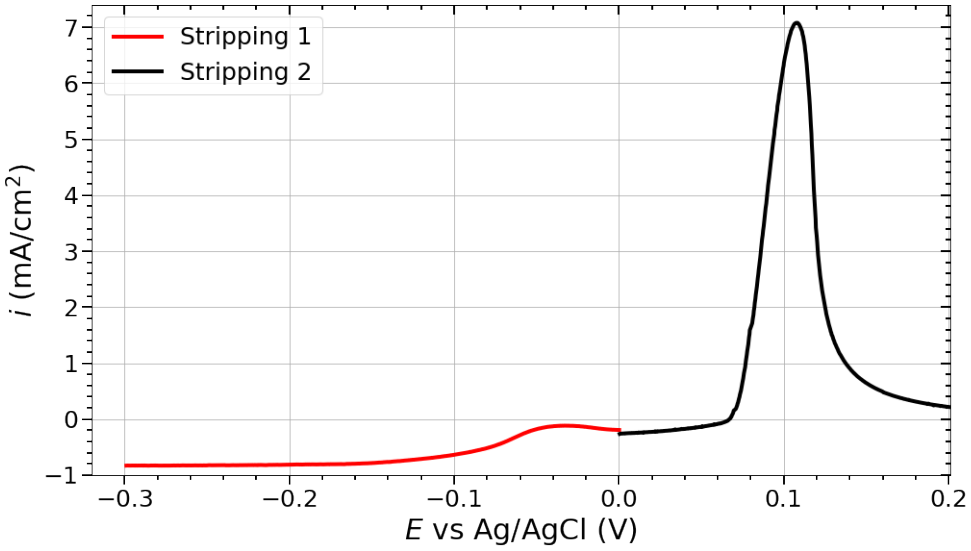

Figure 4.9: Voltammograms of ALSV where the stripping is divided into one slow and one fast scan. The first and second scans were obtained at 5 and $100\,\mathrm{mV\,s^{-1}}$, respectively. The voltammograms were obtained in 1/10 diluted process solution with $1\,\mathrm{mg\,L^{-1}}$ added Ag^{+}-ions after 500 s deposition at $-0.3\,\mathrm{V}$ vs. Ag/AgCl. Rotation rate 1600 rpm.

Figure 4.10 shows the second stripping sweep, as seen in Figure 4.9, from some selected of the repeated measurements. The charge and peak height of the peak at $0.11\,\mathrm{V}$ in all 13 measurements are plotted in Figure 4.11. A trend where the charge and peak height change in the same way over time is seen in the figure. The value of two standard

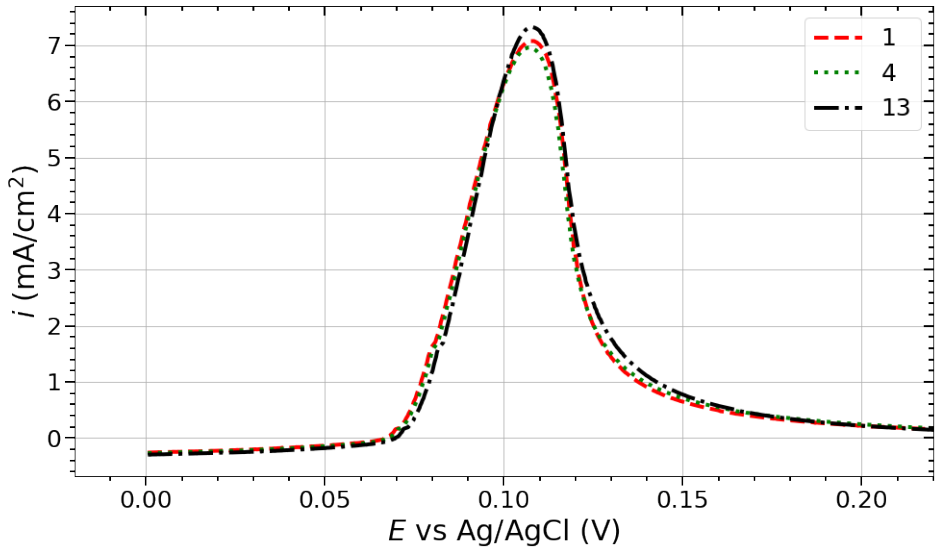

Figure 4.10: Voltammogram showing three of the 13 repeated ALSV measurements after 500 s deposition at −0.3 V vs. Ag/AgCl in a diluted process solution with added silver ions (1 mg L^{-1}). The voltammograms are from the first measurement (1), the one with the lowest peak (4), and the highest and last peak (13). The voltammograms were obtained by stripping at 5 mV s^{-1} after deposition until 0.0 V vs. Ag/AgCl, and a subsequent stripping (the once plotted) at 100 mV s^{-1}. Rotation rate 1600 rpm.

deviations, said to have a 95% accuracy, was found to be 0.3 mA cm^{-2} (4%) and 0.014 mC (2%) for the peak height and charge, respectively (Appendix B).

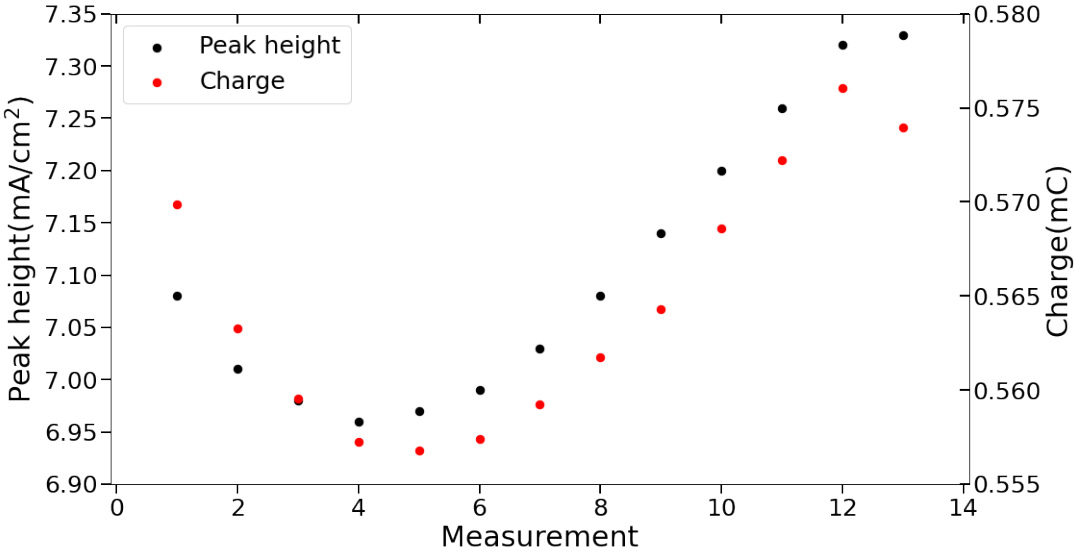

Figure 4.11: Plot showing the peak height and charge trend for the second peak for 13 repeated measurements with divided stripping by ALSV.

Simulation of drift in reference electrode potential. The effect of potential drift is shown in Figures 4.12 a and b for drift of 0.02 V and 0.05 V, respectively, in both the anodic and cathodic directions. This is to simulate drift in the reference electrode (RE). The percentage deviation in peak height and charge from −0.3 V vs. Ag/AgCl is shown in Table 4.2. The peak height deviation is much smaller than the charge deviation. For a drift of 0.05 V in negative direction, two peaks are observed in the voltammogram (Figure 4.12 b).

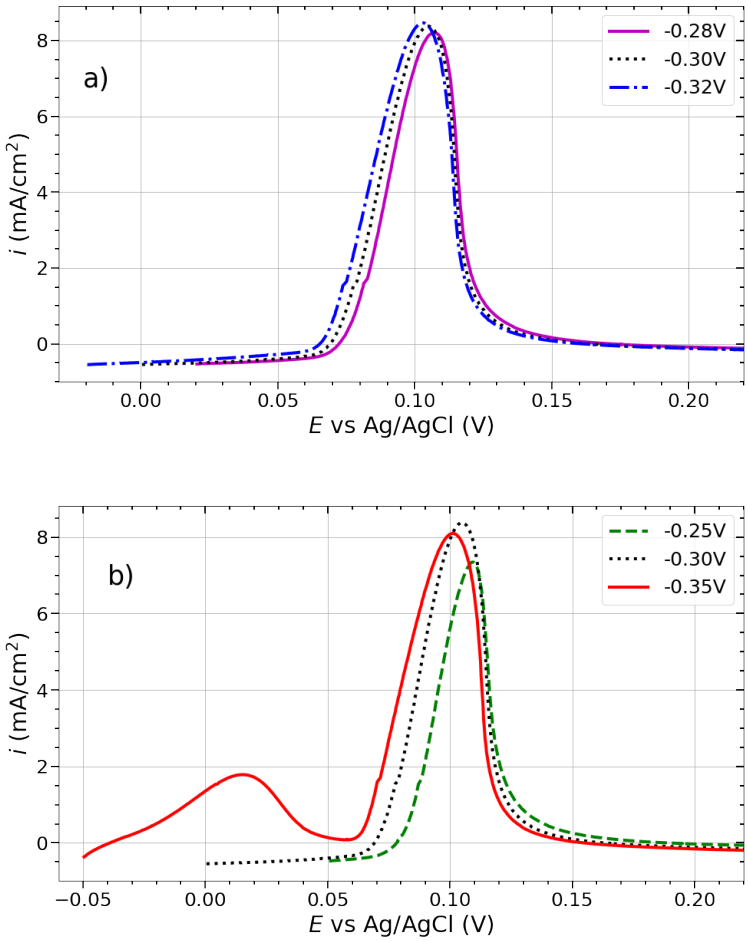

Figure 4.12: Voltammograms of divided stripping with a potential shift of a) 0.02 V and b) 0.05 V in the anodic and cathodic direction from −0.3 V vs. Ag/AgCl. The voltammograms were obtained at 100 mV s^{-1}, after 100 s deposition at −0.25, −0.28, −0.30, −0.32, and −0.35 V vs. Ag/AgCl and stripping at 5 mV s^{-1} until 0.05, 0.02 0.0, −0.02 and −0.05 V vs. Ag/AgCl. Rotation rate 1600 rpm. The solution used was a diluted process solution added silver ions (1 mg L^{-1}).

Table 4.2: Table of the peak height and charge for the different shifts from a deposition potential of −0.3 V vs. Ag/AgCl. The deviation in percent from the results from −0.3 V vs. Ag/AgCl is tabulated for both the peak height and the charge.

Deposition potential [V vs. Ag/AgCl]	Peak height [A cm^{-2}]	Height dev. [%]	Charge [mC]	Charge dev. [%]
-0.25	7.3	12	0.429	24
-0.28	8.2	2.1	0.529	6.5
-0.3	8.4	-	0.565	-
-0.32	8.5	1.0	0.606	7.2
-0.35	8.1	3.3	0.627	10.9

4.3.2 Divided stripping with differential pulse voltammetry

The voltammogram from divided stripping with DPV with three individual sweeps after 500 s deposition is shown in Figure 4.13. The procedure takes about 1180 s and can measure the content approximately three times each hour. A relatively large peak is observed from the first stripping sweep at about −0.21 V. The second stripping sweep shows a very low and decreasing current, with no peaks. The third step shows a large peak at about −0.01 V. The peaks in stripping sweeps 1 and 3 are clearly separated and do not seem to interfere.

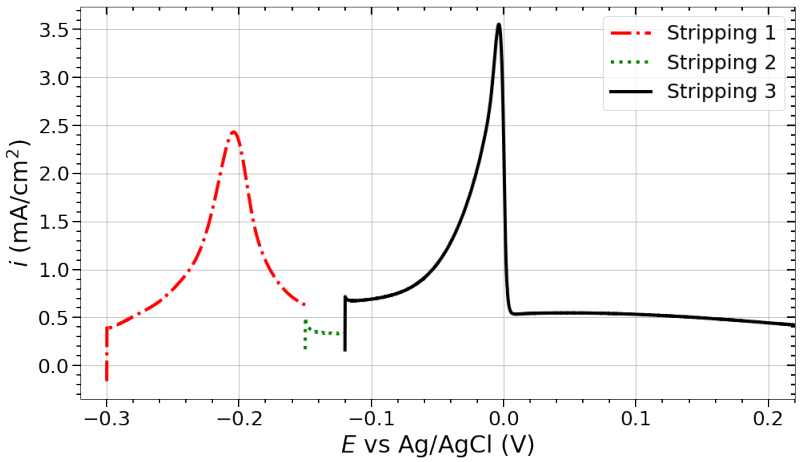

Figure 4.13: Voltammograms from DPV after electrodeposition, where the stripping is divided into three stripping sweeps. The first region is from −0.30 to −0.15 V vs. Ag/AgCl, the second at -0.15-−0.12 V vs. Ag/AgCl, and the third at -0.12-0.40 V vs. Ag/AgCl. The three stripping sweeps have modulation times of 0.05, 0.5, and 0.01 s and modulation amplitudes of -0.15, -0.15, and 0.10 V, respectively.

Figure 4.14 shows the third stripping sweep, as seen in Figure 4.13, from some selected of the repeated measurements. The charge and peak height of all 13 measurements are plotted in Figure 4.15. The peak height shows a decreasing trend, while the charge is first

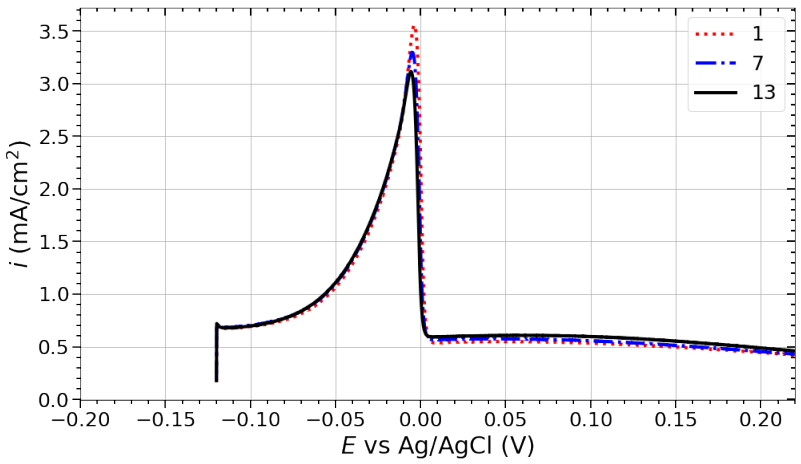

Figure 4.14: Voltammogram showing three of the 13 repeated DPV measurements after 500 s deposition at −0.3 V vs. Ag/AgCl in a diluted process solution with added silver ions (1 mg L^{-1}). The voltammograms are from the measurement 1, 7 and 13. The voltammograms were obtained by divided stripping with three steps, where only the last stripping from −0.12 to 0.40 V vs. Ag/AgCl is plotted. Modulation time 0.01 s and modulation amplitude 0.10 V.

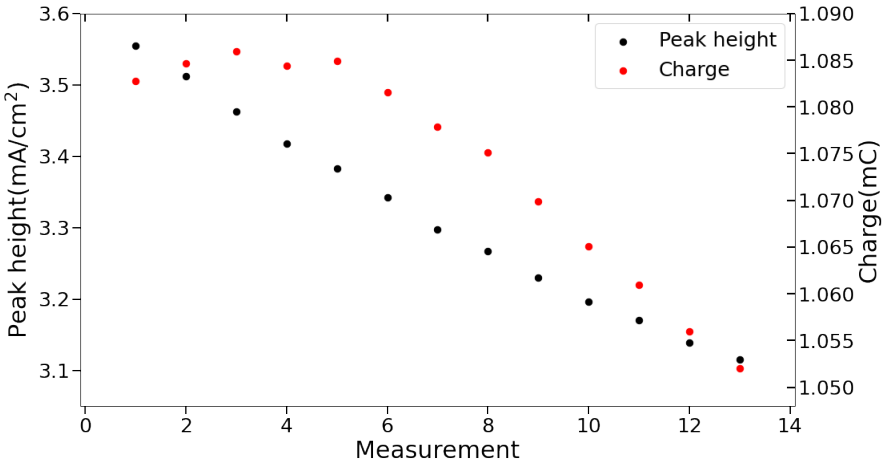

Figure 4.15: The plot shows the peak height and charge trend for 13 repeated measurements with divided stripping by DPV.

increasing before it decreases. The value of two standard deviations, said to have a 95% accuracy, was found to be 0.3 mA cm^{-2} (9%) and 0.02 mC (2%) for the peak height and charge, respectively (Appendix B).

4.4 Calibration for varying silver concentration

Figure 4.16 shows how the peak, from divided stripping by ALSV, changes with different silver ion concentrations. The concentrations given are for the undiluted process solution. The peak increases in both height and area with an increased silver ion concentration. Calibration curves from the linear part of the peak height and charge can be seen in Figures 4.17 a and b, respectively. The coefficient of determination, R^2, of the calibration curve for peak height and charge was 0.9915 and 0.9984, respectively.

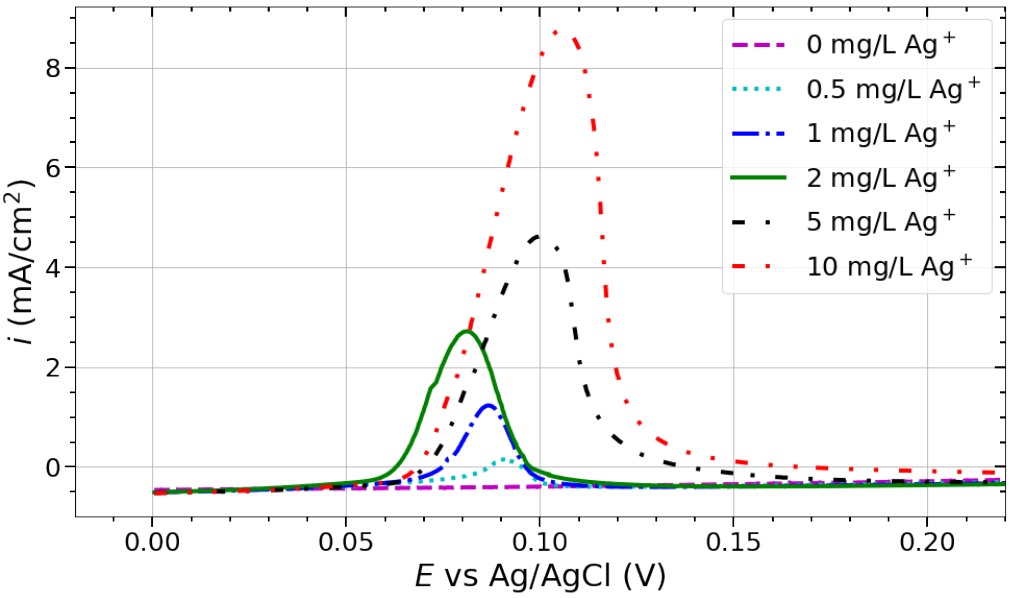

Figure 4.16: Voltammograms of divided stripping by ALSV after electrodeposition in a 1/10 diluted process solution with added silver ion content corresponding to 0, 0.5, 1, 2, 5, and 10 mg L^{-1} in the undiluted process solution. The two stripping sweeps were obtained at 5 and 100 mV s^{-1}, respectively, after 500 s deposition at −0.3 V vs. Ag/AgCl. Rotation rate 1600 rpm.

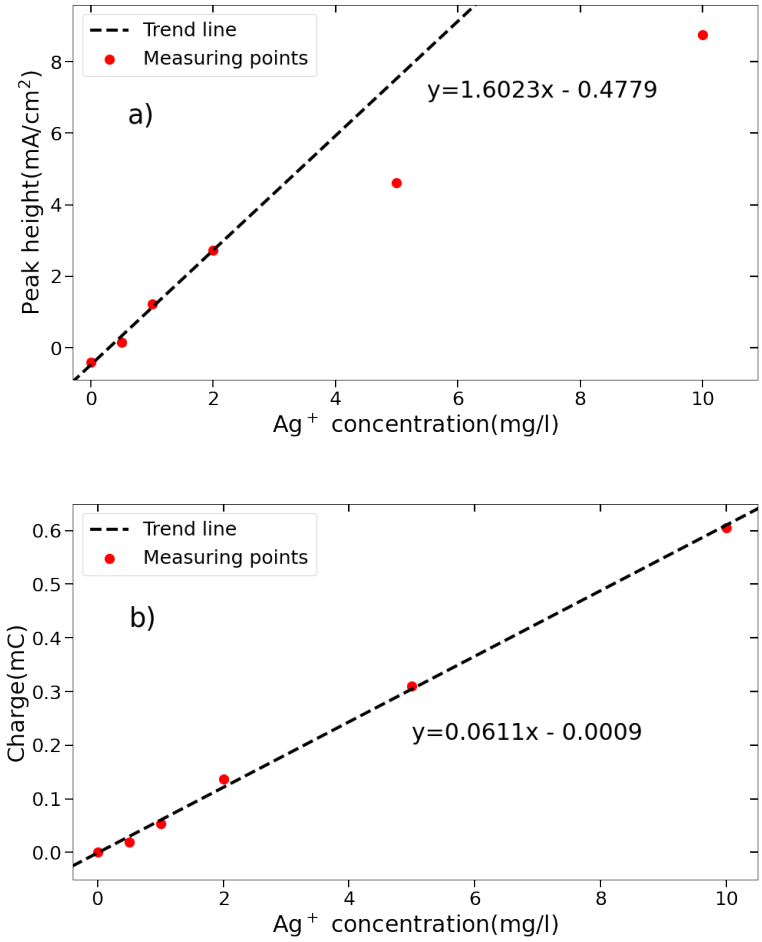

Figure 4.17: Calibration curves for silver detection by a) peak height and b) charge in an 1/10 diluted process solution. The calibration for peak height is based on a content in an undiluted process solution of 0, 0.5, 1, and 2 mg L^{-1} since these showed linearity. Because of linearity, the charge calibration is based on 0, 0.5, 1, 2, 5, and 10 mg L^{-1} Ag^+ in the undiluted process solution.

From the calibration curve for peak height, h_{peak}, the following equation can be used to estimate silver ion concentration, C, in the undiluted solution:

$$C = \frac{h_{peak} + 0.4779}{1.6023} \tag{4.1}$$

The highest peak height for 10 mg L^{-1} silver ions is seen in Figure 4.17 a and is 8.8 mA cm^{-2}. The lowest peak height is seen in Figure 4.10 and is 7.0 mA cm^{-2}. The deviation between these measurements is about 20%.

From the calibration curve for charge, the following equation can be used to estimate

silver ion concentration in the undiluted solution:

$$C = \frac{q + 0.0009}{0.0611} \tag{4.2}$$

The calibration point for charge at $10\,\mathrm{mg\,L^{-1}}$ is 0.611 mC. The charge value from the repeated measurements for ALSV that deviates most from this is 0.557 mC. By using Equation 4.2, the silver ion concentration corresponding to a charge of 0.557 mC is found to be $9.13\,\mathrm{mg\,L^{-1}}$, which gives a deviation of about 9%.

4.5 Nickel as a pseudo-reference electrode

4.5.1 Long term stability of nickel pseudo-reference electrode in process solution

Figure 4.18 shows an open circuit potential (OCP) measurement of a nickel wire vs. Ag/AgCl in a diluted process solution over three weeks. The potential drifted slowly during the period but mainly kept between −0.085 V vs. Ag/AgCl and −0.065 V vs. Ag/AgCl. The potential dip after about 12.5 days is due to refilling the salt bridge with electrolyte. The reason for the potential top after about 17 days is unknown. The

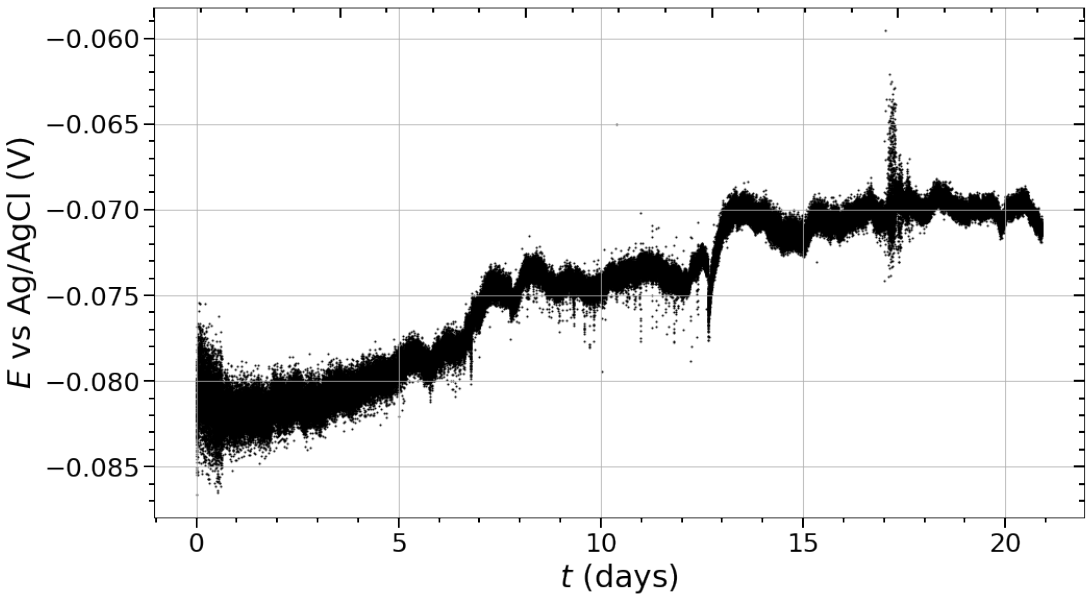

Figure 4.18: OCP measurement of a nickel wire in a diluted process solution for 21 days.

potential seems to drift continuously within a region of 10 mV on the first day and about 5 mV on the following days. Both day 0 and day 17 have a potential drift of more than 10 mV from the minimum to the maximum value.

The Evens diagram for estimation of corrosion rate is seen in Figure 4.19. The corrosion rate is approximated to 1.4 mm/year for a nickel wire of 0.5 mm. For a nickel wire of 5 mm, the corrosion rate would be 0.14 mm/year. The calculation can be seen in Appendix E.

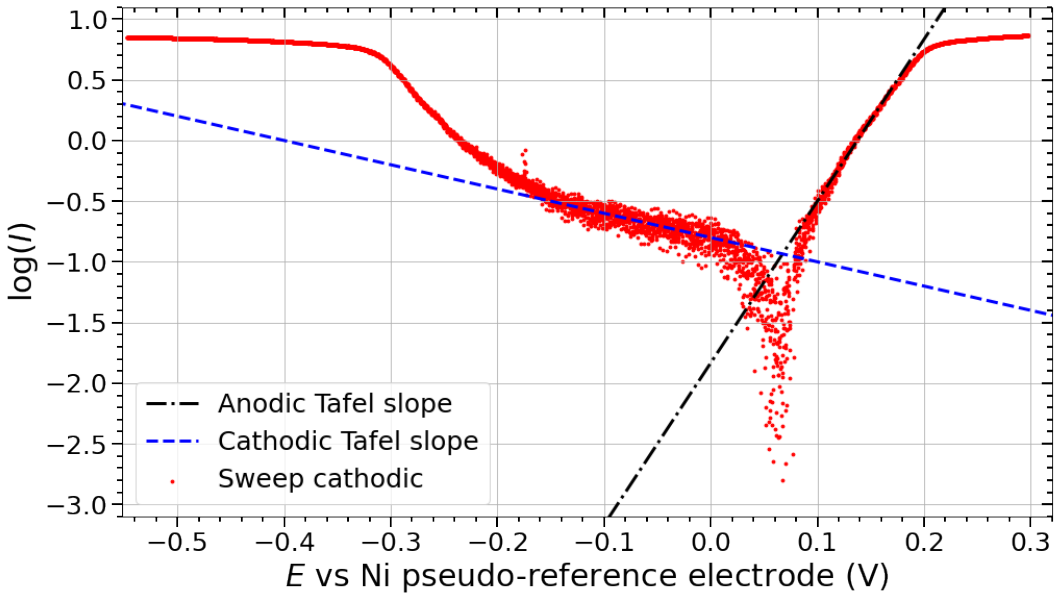

Figure 4.19: Evans diagram of nickel in a diluted process solution. The anodic and cathodic Tafel slopes have been plotted, where the intersect gives the corrosion potential and current. The potential was scanned in the cathodic direction from 0.3 V vs. Ni pseudo-RE to −0.55 V vs. Ni pseudo-RE with a scan rate of 0.5 mV s^{-1}.

4.5.2 Anodic linear sweep voltammetry with nickel pseudo-reference electrode

The voltammogram of ALSV with a nickel pseudo-RE is shown in Figure 4.20. The potential difference between the nickel pseudo-RE and the Ag/AgCl RE was −0.082 V. The applied deposition potential was hence moved 0.082 V in positive direction when a nickel pseudo-RE was used compared to when a Ag/AgCl RE was used (Figure 4.5).

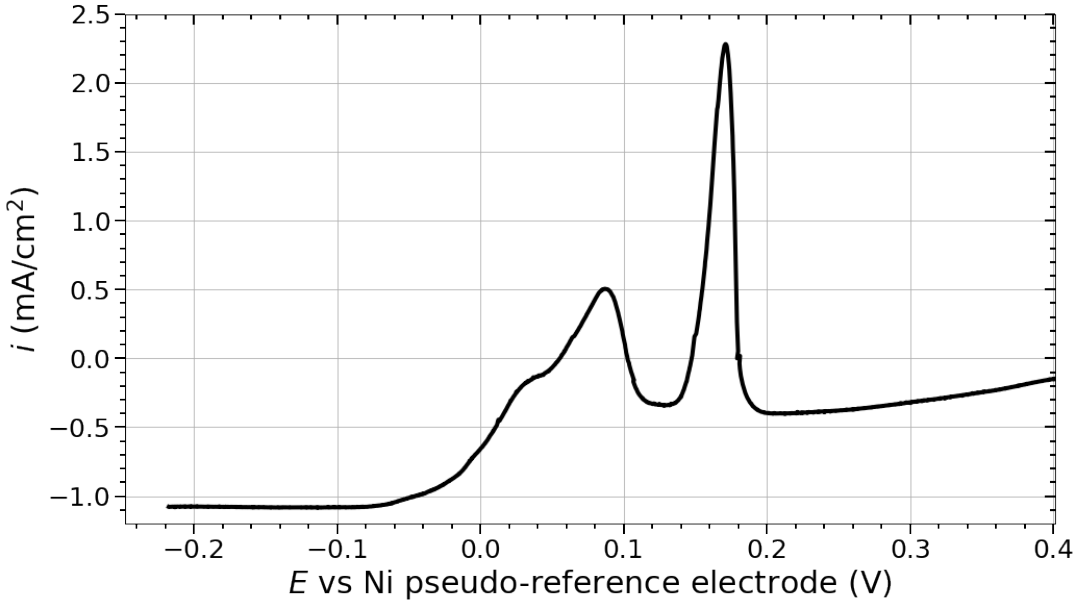

Figure 4.20: Voltammograms of a 1/10 diluted process solution with added silver ions ($1\,\mathrm{mg\,L^{-1}}$). The voltammogram was obtained at $100\,\mathrm{mV\,s^{-1}}$ after 100 s deposition at $-0.218\,\mathrm{V}$ vs. Ni pseudo-RE. Rotation rate 1600 rpm.

4.5.3 Linear divided stripping for nickel pseudo-reference electrode

The voltammogram from anodic stripping with two individual sweeps after 500 s deposition is shown in Figure 4.21 a. The stripping procedure is the same as seen in Chapter 4.3.1, but for a nickel pseudo-RE. The procedure takes about 1180 s and can measure the content about three times each hour. Therefore, the deposition potential and the potential between the two stripping sweeps have been shifted 0.082 V in positive direction. From the first stripping sweep, a very small peak is observed at about 0.04 V. The second stripping sweep has a larger peak, at 0.18 V. The two peaks seem to fit with the peaks observed in Figure 4.9, shifted about 0.07 V in positive direction. This almost corresponds to the potential shift due to the change of RE.

A close-up of the first stripping is shown in Figure 4.21 b. The current response seems relatively unstable compared to the observations from voltammograms obtained by Ag/AgCl RE.

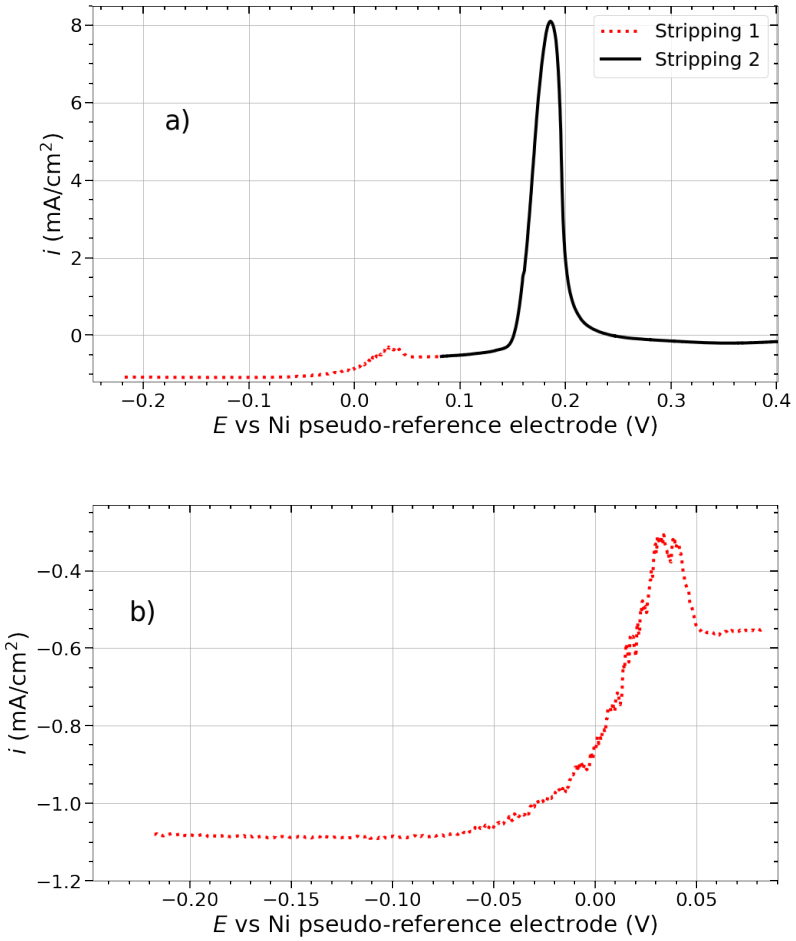

Figure 4.21: Voltammograms of ALSV after electrodeposition, where the stripping is divided into one slow and one fast stripping sweep. a) Shows both stripping sweeps, while b) shows a close-up of the first stripping sweep. Stripping 1 and 2 were obtained at 5 and 100 $\mathrm{mV\,s^{-1}}$, respectively, after 500 s deposition at -0.218 V vs. Ni pseudo-RE and shift between the stripping sweeps at 0.082 V vs. Ni pseudo-RE. Rotation rate 1600 rpm. Measurement is a diluted process solution with added silver ions ($1\,\mathrm{mg\,L^{-1}}$).

Figure 4.22 extracts and emphasizes on the second stripping peak (stripping 2) from Figure 4.21 for selected repeats. The charge and peak height of all 13 repeated measurements are plotted in Figure 4.23. From the figures above, the charge seems to decline minimally, but linearly with time, while the peak height seems to change relatively randomly. The value of two standard deviations, said to have a 95% accuracy, was found to be $0.4\,\mathrm{mA\,cm^{-2}}$

(4%) for the peak height and 0.03 mC (6%) for the charge (Appendix B).

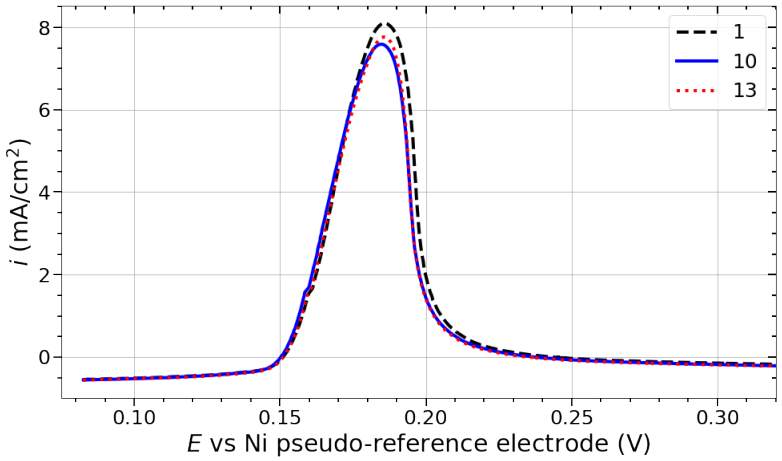

Figure 4.22: Voltammogram showing three of the 13 repeated ALSV measurements after 500 s deposition at −0.218 V vs. Ni pseudo-RE in a diluted process solution with added silver ions (1 mg L^{-1}). The voltammograms are from the first measurement with the highest peak (1), the one with the lowest peak (10), and the last peak (13). The voltammograms were obtained by stripping at 5 mV s^{-1} after deposition until 0.082 V vs. Ni pseudo-RE, and a subsequent stripping (the peak plotted) at 100 mV s^{-1}. Rotation rate 1600 rpm.

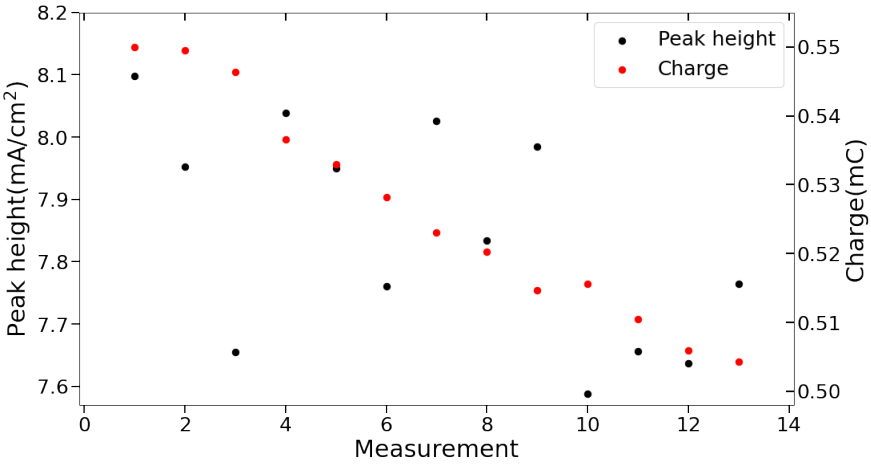

Figure 4.23: Plot showing the peak height and charge trend for 13 repeated measurements with divided stripping by ALSV with a nickel pseudo-RE.

5 Discussion

5.1 Electrochemical silver and bismuth detection

5.1.1 Silver detection by anodic linear sweep voltammetry

Chloride content of $30\,\mathrm{g\,L^{-1}}$ in the real and synthetic diluted process solutions causes silver stripping at about 0.08-0.10 V vs. Ag/AgCl for glassy carbon (GC) electrodes. In both the synthetic and the real diluted process solution, a peak is observed at 0.08-0.10 V vs. Ag/AgCl in only the solutions containing silver ions by anodic linear sweep voltammetry (ALSV) (Figure 4.5 and Figures 4.6 a and b). This potential corresponds well with previously observed silver peaks in solutions containing about $30\,\mathrm{g\,L^{-1}}$ Cl^-.[18] The reversible electrode potential for silver in solutions with this chloride content was calculated to be 0.33 V vs. SHE in Equation 2.37, which is the same as 0.11 V vs.Ag/AgCl. This corresponds well with the observed peaks, and it is reasonable to assume that these are actually due to silver stripping.

Silver can be detected without being affected by bismuth by depositing at −0.1 V vs. Ag/AgCl since only silver is electrodeposited at this potential (Figure 4.6 a). This was also confirmed by energy dispersive spectroscopy (EDS) (Table 4.1). However, using this deposition potential will make the measurements sensitive to potential drift of the reference electrode (RE). A RE will, over time, drift in potential.[20] A drift in RE potential may change the amount of silver electrodeposited radically since the potential difference between the deposition potential (−0.1 V) and the stripping potential (0.08-0.10 V) is relatively small. If the potential drifts in positive direction, silver may not deposit at all due to a potential above the upper potential limit for electrodeposition of silver. Drift in negative direction may increase the silver amount deposited, as well as cause bismuth deposition. A more negative deposition potential may be better even though bismuth will deposit. This is because the measurement may be less affected by drift in the RE at higher potentials.

Only a bismuth peak is observed in voltammograms for solutions not containing silver ions, for deposition potentials below −0.1 V vs. Ag/AgCl. A peak is observed in the voltammogram from the solutions without silver ions, between −0.07 V vs. Ag/AgCl and −0.03 V vs. Ag/AgCl (Figure 4.5 and Figures 4.6 b). This was also confirmed by EDS

(Table 4.1).The peak corresponds well with the observed bismuth peak from previous studies for a chloride concentration of $30\,\mathrm{g\,L^{-1}}$.[18]

The potential of the bismuth peak shifts in positive direction when silver ions are added, from $-0.06\,\mathrm{V}$ vs. Ag/AgCl to $0.0\,\mathrm{V}$ vs. Ag/AgCl (Figure 4.5). This shift in potential fits well with that observed in response to silver ion addition by Krastev et al. [28]. A possible explanation for this is a higher overpotential for bismuth stripping when silver ions are present. This might be because a large part of the electrode surface is covered by silver (Figure 4.3 b and c). Therefore, bismuth has to deposit on silver. The stripping potential will increase as the overpotential for stripping increases.[26] This leads to a smaller distance between the stripping peaks of bismuth and silver and hence a more difficult separation of their current signals.

For electrochemical detection of silver to be reliable, measures need to be taken to distinguish the silver signal from bismuth. The bismuth peak is much larger in the synthetic solution (Figure 4.6 b), where the bismuth concentration is five times higher than in the process solution. The increased bismuth concentration gives less separation of the two peaks. When two peaks are very close to each other, one metal may start stripping before the other metal is completely stripped off. If this happens, the current signals will be altered, leading to wrong estimations of the metal ion content. The bismuth content normally varies in the process solution, and the concentration may be several times as high as in the one used. Silver may therefore be difficult to detect without measures to separate the bismuth signal from the silver signal. If an increased bismuth concentration alters the amount of silver electrodeposited, silver detection may be problematic in a process solution with varying bismuth concentration over time. However, the difference between the silver peak in synthetic and process solution is relatively small, despite a bismuth content five times as high in the synthetic solution (Figures 4.6 b). This indicates that the amount of silver deposited on the electrode will be relatively independent of the bismuth content.

5.1.2 Effect of open circuit after deposition

Without an applied potential below the oxidation potential of silver and bismuth, both metals are unstable in the process solution and will strip off relatively fast. In OCP measurements in a diluted nickel chloride process solution, electrodeposited bismuth will

start to strip off immediately, followed by silver stripping (Figure 4.4 a-c). The potential increases rapidly to a potential plateau at around −0.05 V, depending a little on deposition time. This corresponds well with the potential for the stripping peak of bismuth, as seen in Figure 4.5. After all bismuth has been stripped off, the potential increases to a new potential plateau slightly above 0.05 V, corresponding to the lower potential of the silver stripping peak (Figure 4.5). When all the silver has been stripped off, a stable OCP value of about 0.4 V vs. Ag/AgCl is reached. The stable OCP value of the GC WE in the diluted process solution is higher than both the value for bismuth and silver stripping. Consequently, any deposited silver and bismuth will oxidize unless a potential below their stripping potentials is applied.

The clear division between the stripping of the two metals indicates that there is possible to separate the current signals. Therefor, bismuth can be stripped off while silver stays deposited if a potential between the two stripping potential plateaus is applied for a sufficient time. This can be of great use when trying to isolate the current signal for silver.

5.1.3 Silver detection by differential pulse voltammetry

Both silver and bismuth can be detected by differential pulse voltammetry (DPV). In DPV, the peaks shifts in negative direction corresponding to the modulation amplitude (Figure 4.7 c). This trend fits with a shift in negative direction for the silver peak of 0.05 V from ALSV to DPV, corresponding to the modulation amplitude (Figure 4.8). On the other hand, the bismuth peak seems to shift about 0.05 V from ALSV to DPV. This might be due to the increased sensitivity for bismuth detection in DPV. It seems like both bismuth and silver can be detected by DPV.

When the size of the silver and bismuth peaks increases, it gets more challenging to distinguish between the two metals. When the height of the metal peaks increases, the width of the peaks increases as well (Figure 4.7 a-d). An increased width gives worse separation of the peaks since they can interfere with each other, causing wrong estimation of the metal content. Determination of experimental parameter values will therefore be a trade-off between a strong silver signal and a good separation of the two metal peaks.

DPV is more sensitive toward both bismuth and silver than ALSV, and measures need to

be done to separate the peaks in order to get a reproducible silver signal. This correlates well with theory, saying that DPV has a higher sensitivity due to its ability to reduce the charging current.[29][52] DPV measurement is therefore good for use in trace metal detection. However, the increase in bismuth sensitivity is much larger than the increased silver sensitivity. This leads to a much larger bismuth peak. The bismuth peak has moved more in negative direction than the silver peak compared to ALSV. Therefore, the separation between the two peaks is about the same size for ALSV and DPV, despite the increased bismuth peak. The variation in the real bismuth concentration of the process solution may be large, and the silver ion concentration in the process solution is usually much lower than the concentration used in this work. Measures should be taken to separate or remove the bismuth signal from the silver signal in order to be able to make a reproducible procedure for silver detection.

5.2 Morphology and composition of electrodeposited silver and bismuth on a glassy carbon electrode

The deposited material will start to strip off from the electrode immediately if no potential is applied (Figure 4.4). Therefore, a potential needs to be applied when the electrode is removed from the solution to be studied in the scanning electron microscope (SEM). Both the voltammograms for ALSV (Figure 4.5 and Figures 4.6 a and b) and the plot from deposition(Figure 4.1) show that reactions are happening at the electrodes. The figures also show that the reactions depend on the deposition potential and the electrolyte composition. SEM and EDS can obtain further confirmation of deposited material and its composition and morphology.

5.2.1 Electrodeposition of bismuth

Bismuth appears to form a thin uniform film on the electrode surface, indicating that bismuth has a lower overpotential for depositing on GC than on itself. The surface after bismuth deposition looks like the clean electrode surface (Figure 4.2 a). Bismuth is not visible in SEM, but the EDS confirms that it is present (Table 4.1). This indicates that bismuth has deposited on the electrode surface as a thin film. Deposition as a film can happen when the metal has a lower or equal overpotential for depositing at the surface material compared to depositing on itself.[26]

5.2.2 Process solution with silver

Silver seems to have a lower overpotential for depositing on silver than depositing on GC (Figure 4.3 a). Unlike the bismuth deposition, silver deposits as relatively large nuclei at the surface of the electrode, visible by SEM. After some silver nuclei have formed dispersed across the electrode surface, silver continues to deposit preferentially at these nuclei rather than forming new nuclei at the GC substrate. This indicates that silver might have a lower overpotential for depositing on silver than on GC. This correlates well with the observations by Geboes [66], showing that silver forms nuclei on a GC electrode.

The nucleation rate increases with an increasing deposition overpotential. The number of nuclei increases, and their size decreases with a decreasing deposition potential (Figure4.3 a-c). This correlates well with the experimental observations by Geboes et al. [66] for silver deposition on GC electrodes. The observation also agrees with the hypothesis that the overpotential for silver precipitation on silver is less than silver precipitation on GC. When the applied potential gets lower, the difference in overpotential will be less decisive for the site of deposition.

If the deposition potential is more positive than what is needed for bismuth deposition, but negative of what is needed for silver deposition, only silver will deposit. The EDS for deposition potential of $-0.1\,\mathrm{V}$ vs. Ag/AgCl shows that only silver deposits at this potential (Table 4.1). This correlates with the observed voltammograms seen in Figure 4.6 a, showing only a silver peak.

Fitting the current signals from electrodeposition to plots with instantaneous and progressive nucleation was tested. However, the fit was so bad that it was not considered appropriate to attach the graphs.

5.2.3 Process solution with silver with bismuth removing by chronoamperometry

All deposited bismuth can be removed from the electrode surface without affecting silver to a significant degree by controlling the electrode potential. The data from EDS (Table 4.1) shows that all bismuth has been removed after 1000 s at $0.0\,\mathrm{V}$ vs. Ag/AgCl (Figure 4.3 d), while silver is still deposited. Even though bismuth has been removed, the silver nuclei seem unaffected when comparing Figures 4.3 b and 4.3 d. This correlates well with

the OCP measurements (Figure 4.4 a-c), where bismuth is stripped off before 0.0 V vs. Ag/AgCl, while silver is still deposited at this potential. The results prove that bismuth can be removed while silver is still deposited on the electrode surface. Having a method to remove bismuth without removing silver is very beneficial when developing a method for electrochemical detection of silver since it makes separation of the metal stripping peaks much easier.

5.3 Reproducible measurements by divided stripping

Since bismuth and silver strip off at potentials close to each other, measures need to be taken to isolate the silver signal for the measurements to be reproducible. A possible way to separate the current signals is to divide the stripping into several individual sweeps. Bismuth may then be stripped off by a slow scan rate before silver is stripped off with a fast scan rate. Using a slow scan rate for bismuth removal ensures that all bismuth is removed before changing the scan rate. A faster scan rate for silver stripping gives a larger silver signal. It is also possible to implement a chronoamperometry measurement between the stripping sweeps to ensure complete removal of bismuth. However, this makes the measurement more complex and is desirable to avoid if possible. Adding ammonium buffer was also tested to precipitate other metal ions and increase the silver signal without promising results (Appendix C).

5.3.1 Divided stripping by ALSV

By dividing the stripping in ALSV into two stripping sweeps, the silver peak can be separated from the bismuth peak. Bismuth is stripped off during the first stripping sweep, and silver during the second (Figure 4.9), correlating with the current peaks seen in Figure 4.5. Since bismuth is stripped off by a slow stripping sweep, the current signal is low, and the upper part of the peak is at a lower potential than for higher scan rates. This correlates well with the trend observed in the preliminary experiments by Josefsen [18], where the peak width and height increase with increasing scan rate. The following fast scan where silver is stripped off gives a relatively large and clear silver peak without disturbance from bismuth.

In the second stripping sweep, the silver signal is isolated since all bismuth is removed during the first stripping sweep. The potential region between 0.0 V vs. Ag/AgCl and

the start of the silver stripping top is linear and does not seem to be affected by bismuth (Figure 4.10). If any bismuth were still present on the surface, it would continue to strip off immediately when starting the second stripping sweep. This can be seen from Figure 4.5, where bismuth is stripping off at 0.0 V vs. Ag/AgCl when bismuth is present. The results from EDS, showing no bismuth present after applying a potential of 0.0 V vs. Ag/AgCl (Table 4.1), confirms that all bismuth can be removed at this potential. Since only silver and bismuth deposits on the electrode surface for the used experimental parameters, the silver signal can be completely isolated.

It is possible to establish a reproducible method for electrochemical detection of silver in the studied process solution. By dividing the stripping into two sweeps and adding an OCP measurement at the end, the silver signal had little deviations between repetitive measurements, as seen in Figure 4.11 and Figure 4.10. The time at OCP is to ensure that all deposited material is removed before the next measurement. It is observed in Figure 4.4 that both silver and bismuth will strip off and reach a potential at about 0.4 V vs. Ag/AgCl. An alternative would be to apply a potential of about 0.4 V vs. Ag/AgCl to ensure a clean surface. The deviation was 2% and 4% for charge and peak heights, respectively, which is acceptable deviation in a real measurement. However, it is still uncertain how the method will react to changes in the electrolyte composition.

The deviation in peak height and charge is not normally distributed but changes gradually as a function of time (Figure 4.11). There are several possible explanations for this trend. One explanation is drift in potential due to temperature changes or some degree of memory effect of the RE.[60][61] It is also possible that the method lacks some modifications to get completely reproducible. The glassy carbon surface might also change between measurements, altering the metal deposition. This change in the electrode surface might be due to passivation by deposited material, change in surface roughness, or other mechanisms causing a change in the available surface area. The change in the surface area can be minimized by polishing the surface regularly. However, this is time-consuming and needs to be done manually. Implementing a cleaning step in the procedure, either chemically or electrochemically, may improve reproducibility. This cleaning step might replace the OCP measurements at the end of the procedure.

5.3.2 Divided stripping by differential pulse

The silver peak can be separated from the bismuth peak by dividing the stripping in DPV into three stripping sweeps. Most of the bismuth is stripped off during the first stripping sweep (Figure 4.13). The second sweep is slower to ensure that all bismuth is removed. The third sweep only shows silver stripping. Bismuth, can in other words, be removed to isolate the silver stripping.

It is possible to establish a reproducible method, based on the charge, for detection of silver by DPV in the studied process solution. By dividing the stripping into three sweeps and adding an OCP measurement at the end, the silver signal had little deviations between repetitive measurements, as seen in Figure 4.15 and Figure 4.14. The deviation was 2% for charge and 9% for peak heights. The charge deviation is very good, and the charge is high as well. Even though the charge is high compared to ALSV, the area of the peak is relatively small. The main reason for this is the low scan rate in DPV compared to ALSV. Therefore, the increased charge may give a wrong picture of the sensitivity when different scan rates are used. The deviation in peak height is large and may cause unacceptable deviations. The deviation in the peak height is likely due to the sharp of the peak, with a graduate increase before a sharp edge with a fast current decrease. It is uncertain how the method will react to changes in the electrolyte composition.

The increased sensitivity for silver detection by DPV compared to ALSV is no longer true when divided stripping is used. The peak heights are actually smaller than for ALSV. One reasonable explanation for this is the increased scan rate for ALSV in the divided stripping (Figure 4.9) versus the single stripping (Figure 4.5). Another possible reason is that some silver might have been stripped off during the second stripping sweep for DPV.

ALSV should be further investigated since divided stripping by ALSV is more sensitive and accurate than the divided stripping by DPV. The peak height is much lower for DPV (Figure 4.13) than for ALSV (Figure 4.9). The drift in peak height in percentage is also larger for DPV (9%) than ALSV (4%). The charge is larger for DPV, but the area of the peak is smaller. In addition, the time used for the two measurements is about the same. Therefore, it is most reasonable to use ALSV.

5.4 Calibration curves by divided stripping with ALSV

Calibration curve based on the peak height of the silver stripping peak works for concentrations up to $2\,\mathrm{mg\,L^{-1}}$ Ag^+. The points in the graph for peak height versus silver ion concentration show linearity from 0 to $2\,\mathrm{mg\,L^{-1}}$ (Figure 4.17 a). Higher concentrations show a larger deviation from linearity and may not be estimated by the peak height. Similar observations have been done by Holden [14] in studies of other systems, where the linear trend for the peak height only ranges until a certain upper concentration limit. The coefficient of determination of the curve exceeds 0.99, meaning that over 99% of the variation in peak height can be explained by the variation in concentration.

Calibration curve based on the charge of the silver stripping peak works for concentrations up to $1\,\mathrm{mg\,L^{-1}}$ Ag^+ in the diluted process solution. All points in the graph for charge versus silver ion concentration show linearity, as seen in Figure 4.17 b. The coefficient of determination of the curve exceeds 0.998, meaning that over 99.8% of the variation in peak height can be explained by the variation in concentration. Therefore, a calibration based on the charge will be more accurate and have a broader range for detection than calibrations based on the peak height.

For $10\,\mathrm{mg\,L^{-1}}$ silver ions, the deviation between the highest ($8.8\,\mathrm{mA\,cm^{-2}}$) and lowest ($7.0\,\mathrm{mA\,cm^{-2}}$) peak height is about 20%. This is relatively high and will, in many cases, not be sufficient. The silver ion content of $10\,\mathrm{mg\,L^{-1}}$ is outside the concentration range for the peak height calibration. Therefore, conclusions should not be drawn regarding the reproducibility based on the deviations in the silver peaks for this high silver ion concentration.

The deviation between the charge calibration and the lowest charge measured for $10\,\mathrm{mg\,L^{-1}}$ was about 9%. This is usually acceptable for industrial applications. However, it indicates that further measures can be taken to increase reproducibility.

5.5 Nickel as a pseudo-reference electrode

The total drift observed for the nickel wire during the three-week period is acceptable for use as a pseudo-RE. The potential of a nickel pseudo-RE only varied about 20 mV between maximum and minimum value within a three-week period, as seen from the OCP measurement in Figure 4.18. Since 10 mV drift per day is usually accepted, twice as much

during 21 days will, in most cases, be well within acceptable variation.[20]

Most days, the potential difference between the two extreme values is less than 5 mV (Figure 4.18). However, on day 0 and day 17, the drift is as large as 10 mV or more within a day. This is above the limit of what is generally seen as acceptable.[20] The drift on the first day might be due to a nickel oxide layer on the electrode surface, which had to be removed for the potential to stabilize. This issue could be avoided by immersing the electrode into a diluted process solution some days before using it. The reason for the drift on day 17 is unknown and might cause problems if it happens regularly. However, a likely explanation for the drift is disturbances in the flow caused by irregular magnetic stirring. The nickel wire used is thin and is visibly moved by the flow in the cell. Using a thicker nickel wire might remove such disturbances.

The relatively large potential drift on a short-time basis will likely be removed if the wire thickness is increased. The potential often drifts about 5 mV within a short-time interval (Figure 4.18), which might cause irregular voltammograms. If the potential of the nickel pseudo-RE drifts during the stripping of silver, the peak can change shape and get a different peak height. This can cause wrong estimation of the silver ion content of the solution. Also in this case, the drift is likely due to the vibrations in the nickel wire caused by the stirring. Exchanging the nickel wire with a thicker one that does not move as a result of the stirring might solve the drift.

Silver can be detected electrochemically by using a nickel pseudo-RE. Two peaks are observed in the voltammogram with nickel pseudo-RE, at 0.09 and 0.17 V vs. Ni pseudo-RE (Figure 4.20). These peaks correspond well with the bismuth and silver peaks, respectively, observed in voltammograms with a Ag/AgCl RE (Figure 4.5). The shape of the peaks also looks very similar in the two figures, even though the size is different due to different sweep rates. This means that silver can be detected by using a nickel pseudo-RE. The current signal does not show obvious drift due to drift in RE potential. The reason for this is probably the fast scan rate.

Due to the low corrosion rate of nickel in the diluted nickel solution, nickel as a pseudo-RE will be a cheap and low-maintenance alternative to conventional RE. From the result in Figure 4.19, it has been calculated that the corrosion rate of nickel is about 1.4 mm/year for a 0.5 mm thick nickel wire. The corrosion rate increases with a decreasing thickness.

As the electrode corrodes and becomes thinner, the corrosion rate will increase. If the thickness of the wire is increased to 5 mm, the corrosion rate will decrease to about 0.14 mm/year, and the wire will last several years without needing to be replaced. Nickel is a cheap material, and it will not be a considerable cost related to changing the electrode.

5.5.1 Divided stripping by ALSV with nickel pseudo-RE

The silver signal is isolated from the bismuth signal in divided stripping by ALSV with nickel pseudo-RE. The shape and position of the peaks seen in Figure 4.21 a (Nickel pseudo-RE) correspond well with the position and size of the peaks seen in Figure 4.9 (Ag/AgCl RE). All bismuth seems to have been removed before the silver stripping sweep starts since the curve flattens out at the end of the bismuth stripping (Figure 4.21b). The silver peak is, in other words, isolated from the bismuth peak.

The bismuth signal is disturbed by variation in the potential caused by vibration of the nickel pseudo-RE. Nickel is stripped off by a slow scan rate, and the current signal is visibly affected by the drift in potential (Figure 4.21 b). The observed drift on a short-time basis supports this variation (Figure 4.18). The reason why silver stripping is not visibly affected is likely that it is stripped off using a fast scan rate.

It is important to test how the potential drift from the nickel pseudo-RE will affect the measurements for it to be a reliable RE. The effect of potential drift on the silver signal can be seen in Figures 4.12 a and b for a drift of 0.02 V and 0.05 V, respectively. The change in the silver peak height and charge is acceptable for a drift of 0.02 V. A positive potential drift of 0.05 V will give a relatively large deviation in both peak height and charge. However, for a negative potential drift of 0.05 V, bismuth is still deposited when the fast scan starts (Figure 4.12 b, red curve). The silver signal might be affected by the bismuth content. Hence, the procedure is not reproducible for a positive or negative potential drift of 0.05 V. It has been shown a potential drift of about 0.02 V within a three-week period (Figure 4.18) for a nickel pseudo-RE. If the potential is controlled and calibrated against a known reference once every third week, a nickel pseudo-RE should be possible to use for silver detection.

It is possible to establish a reproducible method for electrochemical detection of silver ions in the studied process solution for a nickel pseudo-RE. ALSV with divided stripping

and an OCP measurement at the end gave little deviations for repeated measurements of silver detection with a nickel pseudo-RE, as seen in Figure 4.23 and Figure 4.22. The deviation is 6% and 4% for charge and peak heights, respectively, which is acceptable deviation in a real measurement. How the measurement will react to the changes in the electrolyte composition is uncertain.

6 Conclusion

Silver ions can be quantitatively detected in a 1/10 diluted process solution by anodic stripping voltammetry. The potentials for both silver and bismuth detection in the process solution correspond well with the observed peaks for a synthetic process solution. Silver ions can be detected both by using linear sweep voltammetry and by differential pulse voltammetry in diluted process solutions. However, since the stripping peaks of bismuth and silver are relatively close in both methods, larger bismuth concentrations might lead to overlapping stripping peaks and, consequently, erroneous results for the silver ion concentration.

Silver and bismuth were shown to deposit on a glassy carbon electrode as large nuclei and a thin film of small nuclei, respectively. Bismuth can be completely removed from the surface while silver is still deposited. This can be done by applying a low scan rate until a potential between the bismuth and silver peaks. EDS has confirmed that all bismuth is actually removed by this method.

The silver signal can be isolated by dividing the stripping in anodic stripping voltammetry into several sweeps with different experimental parameters (divided stripping). This was possible for both linear sweep voltammetry and differential pulse voltammetry. The reproducibility of the linear sweep voltammetry was shown to be relatively good. The deviation in the charge was very low, while the deviation in peak height was larger but still acceptable. Divided stripping by differential pulse voltammetry has lower sensitivity towards silver detection than linear sweep voltammetry and additionally has a higher deviation in repeated measurements.

The deviation in both charge and peak current does not seem random but has a trend as a function of time from the first measurement. Therefore, it may be necessary to implement a cleaning procedure for the working electrode, either chemically or electrochemically, between each measurement to further increase the reproducibility. A drift of 0.02 V gave a change in the charge of less than 10%, which for industrial use will be acceptable deviation. On the other hand, a drift of 0.05 V gave an unacceptable deviation of more than 10%. In addition, an overlap between the bismuth and silver peaks was observed for a drift of 0.05 V in negative direction.

Linear sweep voltammetry with divided stripping was used to make calibration curves for silver detection by both using the peak height and the charge. Silver ions were electrodeposited by using a rotating glassy carbon disk as working electrode, a deposition potential of $-0.3\,\mathrm{V}$ vs. Ag/AgCl for 500 s, and a rotation speed of 1600 rpm. In the first sweep from -0.3 to 0.0 V vs. Ag/AgCl, a scan rate of $5\,\mathrm{mV\,s^{-1}}$ was used. For the second sweep, between 0.0 and 0.4 V vs. Ag/AgCl, a scan rate of $100\,\mathrm{mV\,s^{-1}}$ was used. Finally, the electrode was left in the solution at open circuit for 500 s.

The calibration curve for silver by using the peak height showed linearity until an upper limit for a silver ion concentration corresponding to $2\,\mathrm{mg\,L^{-1}}$ Ag^+ in the undiluted process solution. For calibration by using the charge, the measuring points showed linearity for concentrations up to $10\,\mathrm{mg\,L^{-1}}$ Ag^+ in the undiluted process solution. The lowest silver ion concentration that was tested for silver detection, except for $0\,\mathrm{mg\,L^{-1}}$, was $0.5\,\mathrm{mg\,L^{-1}}$ Ag^+ in the undiluted process solution. The coefficient of determination of the curves was 0.992 and 0.998 for the peak height and charge, respectively.

A nickel wire as a pseudo-reference electrode was found to be a good replacement for a Ag/AgCl reference electrode. Silver detection is possible by linear sweep voltammetry with a nickel pseudo reference electrode. Divided stripping using a nickel pseudo reference electrode by linear sweep voltammetry had relatively good reproducibility. It is visible that the potential drifts on short-time basis affect the voltammograms, especially for slow scan rates. The drift on short-time is likely caused by vibration of the wire due to stirring of the solution. Using a thicker nickel wire will probably lead to less drift within a measurement and in addition last longer before having to be replaced. The corrosion rate of nickel is relatively low in the diluted process solution, reducing the need for maintenance of the reference electrode. The drift over a three-week period was less than 0.02 V, which is acceptable. However, the stability of the reference electrode potential over a longer time period is unknown. Hence, the potential of the nickel pseudo-reference electrode should be checked regularly against a reference electrode with a known potential.

7 Further work

The lower and upper limits for linearity of the calibration for silver ion concentration should be tested for both the peak height and charge. The lowest concentration tested was a concentration of $0.5\,\mathrm{mg\,L^{-1}}$ Ag^+ in the undiluted process solution, except for $0.0\,\mathrm{mg\,L^{-1}}$ Ag^+. In the real process solution, the content may be lower than $0.5\,\mathrm{mg\,L^{-1}}$ Ag^+. If possible, it is desirable to be able to detect even lower silver ion concentrations.

Square wave voltammetry should be investigated as a possible method for silver detection. It is a fast measuring method that can be very sensitive. This method might not even need a deposition step for the right set of parameters. However, separating bismuth and silver might be more difficult than for the other types of anodic stripping voltammetry. Therefore, measures need to be taken to get a silver signal that is not affected by bismuth.

Since only one specific sample of the nickel process solution has been tested, little information has been gathered about how the detection is affected by a change in the electrolyte composition. Testing the effect of the solution content, especially the bismuth and chloride concentrations, will be important to get a reliable measurement. By testing for the minimum and maximum values for the concentration of the most important elements, the settings can be modified to work for the entire concentration range.

Measurements at different temperatures can be executed to investigate the effect of temperature on the system. The potential of the reference electrode is temperature-dependent. Therefore, tests of the temperature dependence should be executed for both the nickel pseudo-reference electrode and the Ag/AgCl reference electrode.

Nickel should be further investigated as a pseudo-reference electrode. A thicker nickel wire should be tested to decrease the short-time drift of the potential. Monitoring the potential drift for the electrode over a longer time period should be tested to find the required time interval for calibration of the pseudo-reference electrode potential. A calibration curve should also be made by linear sweep voltammetry with divided stripping for a nickel pseudo-reference electrode. This is for a final confirmation of the stability of the nickel pseudo-reference electrode.

The open circuit potential measurement at the end of the measurement should be exchanged by an electrochemical cleaning procedure. This can be a chronoamperometry

measurement at a high potential or a cyclic voltammetry measurement. This will likely decrease the time between measurements and may also increase the reproducibility of the measurement.

An electrochemical online monitoring system should be implemented in the real process to test how the variations in the process solution affect the reproducibility of the system. By making a calibration and measuring the silver ion content over time, the measured silver ion content can be compared to the silver ion content measured by another instrument, for example atomic absorption spectrometer. Optimization of the settings used by the electrochemical online monitoring system should be done by testing in the real process. The deposition time should be chosen based on the wanted lower detection limit for silver ions and the frequency of measurements needed. The choice of scan rate for the first scan should be based on the maximum bismuth concentration in the process solution.

References

[1] W. J. Rankin, *Minerals, Metals and Sustainability: Meeting Future Material Needs*. Victoria: CSIRO Publishing, 2011.

[2] S. Saracoglu, M. Soylak, and L. Elci, "Separation/preconcentration of trace heavy metals in urine, sediment and dialysis concentrates by coprecipitation with samarium hydroxide for atomic absorption spectrometry," *Talanta (Oxford)*, vol. 59, no. 2, pp. 287–293, 2003.

[3] L.-G. Danielsson, B. Magnusson, and S. Westerlund, "An improved metal extraction procedure for the determination of trace metals in sea water by atomic absorption spectrometry with electrothermal atomization," *Analytica Chimica Acta*, vol. 98, no. 1, pp. 47–57, 1978.

[4] G. Currell, *Analytical instrumentation : performance characteristics and quality*. Analytical techniques in the sciences, Chichester: Wiley, 2000.

[5] E. d. Hoffmann, *Mass spectrometry : principles and applications*. Chichester: Wiley, 3rd ed. ed., 2007.

[6] J. W. OLESIK, "10.9 - icp-oes: Inductively coupled plasma-optical emission spectroscopy," in *Encyclopedia of Materials Characterization* (C. R. Brundle, C. A. Evans, and S. Wilson, eds.), pp. 633–644, Boston: Butterworth-Heinemann, 1992.

[7] P. J. Potts, *Ion-selective electrodes*, pp. 213–225. Boston, MA: Springer US, 1992.

[8] K. N. Mikhelson, *Ion-Selective Electrodes*, vol. 81 of *Lecture Notes in Chemistry*. Berlin, Heidelberg: Springer Berlin Heidelberg : Imprint: Springer, 1st ed. 2013. ed., 2013.

[9] C. E. Housecroft, *Chemistry : an introduction to organic, inorganic, and physical chemistry*. Harlow: Pearson Prentice Hall, 3rd ed. ed., 2006.

[10] J. Wang, *Analytical electrochemistry*. Hoboken, N.J: Wiley-VCH, 3rd ed. ed., 2006.

[11] B. Welz, *Atomic absorption spectrometry*. Weinheim: Wiley-VCH, 3rd, completely rev. ed. ed., 1999.

[12] O. Mikkelsen, K. Strasunskiene, S. Skogvold, K. H. Schrøder, C. C. Johnsen, M. Rydningen, P. Jonsson, and A. Jonsson, "Automatic voltammetric system for continuous trace metal monitoring in various environmental samples," *Electroanalysis (New York, N.Y.)*, vol. 19, no. 19-20, pp. 2085–2092, 2007.

[13] R. G. Compton, *Understanding voltammetry*. Hackensack New Jersey: World Scientific, third edition. ed., 2018.

[14] M. C. H. Holden, "Utvikling av prosedyre for overvåking av nikkel og kobolt i avløpsvann fra metallurgisk industri," Master's thesis, NTNU, 2014.

[15] D. Pletcher, *A first course in electrode processes*. Cambridge: RSC Publ, 2nd ed. ed., 2009.

[16] "Nickel," Oct. 13, 2021 [Online]. https://www.mining.com/markets/commodity/nickel/all/.

[17] "Silver," Oct. 13, 2021 [Online]. https://www.mining.com/markets/commodity/silver/all/.

[18] B. Josefsen, "Electrochemical detection of silver in chloride electrolytes," Master's thesis, NTNU, 2021.

[19] P. Sebastián, E. Vallés, and E. Gómez, "First stages of silver electrodeposition in a deep eutectic solvent. comparative behavior in aqueous medium," *Electrochimica Acta*, vol. 112, pp. 149–158, 2013.

[20] Springer, A. Lewenstam, F. Scholz, and G. Inzelt, *Handbook of Reference Electrodes*. Berlin, Heidelberg: Springer Berlin / Heidelberg, 2013 ed., 2013.

[21] K. Oldham, J. Myland, and A. Bond, *Electrochemical Science and Technology: Fundamentals and Applications*. Hoboken: John Wiley & Sons, Incorporated, 2011.

[22] C. Hamann, *Electrochemistry*. Weinheim: Wiley, 2nd, completely rev. and updated ed. ed., 2007.

[23] D. Pletcher, R. Greff, R. Peat, L. Peter, and J. Robinson, "4 - convective diffusion systems – the rotating disc and ring-disc electrodes," in *Instrumental Methods in Electrochemistry* (D. Pletcher, R. Greff, R. Peat, L. Peter, and J. Robinson, eds.), pp. 113–148, Woodhead Publishing, 2010.

[24] A. J. Bard, *Electrochemical methods : fundamentals and applications*. New York: Wiley, 2nd ed. ed., 2001.

[25] E. Gileadi, M. Urbakh, M. Stratmann, and A. Bard, *Encyclopedia of electrochemistry : Vol. 1 : Thermodynamics and electrified interfaces*, vol. Vol. 1. Weinheim: Wiley-VCH, 2002.

[26] M. Paunovic, *Fundamentals of electrochemical deposition*. Electrochemical Society series, Hoboken, N.J.: Wiley-Interscience, 2nd ed. ed., 2006.

[27] K. McCay, *Tin and Tin Alloys for Low Cost Bipolar Plates in PEM Fuel Cells*. PhD thesis, NTNU, 2020.

[28] I. Krastev, T. Valkova, and A. Zielonka, "Effect of electrolysis conditions on the deposition of silver-bismuth alloys," *Journal of applied electrochemistry*, vol. 33, no. 12, pp. 1199–1204, 2003.

[29] F. Scholz, *Electroanalytical Methods: Guide to Experiments and Applications*. Berlin, Heidelberg: Springer-Verlag, 2. aufl. ed., 2010.

[30] J. Wang, *Stripping analysis : principles, instrumentation, and applications*. Deerfield Beach, Fla: VCH, 1985.

[31] K. I. Popov, S. S. Djokic´, N. D. Nikolic´, and V. D. Jovic´, *Morphology of Electrochemically and Chemically Deposited Metals*. Cham: Springer International Publishing AG, 1st ed. 2016 ed., 2016.

[32] B. Scharifker and G. Hills, "Theoretical and experimental studies of multiple nucleation," *Electrochimica Acta*, vol. 28, no. 7, pp. 879–889, 1983.

[33] M. E. Hyde, O. V. Klymenko, and R. G. Compton, "The theory of electrodeposition in the presence of forced convection:: Transport controlled nucleation of hemispheres," *Journal of electroanalytical chemistry (Lausanne, Switzerland)*, vol. 534, no. 1, pp. 13–17, 2002.

[34] S. M. Skaftun, *Manganese oxide in zinc electrowinning : deposition and removal at platinum, gold and $IrO_2Ta_2O_5$/Ti anodes in sulphuric acid*. PhD thesis, NTNU, Trondheim, 2021.

[35] G. B. Popov KI, Djokic´ SS, *Fundamental aspects of electrometallurgy*. New York: Kluwer Academic/Plenum Publishers, 1st ed. ed., 2002.

[36] T. Åkre, *Electrowinning of cobalt from chloride solutions : anodic deposition of cobalt oxide on DSA*. PhD thesis, Norwegian University of Science and Technology, Trondheim, 2008.

[37] J. Jansz, "Estimation of ionic activities in chloride systems at ambient and elevated temperatures," *Hydrometallurgy*, vol. 11, no. 1, pp. 13–31, 1983.

[38] K. W. Krakhella, M. Morales, R. Bock, F. Seland, O. S. Burheim, and K. E. Einarsrud, "Electrodialytic energy storage system: Permselectivity, stack measurements and life-cycle analysis," *Energies (Basel)*, vol. 13, no. 5, p. 1247, 2020.

[39] R. H. Petrucci, *General chemistry : principles and modern applications*. Upper Saddle River, N.J: Pearson Prentice Hall, 9th ed. ed., 2007.

[40] B. Averill, *Chemistry : principles, patterns, and applications*. San Francisco: Benjamin Cummings, pearson international ed. ed., 2005.

[41] S. Dong and Y. Wang, "A nafion/crown ether film electrode and its application in the anodic stripping voltammetric determination of traces of silver," *Analytica Chimica Acta*, vol. 212, pp. 341–347, 1988.

[42] D. E. Schildkraut, P. T. Dao, J. P. Twist, A. T. Davis, and K. A. Robillard, "Determination of silver ions at submicrogram-per-liter levels using anodic square-wave stripping voltammetry," *Environmental toxicology and chemistry*, vol. 17, no. 4, pp. 642–649, 1998.

[43] A. G. Blackman, *Aylward and Findlay's SI chemical data*. Wiley, 7th ed., 2014.

[44] I. Lampre, P. Pernot, and M. Mostafavi, "Spectral properties and redox potentials of silver atoms complexed by chloride ions in aqueous solution," *The Journal of Physical Chemistry B*, vol. 104, no. 26, pp. 6233–6239, 2000.

[45] T. Renner, M. Quack, J. Stohner, H. L. Strauss, M. Takami, A. J. Thor, E. R. Cohen, T. Cvitas, J. G. Frey, and B. Holström, *Quantities, units, and symbols in physical chemistry*. Cambridge, UK: RSC Pub., 3rd ed. ed., 2007.

[46] J. R. Rumble, "Crc handbook of chemistry and physics," *CRC Press/Taylor and Francis*, vol. 102nd Edition (Internet Version 2021), 2021.

[47] D. A. Skoog, *Fundamentals of analytical chemistry*. Boston: Brooks/Cole Cengage Learning, 9th ed. ed., 2014.

[48] P. Atkins, *Atkins' physical chemistry*. Oxford: Oxford University Press, 10th ed. ed., 2014.

[49] T. Seward, "The stability of chloride complexes of silver in hydrothermal solutions up to 350°c," *Geochimica et Cosmochimica Acta*, vol. 40, no. 11, pp. 1329–1341, 1976.

[50] E. Bardal, *Corrosion and protection*. Engineering materials and processes, London: Springer, 2004.

[51] A. J. Bard, G. Inzelt, and F. Scholz, *Electrochemical Dictionary*. Berlin, Heidelberg: Springer-Verlag, 2. aufl. ed., 2012.

[52] J. Gonzalez and A. Molina, *Pulse Voltammetry in Physical Electrochemistry and Electroanalysis: Theory and Applications*. Monographs in Electrochemistry, Cham: Springer International Publishing AG, 2015.

[53] V. Mirceski, *Square-wave voltammetry : theory and application*. Monographs in electrochemistry, Berlin: Springer, 2007.

[54] T. Greibrokk, *Kromatografi : separasjon og deteksjon*. Oslo: Universitetsforlaget, 3. utg. ed., 1994.

[55] J. N. Miller, "Basic statistical methods for analytical chemistry. pt.2: calibration and regression methods," *Analyst (London)*, vol. 116, pp. 3–14, 1991.

[56] B. N. Popov, *Corrosion Engineering: Principles and Solved Problems*. Amsterdam: Elsevier, 2015.

[57] P. Pedeferri, *Corrosion Science and Engineering*. Engineering Materials, Cham: Springer International Publishing : Imprint: Springer, 1st ed. 2018. ed., 2018.

[58] R. Holze, *Experimental electrochemistry : a laboratory textbook*. Weinheim: Wiley-VCH, 2009.

[59] A. Torriero, "Understanding the differences between a quasi-reference electrode and a reference electrode," *Medicinal & Analytical Chemistry International Journal*, vol. 3, 01 2019.

[60] D. A. Lowy and L. Oniciu, "Reference electrode for potentiometric analysed in corrosive media," *Analyst (London)*, vol. 121, no. 3, pp. 363–368, 1996.

[61] M. Ciobanu, J. P. Wilburn, N. I. Buss, P. Ditavong, and D. A. Lowy, "Miniaturized reference electrodes based on ag/agix internal reference elements. i. manufacturing and performance," *Electroanalysis (New York, N.Y.)*, vol. 14, no. 14, pp. 989–997, 2002.

[62] R. Beanland, F. J. Humphreys, and P. J. Goodhew, *Electron Microscopy and Analysis, Third Edition*. CRC Press, 2000.

[63] J. Hjelen, *Scanning elektron-mikroskopi*. Trondheim: SINTEF, 1989.

[64] K. L. Scrivener, "Backscattered electron imaging of cementitious microstructures: understanding and quantification," *Cement & concrete composites*, vol. 26, no. 8, pp. 935–945, 2004.

[65] Z. Alobad, *Designing PU Resins for Fibre Composite Applications*. PhD thesis, University of Babylon, 03 2018.

[66] B. Geboes, B. Vanrenterghem, J. Ustarroz, D. Pauwels, S. Sotiropoulos, A. Hubin, and T. Breugelmans, "Influence of the morphology of electrodeposited nanoparticles on the activity of organic halide reduction," *Chemical engineering transactions*, vol. 41, 2014.

[67] S. Musabikha, M. Mukhtasor, J. Wharton, and R. Wood, "Effects of nickel–aluminum bronze pre-oxidized films on the cathodic kinetics of oxygen reduction," *Analytical Letters*, vol. 53, pp. 1218–1232, 01 2020.

A Chemical content and calculation

The silver nitrate solution should be 0.5 L and give a silver ion concentration of 1 mg L^{-1} when 1 mL is added to a 0.15 L glass cell. The total silver ion content can be found as follows:

$$m_{Ag^+} = \frac{500\,\text{mL} \cdot 1\,\text{mg}\,\text{L}^{-1} \cdot 0.15\,\text{L}}{1\,\text{mL}} = 75\,\text{mg}Ag^+ \tag{A.1}$$

The molar mass of silver nitrate is 169.87 g mol^{-1}, while the molar mass of silver is 107.87 g mol^{-1}. The amount of silver nitrate needed can then be calculated as follows:

$$m_{AgNO_3} = \frac{169.87\text{g}\,\text{mol}^{-1}AgNO_3}{107.87\text{g}\,\text{mol}^{-1}Ag^+} \cdot 75\,\text{mg}Ag^+ = 118\,\text{mg}AgNO_3 \tag{A.2}$$

The content of some of the most important elements in the undiluted process solution is shown in Table A.1.

Table A.1: Content of some chosen elements in the used undiluted process solution.

Element	Unit	Concentration
Ni^{2+}	g L^{-1}	240
Cl^-	g L^{-1}	280
$SO_4{}^{2-}$	g L^{-1}	35
Fe^{2+}	g L^{-1}	9
Bi^{2+}	mg L^{-1}	10
Ag^+	mg L^{-1}	<0.05

B Statistic in measurements for reproducibility

The peak height and charge from 13 repeated measurements of divided stripping by ALSV with a Ag/AgCl reference electrode, differential pulse voltammetry, and ALSV with a nickel pseudo-reference electrode is shown in Table B.1, Table B.2, and B.3, respectively. The average value, standard deviation, two standard deviations, and deviation in percent is also shown in the table. The deviation is for 95% probability.

Table B.1: Table of the peak height and charge for each of the 13 repeated measurements for ALSV with AgAgCl RE. In addition, the average, the standard deviation, the value of two standard deviations, and the deviation in percent for two standard deviations are shown.

Measurement	Peak height [A cm^{-2}]	Charge [mC]
1	7.1	0.570
2	7.0	0.563
3	7.0	0.560
4	7.0	0.557
5	7.0	0.557
6	7.0	0.557
7	7.0	0.559
8	7.1	0.562
9	7.1	0.564
10	7.2	0.569
11	7.3	0.572
12	7.3	0.576
13	7.3	0.574
Average	7.1	0.565
Standard deviation	0.14	0.007
Two standard deviations	0.3	0.014
Deviation	4%	2%

Table B.2: Table of the peak height and charge for each of the 13 repeated measurements for differential pulse voltammetry. In addition, the average, the standard deviation, the value of two standard deviations, and the deviation in percent for two standard deviations are shown.

Measurement	Peak height [A cm^{-2}]	Charge [mC]
1	3.6	1.08
2	3.5	1.08
3	3.5	1.09
4	3.4	1.08
5	3.4	1.08
6	3.3	1.08
7	3.3	1.08
8	3.3	1.08
9	3.2	1.07
10	3.2	1.7
11	3.2	1.06
12	3.1	1.06
13	3.1	1.05
Average	3.3	1.07
Standard deviation	0.14	0.012
Two standard deviations	0.3	0.02
Deviation	9%	2%

Table B.3: Table of the peak height and charge for each of the 13 repeated measurements for ALSV with a nickel pseudo-RE. In addition, the average, the standard deviation, the value of two standard deviations, and the deviation in percent for two standard deviations are shown.

Measurement	Peak height [A cm^{-2}]	Charge [mC]
1	8.1	0.55
2	8.0	0.55
3	7.7	0.55
4	8.0	0.54
5	7.9	0.53
6	7.8	0.53
7	8.0	0.52
8	7.8	0.52
9	8.0	0.52
10	7.6	0.52
11	7.7	0.51
12	7.6	0.51
13	7.8	0.50
Average	7.8	0.53
Standard deviation	0.2	0.016
Two standard deviations	0.4	0.03
Deviation	4%	6%

C Silver detection with ammonium buffer

An ammonium buffer was made by mixing 50 mL of 25% NH_3 and 50 mL of deionized water. Anodic linear sweep voltammetry (ALSV) was conducted in diluted synthetic process solution added 0, 1, 5, 10, and 15 mL of the ammonium buffer solution. The parameters were the same as in Table 3.6 in Subsection 3.2 but only -0.2 V was used as deposition potential.

A pH-meter was used to monitor the pH change when adding the buffer solution. The buffer solution was added in steps of 1 mL from 0 to 15 ml with continuous stirring by a magnetic stirrer. The pH was measured after each addition but in a separate beaker and not directly in the solution used for the electrochemical measurements.

Addition of ammonium buffer has little effect on the silver peak before 10 mL buffer is added, and the silver peak disappears (Figure C.1). Precipitation of a dark substance was observed after addition of 10 mL buffer.

In the diluted synthetic process solution, the change in the pH as a function of the amount of buffer added to the solution can be seen in Figure C.2. The pH changed little the first 4 mL added. From 4 to 5 mL, the pH changed from 1.1 to 5.6, and precipitation of a dark material was observed. Further addition of buffer changed the pH relatively linearly to pH of 7.4 after adding 15 mL of the buffer.

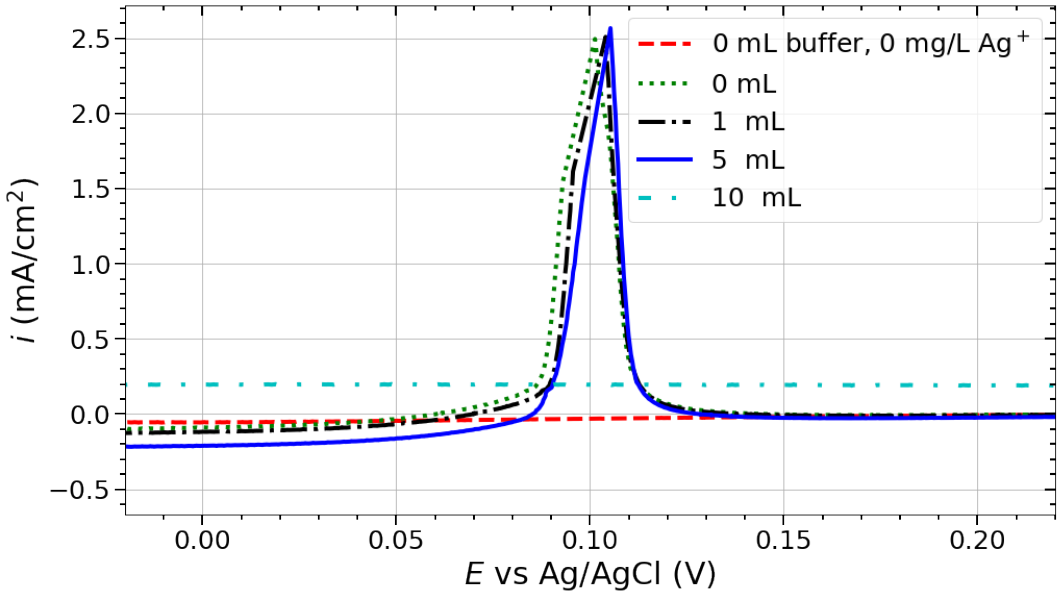

Figure C.1: Voltammograms of silver ion detection in a synthetic electrolyte containing 25 g L^{-1} Ni^{2+}, 1.2 g L^{-1} Fe^{2+}, 1 mg L^{-1} Mn^{2+}, and 30 g L^{-1} Cl^{-} by a GC electrode. The figure shows voltammograms for solutions without silver ions and with 1 mg L^{-1} Ag^{+} in addition to 0, 1, 5, and 10 mL ammonium buffer. The experimental parameters used are as follows: 100 mV s^{-1} scan rate, 100 s deposition time, rotation rate of 1600 rpm, and deposition potential of −0.2 V vs. Ag/AgCl.

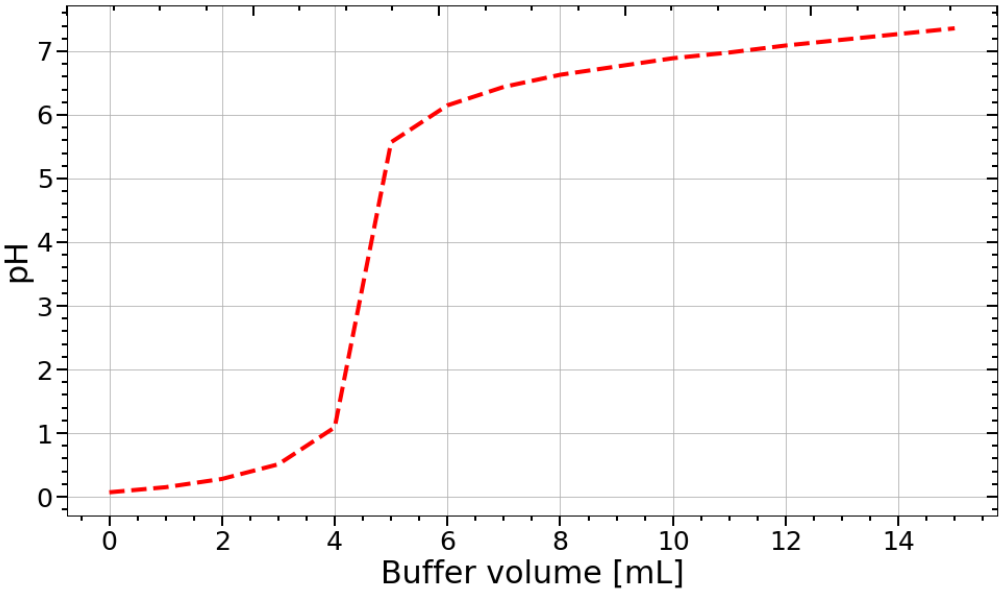

Figure C.2: Graph of the pH as a function of the volume of ammonium buffer added.

D Electrode surfaces and EDS spectra

D.1 SEM and EDS after deposition in solution without silver ions

SEM images after 1000 s deposition in a diluted process solution without silver ions can be seen in Figure D.1 and Figure D.2 for deposition potential of -0.1 and $-0.2\,\mathrm{V}$ vs. Ag/AgCl, respectively. The results from EDS can be seen in Figure D.3, Figure D.4, and Figure D.5 for deposition potentials of -0.1, -0.2, and $-0.3\,\mathrm{V}$ vs. Ag/AgCl, respectively.

D.2 SEM and EDS after deposition in solution with silver ions

The results from EDS can be seen in Figure D.6, Figure D.7, and Figure D.8 for deposition potentials of -0.1, -0.2, and $-0.3\,\mathrm{V}$ vs. Ag/AgCl, respectively. This is for a diluted process solution with a silver ion content of $1\,\mathrm{mg\,L^{-1}}$, corresponding to a concentration of $10\,\mathrm{mg\,L^{-1}}$ Ag^+ in the undiluted process solution.

D.3 EDS of electrode after deposition and OCP

EDS of an electrode after 1000 s deposition, followed by about 50 s OCP, can be seen in Figure D.9 for a deposition potential of $-0.3\,\mathrm{V}$ vs. Ag/AgCl. The spectrum shows silver and chloride present, indicating that silver chloride might have been formed at the surface during OCP.

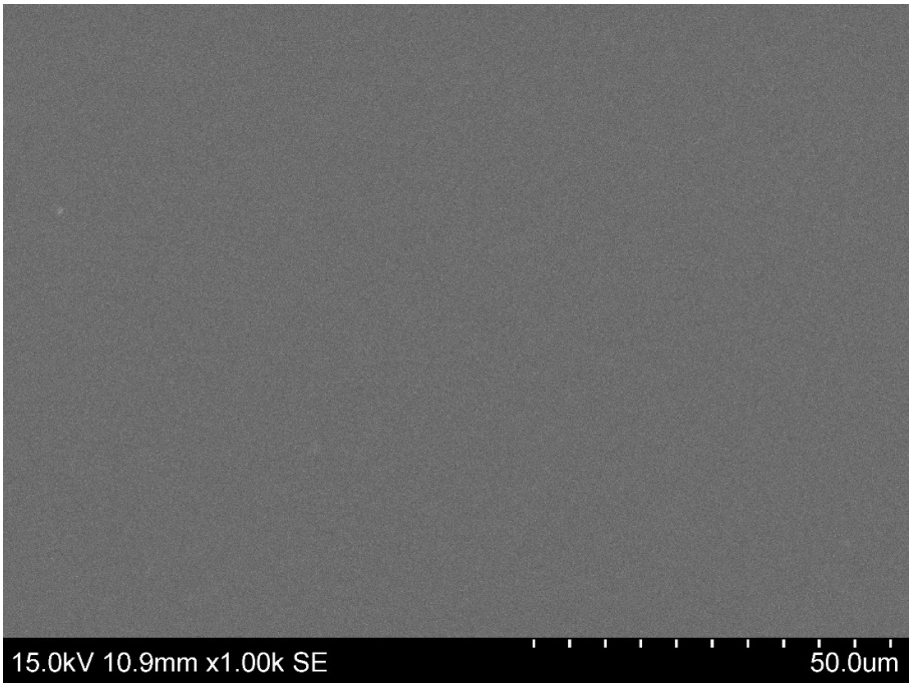

Figure D.1: SEM image of a GC electrode after electrodepositing at −0.1 V vs. Ag/AgCl for 1000 s in a diluted process solution without silver ions.

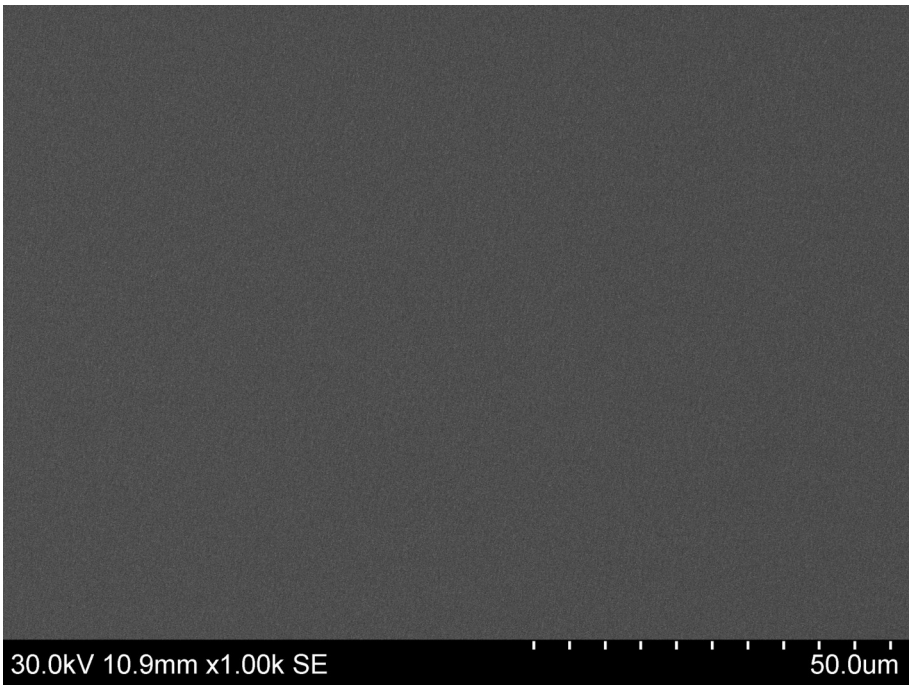

Figure D.2: SEM image of a GC electrode after electrodepositing at −0.2 V vs. Ag/AgCl for 1000 s in a diluted process solution without silver ions.

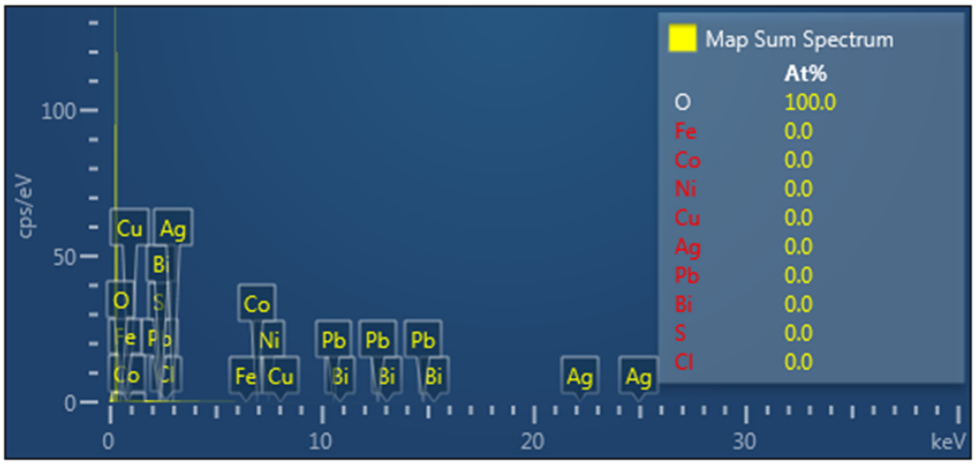

Figure D.3: EDS spectrum of a GC electrode after electrodepositing at −0.1 V vs. Ag/AgCl for 1000 s in a diluted process solution without silver ions.

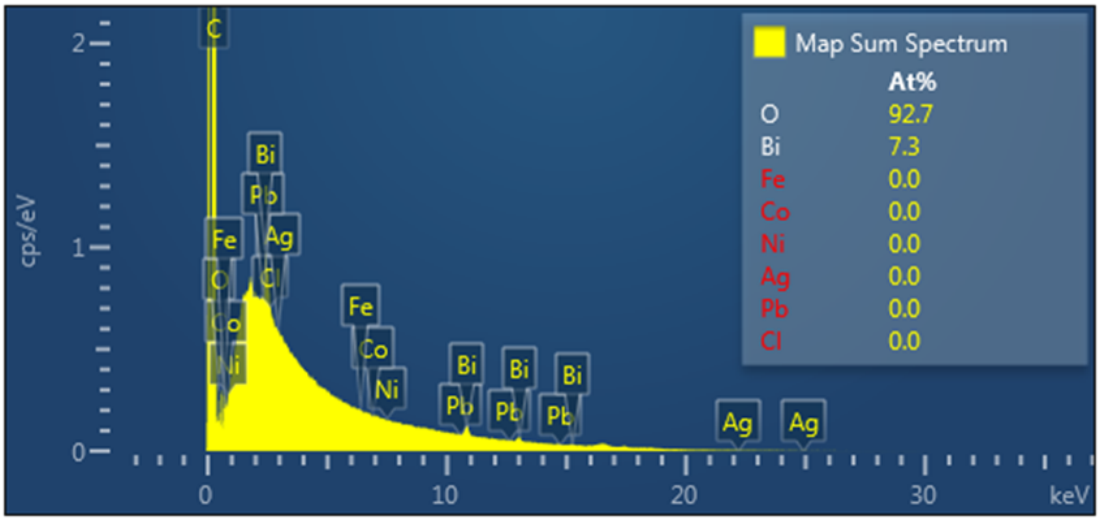

Figure D.4: EDS spectrum of a GC electrode after electrodepositing at −0.2 V vs. Ag/AgCl for 1000 s in a diluted process solution without silver ions.

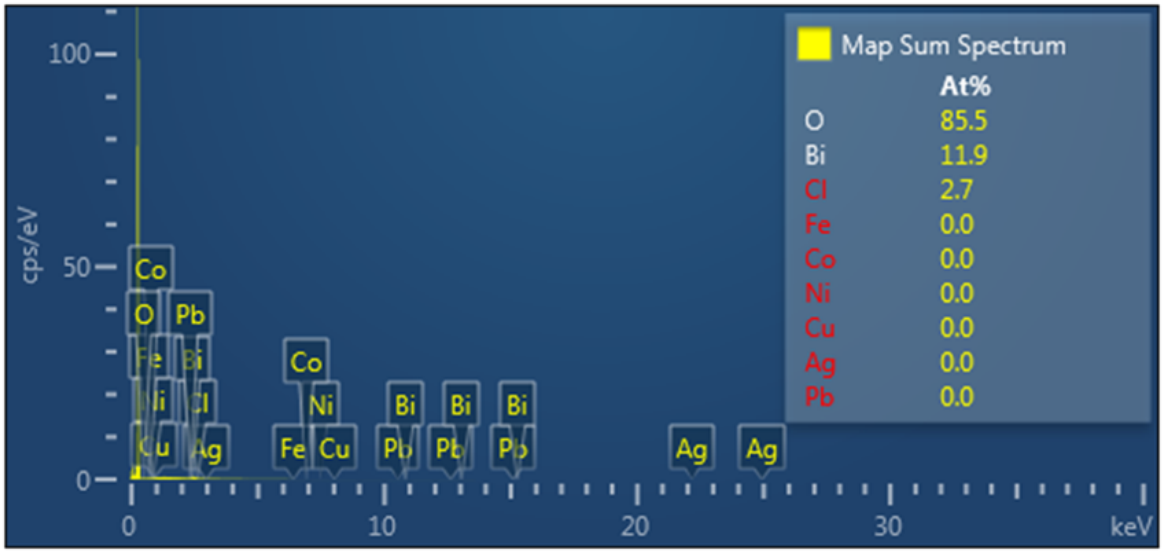

Figure D.5: EDS spectrum of a GC electrode after electrodepositing at −0.3 V vs. Ag/AgCl for 1000 s in a diluted process solution without silver ions.

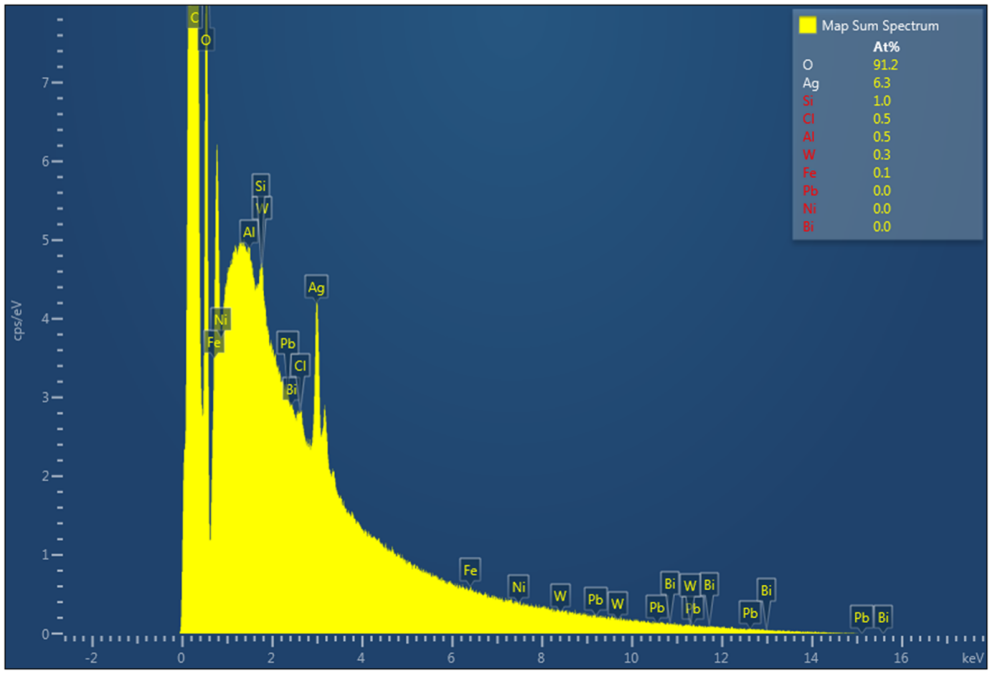

Figure D.6: EDS spectrum of a GC electrode after electrodepositing at −0.1 V vs. Ag/AgCl for 1000 s in a diluted process solutions a silver ion content of 1 mg L^{-1}.

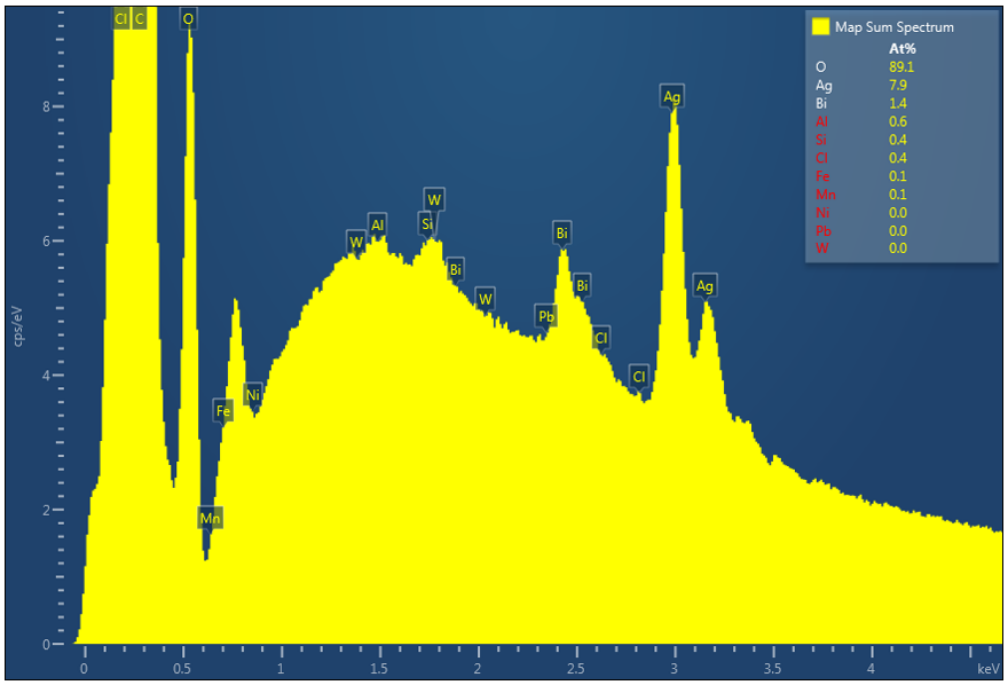

Figure D.7: EDS spectrum of a GC electrode after electrodepositing at −0.2 V vs. Ag/AgCl for 1000 s in a diluted process solutions a silver ion content of 1 mg L^{-1}.

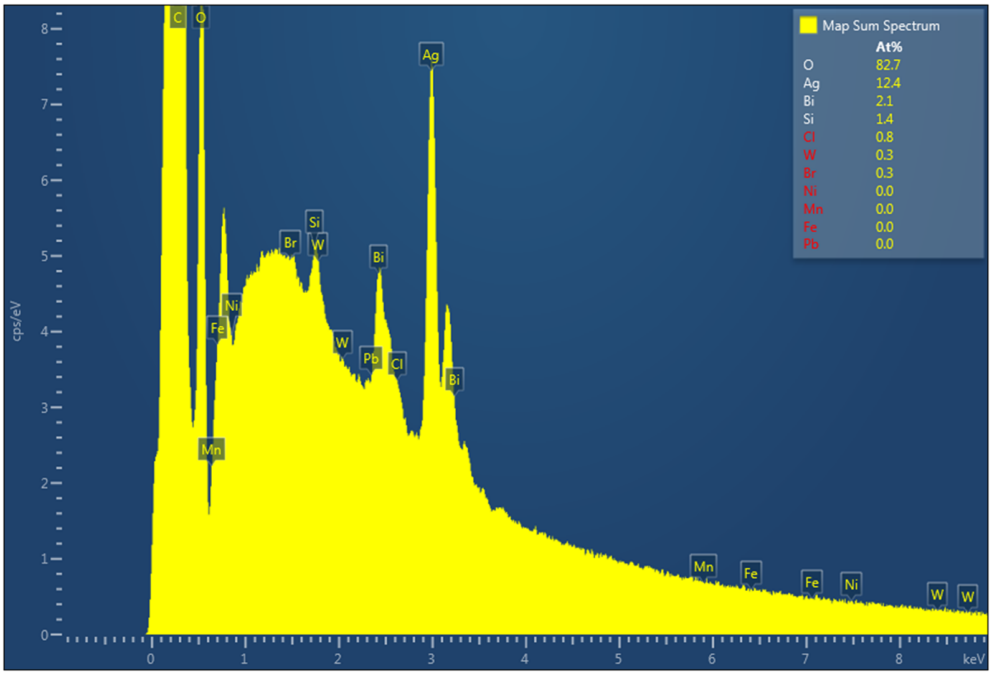

Figure D.8: EDS spectrum of a GC electrode after electrodepositing at −0.3 V vs. Ag/AgCl for 1000 s in a diluted process solutions a silver ion content of 1 mg L^{-1}.

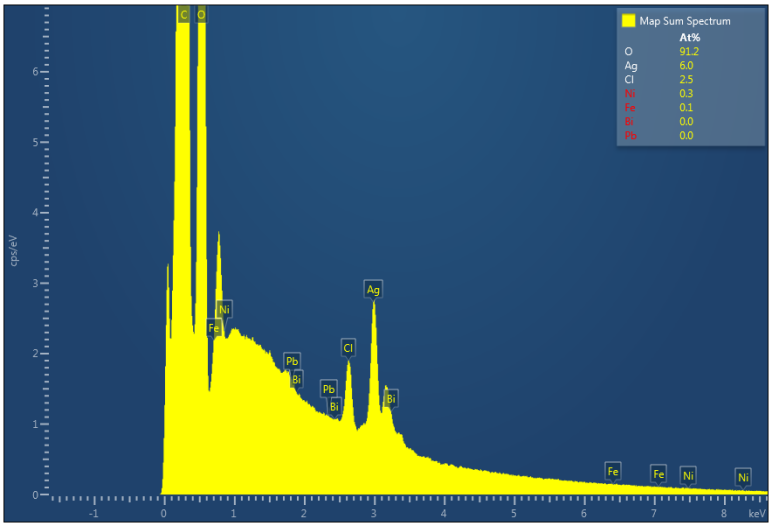

Figure D.9: EDS spectrum of a GC electrode after electrodepositing at $-0.3\,\mathrm{V}$ vs. Ag/AgCl for 1000 s in a diluted process solutions a silver ion content of $1\,\mathrm{mg\,L^{-1}}$, followed by about 50 s OCP.

E Corrosion rate

A polarisation curve for estimation of the corrosion rate of a nickel wire is shown in Figure 4.19. The Tafel slopes intersect at approximately $log(I) = -0.95$. The molar mass of nickel is $58.69\,\mathrm{g\,mol^{-1}}$, the number of electrons transferred is 2, and the area of the nickel wire is about $0.86\,\mathrm{cm^2}$. The corrosion rate can be calculated from these values by using the Faradays law (Equation 2.38):

$$\frac{\Delta s}{\Delta t} = 3268 \frac{58.69 \cdot 10^{-0.95} \cdot \frac{1}{1000} / 0.86}{2 \cdot 8.902} = 1.4\mathrm{mm/year} \tag{E.1}$$